Title
Development and Assessment of Gene Therapies for

Author
Kolstad, Kathleen Durgin

Publication Date
2009

Peer reviewed|Thesis/dissertation

Development and Assessment of Gene Therapies for Inherited Blinding Diseases

By

Kathleen Durgin Kolstad

B.S. Bates College (2004)

Dissertation submitted in partial fulfillment of the requirements for the degree of

Doctor of Philosophy

in

Molecular and Cell Biology

in the

Graduate Division

of

University of California, Berkeley

Committee in charge:
Professor John G. Flannery, Chair
Professor Yang Dan
Professor Ehud Y. Isacoff
Professor David V. Schaffer

Fall, 2009

Abstract

Development and Assessment of Gene Therapies for Inherited Blinding Diseases

By

Kathleen Durgin Kolstad

Doctor of Philosophy in Molecular and Cell Biology

University of California, Berkeley

Professor John Flannery, Committee Chair

There are two therapeutic approaches for inherited retinal disease addressed in this dissertation: we sought to slow retinal degeneration and reverse visual loss after complete photoreceptor apoptosis. In the first approach, by viral gene transfer to the support cells of the retina, Müller glia (RMCs), we achieved sustained secretion of human glial derived neurotrophic factor (hGDNF) (Chapter 3). We hypothesized that hGDNF production by retinal glia will enhance the protective affects of RMCs in the diseased retina and help slow photoreceptor degeneration. Furthermore, this method avoids extra photoreceptor stress caused by direct hGDNF gene transfer to cells that are already stressed. We were able to optimize gene transfer to RMCs and observe the beginnings of functional rescue in an animal model of autosomal dominant retinitis pigmentosa with this technique. One major advantage of this therapeutic approach is that it is applicable to multiple retinal disease genotypes.

The second approach to ocular gene therapy presented in this dissertation was to re-introduce photosensitivity to the retina after complete photoreceptor degeneration

(Chapter 4). To this end, we employed the engineered light activated glutamate receptor (LiGluR) to confer light sensitivity on retinal ganglion cells (RGCs) in the diseased retina. We first showed LiGluR mediated RGC photo-activation in *in vitro* retinal tissue preparation. We then characterized in vivo cell population responses (visually evoked potentials, VEPs) in V1 when retinal input was limited to LiGluR induced activity in the retina. VEPs driven by LiGluR are approximately 50% of the amplitude of full field light flash driven responses in the wild type animal. LiGluR driven cortical responses in blind animals suggest that it is a promising therapy for restoring visual function and processing in the late stages of retinal degeneration.

In the third part of this dissertation (Chapter 2a and 2b), the goal was to develop and assess methods of making ocular gene therapies safer and more efficacious. Current gene therapies for retinal degenerative diseases rely on subretinal delivery of viral vectors carrying therapeutic DNA. However, this method of delivery limits the viral transduction profile to the region of injection and seriously compromises the retina during detachment. We have identified natural barriers to viral vector delivery to the outer retina from the vitreous. Furthermore, we have developed artificial methods and characterized disease states that allow these barriers to be overcome. The understanding of and the ability to manipulate barriers to vitreal delivery of viral vectors will help avoid the limitations, risks, and damage associated with subretinal injections.

Professor John G. Flannery _____Date _____

Acknowledgements

First and foremost, I would like to thank my adviser, Dr. John Flannery. John has not only provided me with scientific guidance, but also the trust and tools for me to independently pursue scientific questions, make mistakes, and ultimately learn in a way that suits me. John also supported and encouraged collaboration, which allowed me to not only develop life long friendships, but also discover that scientific progress requires a combination of experimental approaches and perspectives. Finally, I do not think I would be following the career path I am now on, if it were not for John. He has taught me that progress and results come from a balanced life and an excitement and passion for what lies ahead.

I would also like to express my gratitude to my wonderful friends and fabulous colleagues, Natalia Caporale, Deniz Dalkara, and Karen Guerin. You have taught me more than you know about experimental science, hard work, and the value of collaboration combined with a good sense of humor. Thank you to Meike Visel, for her interminable hard work to support our research, valuable discussion, and positive attitude and Ryan Klimczak for his constant good humor. Thank you to Richard Kow, Natalie Hoffman, and Kim Nguyen for their assistance and patience with me as a teacher. And thank you to the Berkeley faculty, namely my dissertation committee members, for valuable scientific discussion and guidance throughout my PhD.

And lastly, I would like to thank my family and friends. This dissertation is dedicated to my parents, Charlie and Valerie Kolstad, and my brother, Jonathan Kolstad. The three of you have provided me with the love, support, dialogue, and inspiration to learn that I need to keep my life balanced and priorities in place, and the motivation to

continue asking questions. I would also like to acknowledge some of the most important role models in my life: my grandparents, Christine Kolstad and Dorothy and Gilbert Thompson and Aunt Ruth and Uncle Lu Fernandez, and in loving memory of my grandfather, George Kolstad. I am also grateful to my sister-in-law, Katrina Abuabara for your early and continuing career guidance and, of course, great sense of fun. Thank you Max Baumhefner for your optimism, warmth, and conversation. You inspire me to always look on the bright side of life. And, finally, thank you Rosie Ueng, Kim Cooney, and Atticus Finch for keeping me laughing, enjoying life, and exploring the world around me.

Table of Contents

Figure and Table Legend

Chapter 1

Chapter 2

Chapter 2a

Chapter 2a

Chapter 3

Chapter 4

Chapter 1

Introduction

Processing visual information allows us to understand facial expressions, appreciate natural beauty, and navigate through the world around us. Inherited diseases like retinitis pigmentosa result in progressive retinal degeneration that ultimately leads to blindness and the loss of the capabilities many take for granted. Enhancing our understanding of the molecular mechanisms responsible for retinal degeneration and developing therapies to either slow or reverse disease progression are necessary steps toward providing patients with viable treatments in the future.

The Retina

The retina performs the initial stages of visual image processing via its intricate neural circuitry. Retinal tissue is organized into distinct functional and structural layers. Photoreceptors (rods and cones) are the light sensitive cells situated at the back of the eye, directly adjacent to the retinal pigment epithelium. The photosensitive compound, retinal, that is found in the photoreceptor outer-segments, changes its three-dimensional structure as it absorbs photons. This structural change activates the protein, opsin, that in turn signals the G-protein, transducin, to initiate cyclic-GMP phosphodiestarase activity. In the dark, cGMP gated cation channels remain open, leading to the maintenance of a depolarized membrane potential. However, photo-activation of the biochemical-signaling cascade results in cGMP gated channels to shut, hyperpolarizing the membrane and altering glutamate release and the electrical microenvironment at the outer plexiform

layer. Changes at the outer plexiform signal further information processing by second order neurons in the inner nuclear layer (INL), bipolar and horizontal cells. Retinal ganglion cells (RGCs) collect information from the INL and are the final output neuron of the retina (Figure 1.1). The information is then sent to the lateral geniculate nucleus and on to the visual cortex.

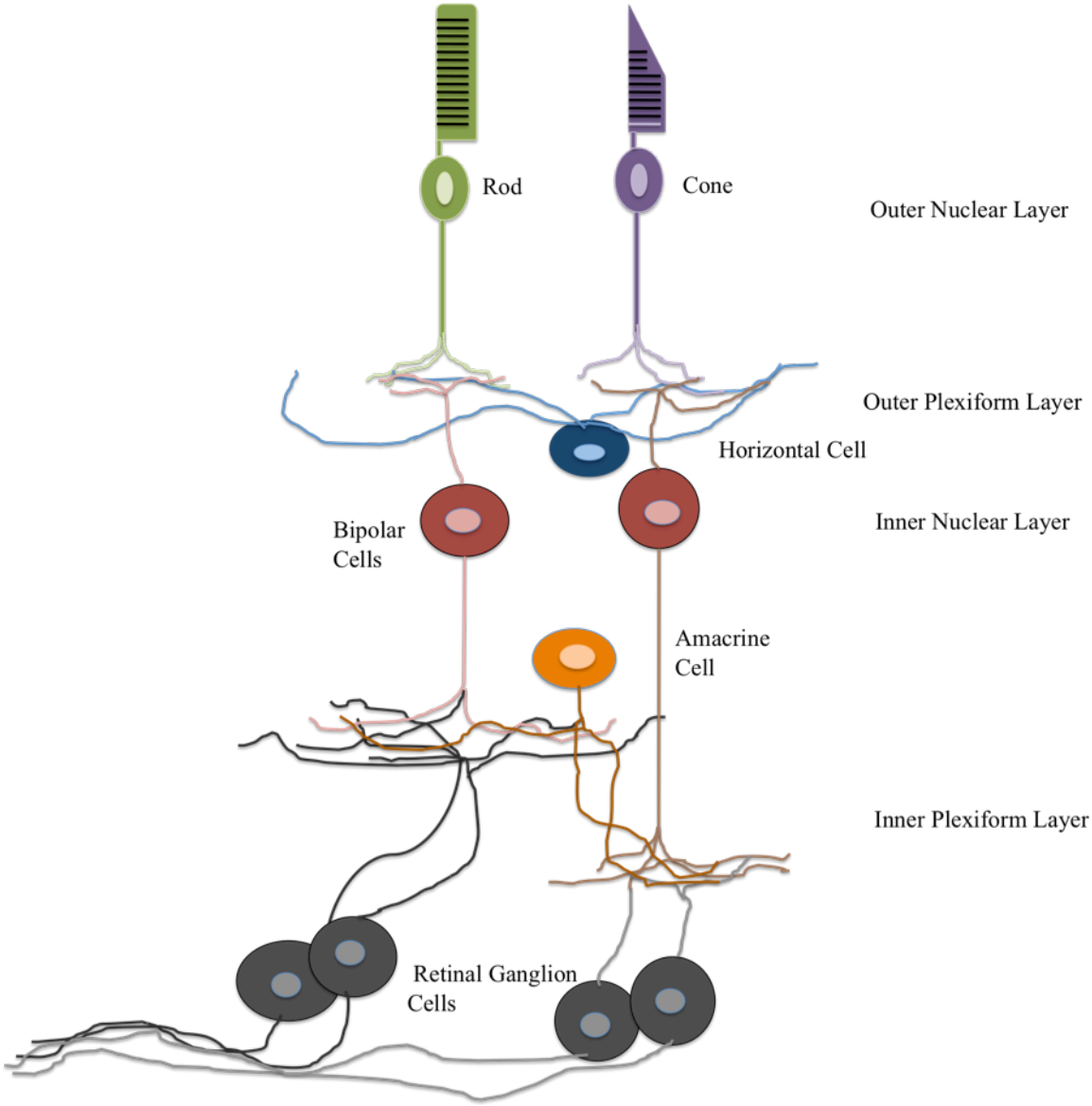

Figure 1.1. Diagram of retinal layers; photoreceptors (rods and cones) synapse on to bipolar cells and horizontal cells at the outer plexiform layer. Bipolar cells synapse onto retinal ganglion cells and amacrine cells at the inner plexiform layer.

Parallel processing in the retina results in multiple distinct neural representations of a visual image. Researchers have categorized these neural representations based on the morphological and physiological characteristics of particular retinal cells. The lamination of second order retinal bipolar cell axons and third order retinal ganglion cell dendrites reflects a level of functional organization at the inner plexiform layer (Nelson *et al.,* 1978; Roska *et al.,* 2006; Roska and Werblin, 2001; Werblin *et al.,* 2001; Wu *et al.,* 2000) (Figure 1.2). OFF ganglion cells projecting their dendritic arbor to the distal portion of the IPL spike outside the stimulus boundaries at light ON and within the stimulus boundaries at light OFF. Conversely, ON ganglion cells that project to the proximal region of the IPL spike at light ON within the spatial boundaries of the stimulus (Awatramani and Slaughter, 2000; Bloomfield and Miller, 1986; Roska *et al.,* 2006; Roska and Werblin, 2001; Werblin *et al.,* 2001). Ganglion cells that project to the border between ON and OFF strata tend to demonstrate transient responses while more proximal and distal projecting cells exhibit sustained responses (Awatramani and Slaughter, 2000; Roska *et al.,* 2006; Roska and Werblin, 2001; Werblin *et al.,* 2001).

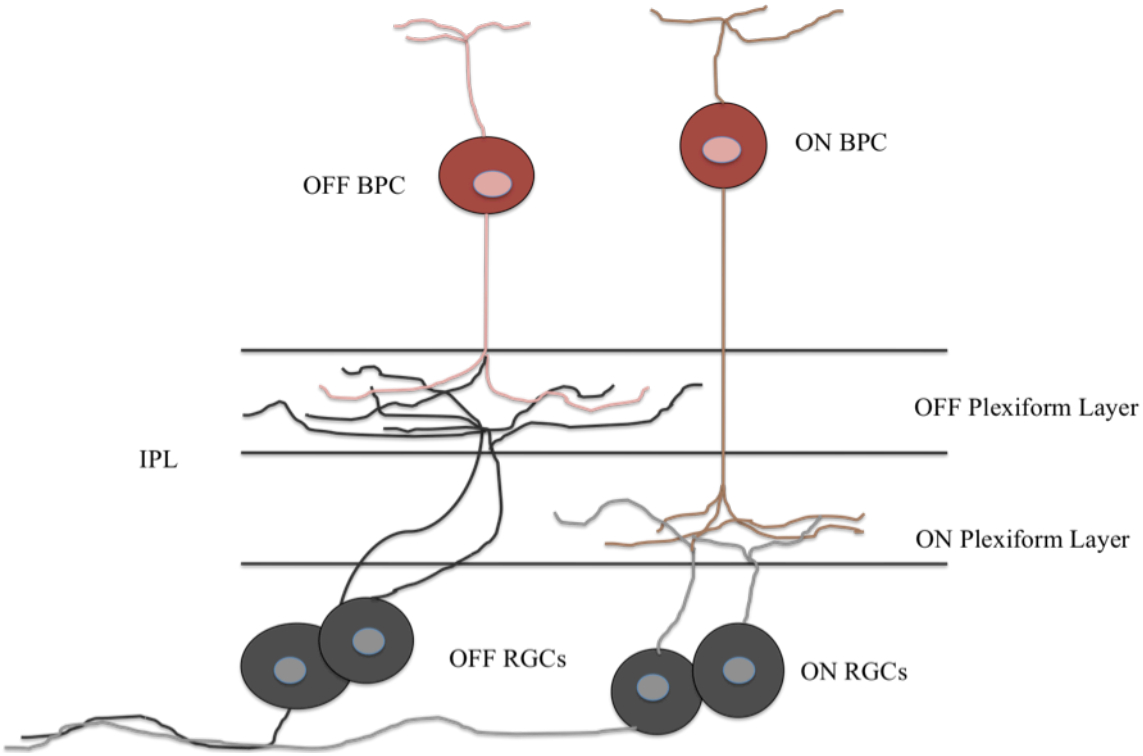

Figure 1.2. Functional organization of ON and OFF bipolar cells, and ON and OFF retinal ganglion cells at the inner plexiform layer (IPL). Visual input originates from cone and rod photoreceptors.

The retina is a highly specialized tissue that is necessary for the initial stages of visual processing. The precise anatomical and functional organization is crucial for the appropriate cortical interpretation of the surrounding world, thus diseases that affect this fine balance can be severely damaging to vision.

Inherited Retinal Diseases

Inherited retinal diseases greatly vary in genetic profile (mutations in different genes can cause the same disease), allelic makeup (different mutations in the same gene can cause the same or different disease), and clinical manifestation (Sullivan and Daiger, 1996). Retinal diseases can be monogenic or digenic. Monogenic disease are more common and are inherited as autosomal dominant, autosomal recessive, or x-linked. The one commonality between all inherited retinal diseases is retinal degeneration, as seen in patients with retinitis pigmentosa (RP), Leber's congenital ameurosis (LCA), congenital stationary night blindness, macular degeneration, Stargart's macular dystrophy, and usher syndrome (Sullivan and Daiger, 1996). Retinitis Pigmentosa (RP) is the largest and most genetically heterogeneous inherited retinal disease (http://www.sph.uth.tmc.edu/retnet/, Travis, 1998, Hims *et al.,* 2003; Sullivan and Daiger, 1996). In fact, RP is the most common blinding disease in the developed world, affecting 1 in 3,000 individuals (Bessant *et al.,* 2001). The clinical manifestations of RP are night blindness, the development of tunnel vision, and ultimately complete blindness.

The majority of mutations resulting in photoreceptor degeneration are found in genes expressed in photoreceptors and the RPE (Daiger *et al.,* 2007; Travis, 1998). Many affected proteins are found in the phototransduction cascade, including rhodopsin (Daiger *et al.,* 2007; Shastry, 1997), transducin (Dryja *et al.*, 1996), and the α and β subunits of cGMP phosphodieesterase (Huang *et al.,* 1995, McLaughlin *et al.,* 1995). Other major proteins implicated in photoreceptor degeneration are expressed in the RPE. These proteins typically assist in photoactivation of rods and cones. Two examples of RPE expressed genes that are subject to mutation and resulting retinal degeneration are

CRALBP (cellular retinaldehyde binding protein) (Maw *et al.,* 1997) and RPE65 (Gu *et al.*, 1997, Marlhens *et al.,* 1997). Both proteins are necessary for all-trans-retinol isomerization (Saari *et al.,* 2001).

The molecular details of how and why photoreceptors die during retinal degeneration are yet to be completed elucidated, however it is generally agreed that the final steps of cellular loss are a result of apoptosis, pre-programmed cell death (Reme *et al.*, 2000, Chang *et al.,* 1993). Stressful endogenous and exogenous stimuli induce a signaling cascade that results in the activation of multiple proteases and caspases. After protealytic cleavage of the cell, debris is phagocytosed. The main signs of apoptosis are condensation of nuclear chromatin, cell soma shrinkage, blebbing of the plasma membrane, and the breakdown of the cell into apoptotic bodies.

Apoptosis is the final common pathway of retinal diseases but is also necessary for appropriate retinal development (Linden *et al.,* 1999; Chang *et al.,* 1993). Some of the earliest work to identify apoptosis as the common pathway to retinal degeneration was conducted by Chang and colleagues (1993). This study showed that DNA fragmentation occurs in three different models of retinal degeneration: the rd (retinal degeneration), rds (retinal degeneration slow), and rhodopsin mutant mice. All three of these animal models possess different genetic backgrounds that result in a shared phenotype, retinal degeneration. Though the trigger of apoptosis must be different for the various mutations, they share a common phenotype and apoptosis as the ultimate step in cell death (Chang *et al.,* 1993). Other studies of different animal models of RP have shown similar results that apoptosis is the final step in photoreceptor death (Travis 1998; Tso *et al.,* 1994).

Therapies for Inherited Retinal Diseases

The eye is an attractive organ for targeted gene therapy as it is immune privileged, accessible for the introduction of therapeutic material, and many animal models of different forms of inherited retinal diseases exist (Buch *et al*., 2008; Chang *et al.,* 2002). Over the past ten years there have been multiple strategies taken to either slow photoreceptor degeneration or reverse vision loss. These attempts have recently culminated with three clinical trials currently in progress aimed at treating patients with inherited blinding diseases (Bainbridge *et al*., 2008; Cideciyan *et al*., 2008; Hauswirth *et al*., 2008; Maguire *et al*., 2008). Modern approaches to treating retinal degenerative diseases include gene replacement (the introduction of wild-type DNA to replace the mutant endogenous gene activity or lack there of), RNA mediated knock-down of dominant-negative mutant genes, the delivery of trophic factors to slow photoreceptor death, and retinal prosthetics. Some of the novel and/or ground-breaking therapeutic techniques relevant to the current dissertation work are highlighted below.

Gene Replacement Therapy

Gene replacement experiments have been shown to be a viable option for certain forms of retinal disease. Viral vectors are used to introduce wild type DNA encoding for a mutated, loss of function, gene. This technique has been successful in a variety of animal models and is now being tested in human clinical trials (Bainbridge *et al*., 2008; Cideciyan *et al*., 2008; Hauswirth *et al*., 2008; Maguire *et al*., 2008). For example, rodent models with a defect in the perpherin gene (Prph2 Rd2/Rd2) demonstrate both electrophysiological and morphological rescue as shown by the generation of normal

photoreceptor outer segments and recovered electroretinogram when the wild type gene is delivered to the retina (Ali *et al.,* 2000). More recent loss-of-function gene replacement therapies have recovered retinal ultrastructure and physiological function in rodent models of X-linked retinoschisis and RCS rats lacking the functional MERTK gene that is necessary for the phagocytosis of shed photoreceptor outer segments (Buch *et al.,* 2008, Min *et al.,* 2005, Park *et al.,* 2009; Smith *et al.,* 2003, Vollrath *et al.,* 2001).

A substantial advance in ocular gene therapy has recently been made with phase I clinical trials to treat patients with Leber's congenital ameurosis (LCA) (Bainbridge *et al*., 2008; Cideciyan *et al*., 2008; Hauswirth *et al*., 2008; Maguire *et al*., 2008). LCA is a severe autosomal recessive retinal dystrophy marked by visual loss starting at birth. There are multiple genetic mutations, 14 discovered to date, that can cause LCA (den Hollander, 2008). These mutations can affect a range of retinal functions including phototransduction, photoreceptor development, and outer segment phagocytosis (den Hollander, 2008). Mutations resulting in the loss-of-function of the RPE65 gene have been the main focus of recent therapeutic developments. The protein product of the RPE65 gene is expressed in the retinal pigment epithelium and is responsible for vitamin A cycling (i.e. the regeneration of photoactive 11-cis-retinaldehdye from all-trans-retinaldehyde).

One benefit of studying RPE65 LCA is that multiple animal models of the disease exist. Pang and colleagues achieved morphological, functional, and behavioral rescue in the rd12 mouse model of LCA (Pang *et al.,* 2006). The naturally occurring rd12 mouse possesses a recessive nonsense mutation in RPE65. Viral vector delivery of wild-type RPE65 cDNA to the subretinal space resulted in restored ERG, an increase in

rhodopsin levels, recovery of retinal structure, and restored vision-dependant behavior as shown by the Morris water maze test (Pang *et al.,* 2006).

The existence of the naturally occurring RPE65-/- Briard dog has assisted translation of therapeutic developments across species. Multiple studies have shown physiological, behavioral, and cellular function rescue in the RPE65 null canine (Acland *et al.,* 2001; Acland *et al.,* 2005; Le Meur *et al.,* 2007; Narfstrom *et al.,* 2003; Rolling F *et al.,* 2006). The original work done by Acland and colleagues showed visual recovery after vector introduction of RPE65 to the subretinal space by ERG, pupillometry, and behavior. More recent fMRI studies demonstrate a recovery in amplitude and volume of visual cortex responses to light stimuli after gene-replacement therapy in the Briard dog (Aguirre *et al.,* 2007).

The thorough experimentation conducted to develop RPE65 LCA gene therapy strategies has expedited the implementation of phase I clinical trials in humans. To date, three LCA trials in RPE65 loss of function patients are in progress (Bainbridge *et al*., 2008; Cideciyan *et al*., 2008; Hauswirth *et al*., 2008; Maguire *et al*., 2008). Differences in promoter used and patient genotype distinguish the trials. Overall, a recovery of visual behavior and acuity, fixation, and pupillometry was seen in treated patients with minimal adverse affects. These proof-of principle gene therapy trials have now paved the way for future ocular therapies that will ideally target a greater number of patients with a wider range of genotypes, and with optimized methodology.

Trophic Factor Therapy

A major limitation of gene replacement therapy is that the treatment can only be applied to individuals with a common genotype. One way to simultaneously target multiple genetic manifestations of retinal disease is to introduce a neurotrophic factor to slow photoreceptor degeneration. LaVail and colleagues explored the effects of different survival factors (bFGF, BDNF, and CNTF) in animal models of retinal degeneration (LaVail *et al.,* 1998; LaVail *et al.,* 1992). These experiments showed that certain factors slow photoreceptor death, depending on the model and species. This work has been followed by the optimization of trophic factor delivery and careful assessment of functional and morphological rescue in animal models of retinal disease by specific survival proteins, namely CNTF, bFGF, and GDNF (Dinculescu *et al.,* 2005; Frasson *et al.,* 1999; Green *et al.,* 2001; Lau *et al.,* 2000; Liang *et al.,* 2001; McGee-Sanftner *et al.,* 2001; Wu *et al.,* 2002). More recent studies have shown that an appropriate balance of neurotrophic factors in the retina, primarily acting through Müller glia, is necessary to achieve photoreceptor protection (Harada *et al.,* 2000; Zack, 2000).

Glial derived neurotrophic factor (GDNF) is a member of the transforming growth factor β (TGF-β) super family and binds the GFRα and RET receptors that are localized to retinal Müller cells (Reviewed in Airaksinen and Saarna, 2001; Hauck *et al.,* 2006). GDNF has been shown to protect dopamine neurons from degeneration in an animal model of Parkinsons and plays a crucial role in organ and neural development (Baloh *et al.,* 2000; Costantini and Shakya, 2006; Kordower *et al.,* 2000). Previous studies have shown that hGDNF has anti-apoptotic and pro-survival effects on retinal neurons during disease (Andrieu-Soler *et al.,* 2005; Frasson *et al.,* 1999; McGee-

Sanftner *et al.,* 2001; Wu *et al.,* 2002). More specifically, viral delivery of hGDNF to the photoreceptors has been shown to slow the disease progression of the S334-ter rat model of autosomal dominant retinitis pigmentosa, as demonstrated by functional (ERG) and histological rescue (McGee-Sanftner *et al.,* 2001). As GDNF has shown great potential as a therapeutic factor for retinal disease, we set out to optimize GDNF's protective effects during retinal degeneration by targeting gene delivery to the support cells of the retina, Müller glia (Bringmann *et al.,* 2006; Bringmann and Reichenbach, 2001; Newman and Reichenbach, 1996).

Restoring Visual Sensitivity in Late Stages of Disease

One major goal of this dissertation is to develop therapies that can be applied to multiple genotypes and disease stages. The use of trophic factors is one discussed method of targeting multiple genetic manifestations of retinitis pigmentosa. However, currently there are few options to restore photosensitivity in patients who have undergone disease progression to the point where few or no photoreceptors remain. Three particularly promising methods of restoring visual sensitivity in late stages of retinal degeneration are receiving substantial attention today: electrical stimulation via implanted microelectrodes, stem cell therapy to reintroduce photoreceptors, and optogenetic tools to confer light sensitivity on residual neurons.

"Chip" based retinal prosthetics restore light sensitivity to the retina through electrical activation of residual neurons by an implanted microelectrode array (Weiland *et al.,* 2005). The electrode chip can be placed either at the inner limiting membrane or into the subretinal space. The chip requires receptors for externally processed and

wirelessly transmitted visual information (ILM approach) or a built in array of solar cells to act as sensors of light (subretinal approach). The electrodes interface with retinal neurons, namely retinal ganglion cells or bipolar cells, respectively (Reviewed in Weiland *et al.,* 2005). The subretinal method is limited by the small area for implantation in the space between the RPE and retinal tissue but has its advantages as the stimulation of bipolar cells allows for signal amplification and the restoration of retinal processing between bipolar and ganglion cells. The epiretinal implant does not benefit from retinal amplification or natural information processing, but implantation is more straightforward and there is a larger space for the introduction of more activation channels. One of the main limitations of any implanted prosthetic is the low resolution of stimulation. Current technology affords the chip approximately 100 stimulatory channels, while retinal ganglion cells normally receive millions of inputs from second order neurons (Humayun *et al.,* 1999; Weiland *et al.,* 2005). Increasing the number of channels is limited by the size of the chip that can be successfully implanted. Furthermore, when the retina has been severely damaged during degeneration, the efficacy of stimulation is reduced (Reviewed in Weiland *et al.,* 2005).

Stem cell therapy is a method of restoring a population of neurons by introducing pluripotent cells into an environment with the necessary cues to initiate appropriate differentiation and synaptic development (Baker and Brown, 2009). Injection of photoreceptor precursor cells isolated from an embryonic retina into an animal model of retinal degeneration has been shown to reverse photoreceptor loss (MacLaren *et al.,* 2006). Newly formed photoreceptor cells were able to make synaptic contacts with bipolar cells and light-evoked extracellular field potentials in the retinal ganglion cell

layer and pupillary reflexes were restored. Though this study is very promising, there are many issues that remain surrounding stem cell therapy for retinal degenerative diseases. Namely, ethical concerns have been raised as many researchers are relying on isolating cells from the fetus during embryonic development (MacLaren *et al.,* 2006; Yu and Silva, 2008). Finally, it is still necessary to identify optimal retinal conditions and the best stem cells for appropriate differentiation and synaptic development.

Another method of treating late stage retinal disease is to confer light sensitivity on surviving neurons by gene transfer of photosensitive proteins. There has been a recent burst of research to optimize naturally occurring light sensitive proteins and engineer existing proteins to respond to light for this purpose (Reviewed in Zhang *et al.,* 2006). Channelrhodopsin 2 (ChR2), a seven transmembrane microbial-type rhodopsin that is non-selectively permeable to cations, is capable of driving temporally and spatially precise neuronal activity upon illumination (Boyden *et al.,* 2005). ChR2 has been employed to re-establish light sensitivity in the retina after severe retinal degeneration (Bi *et al.,* 2006; Lagali *et al.,* 2008). This method of introduced light sensitivity in the retina is capable of driving electrophysiological responses in the visual cortex and visually driven behavior (Lagali *et al.,* 2008). The limitations of ChR2 include low conductance and fast inactivation, though many researchers are attempting to optimize the properties of the channel (Lin *et al.,* 2009).

To improve upon the properties of naturally occurring light sensitive proteins, researchers are engineering endogenous receptors and channels to respond to light (Chambers and Kramer, 2009). More specifically, the synthetic photoisomerizable, azobenzene regulated K+ channel (SPARK) and light activated glutamate receptor

(LiGluR) were recently developed (Banghart *et al.,* 2004; Chambers and Kramer, 2009; Volgraf *et al*., 2006). Azobenzene is a compound that changes confirmation upon illumination with specific wavelengths of light. When azobenzene is attached to specific receptors and receptor agonists or antagonists, this combination is termed a photoswitch. SPARK channel activity is controlled by a photoswitch attachment that contains a K+ channel blocker. Illumination of SPARK can drive potassium currents across the membrane in oocytes and turn on and off spiking in cultured hippocampal neurons and ganglion cells of flat-mount, *in vitro,* retina preparation (Banghart *et al.,* 2004; Borges & Greenberg unpublished data). The light activated glutamate receptor (LiGluR) also employs a "photoswitch" attachment that contains a glutamate analogue to induce light mediated glutamate receptor activity (Volgraf *et al*., 2006). LiGluR is capable of reversibly driving neuronal activity at high temporal (millisecond scale) and spatial (less than a micron) resolution, characteristics that make it an attractive tool for re-storing visual sensitivity in the degenerated retina (Szobota *et al.,* 2007).

Gene Delivery to the Retina

For any gene therapy approach, the greatest challenge is achieving targeted delivery and stable expression of therapeutic cDNA. Today, viral vectors are the method of choice for gene delivery. Over the past ten years, lentivirus and adeno-associated virus (AAV) have received the most attention for their promise as vehicles for ocular gene therapy.

Lentivirus is a retrovirus that stably and efficiently infects non-dividing cells (Naldini *et al.,* 1996). Lentivirus possesses an RNA genome that is converted to DNA in

infected cells (Verma *et al.,* 2000). The most common lentiviral vector is derived from HIV (human immunodeficiency virus). To create a lentiviral vector for gene therapy, the viral genes (*gag, pol, cap,* and six other accessory genes) are replaced by the therapeutic transgene. The therapeutic transgene is flanked by LTRs (long terminal repeats) that are required for the integration of the transgene into the host genome and placed downstream of the packaging signal sequence (φ) (Naldini *et al.,* 1996). One benefit of lentivirus is the transgene packaging capacity is roughly 8-10 kilobases, which is substantially larger then AAV (Sinn *et al.,* 2005). Furthermore, pseudotyping lentivirus with specific envelope proteins in combination with cell type specific promoters allows for efficient transduction of RPE, photoreceptors, and more recently, retinal Müller cells (Miyoshi *et al.,* 1997; Greenberg *et al.,* 2007). One potential drawback of lentiviral vectors is that in order to successfully function as a gene delivery vector, the transgene must integrate into chromosomal DNA, which could result in insertional mutagenisis (Naldini *et al.,* 1996). Recently, a non-integrating lentiviral vector was developed that could be used to avoid this risk (Philpott and Thrasher, 2007; Yáñez-Muñoz *et al.,* 2006).

AAV is a nonpathogenic parvovirus composed of a 4.7 kb linear single-stranded DNA genome enclosed within a 25 nm icosahedral capsid (Alexander and Hauswirth, 2008; Buning *et al.,* 2008). For gene therapy purposes, genes encoding for replication and capsid proteins from the wild type AAV genome are replaced by a promoter and therapeutic transgene cassette flanked by the normal AAV inverted terminal repeats that are required for packaging and replication (Goncalves, 2005). Twelve distinct AAV serotypes (AAV1-12) and over one hundred AAV variants have currently been identified

(Gao *et al.,* 2004; Wu *et al.,* 2006).

AAV is currently the most successful vector for ocular gene therapy, as different serotypes are capable of stably transducing a variety of retinal cell types with minimal immunogenicity (Auricchio, 2003; Buning *et al*., 2008; Buch *et al*., 2008; Surace and Auricchio, 2003). AAV serotypes are distinguished by the amino acid sequence of the viral capsid that controls initial receptor attachment, cellular entry, and trafficking. AAV serotypes 1, 2, 5, 8, and 9 are extremely efficient at transducing RPE and photoreceptors following subretinal delivery. AAV2 transduces retinal ganglion cells when introduced from the vitreous (Auricchio, 2003; Buch *et al*., 2008; Harvey *et al*., 2002; Lebherz *et al*., 2008; Martin *et al*., 2002; Rolling, 2004). However, AAV is limited by the small packaging capacity (4.7kb) (Buning *et al.,* 2008). Furthermore, like lentivirus, the subretinal injection is currently required to transduce RPE and photoreceptors. Therefore, to enhance the efficacy of any ocular gene therapy approach, methods to reduce barriers to intravitreal viral vector delivery to the outer retina will be necessary.

Summary

Ocular gene therapies will benefit from the enhancement of viral vector gene transfer efficacy and the development of treatments that can be applied across genotypes and stages of retinal disease. To this end, this dissertation describes methods of both artificially and naturally reducing barriers to gene delivery to the outer retina from the vitreous. We have also achieved sustained secretion of a trophic factor from the natural support cell of the retina, Müller glia, to slow the rate of vision loss in an animal model of retinitis pigmentosa. This therapeutic approach could be applied to multiple disease

genotypes. Finally, we have re-introduced light sensitivity to remaining retinal neurons in the very late stages of retinal degeneration with an engineered photosensitive protein. This technique not only recovers retinal photosensitivity, but also restores cortical responses to visual stimuli. We are confident that the data presented in this dissertation will contribute to making future gene therapies safer, more efficacious, and applicable to a wider spectrum of patients.

Chapter 2

The Breakdown of Barriers to Vitreal Delivery of Adeno-Associated Virus to the Outer Retina and RPE

Chapter 2a

Inner Limiting Membrane Barriers to AAV Mediated Retinal Transduction from the Vitreous

Preface: This work was done in collaboration with Dr. Deniz Dalkara, a postdoctoral fellow in the Flannery and Schaffer Labs at UC Berkeley. Natalie Hoffman and Meike Visel provided technical assistance. Natalia Caporale, a post-doctoral fellow in Dr. Yang Dan's lab at UC Berkeley, conducted the cortical experiment. Jessie Lee provided valuable technical assistance for TEM experiments.

This chapter has been accepted and is in press in the journal, *Molecular Therapy*: D. Dalkara, K.D. Kolstad, N. Caporale, M. Visel, R.R. Klimczak, D.V. Schaffer, J.G. Flannery (2009).

Abstract

Adeno-associated viral gene therapy has shown great promise in treating retinal disorders, with three clinical trials in progress. Numerous AAV serotypes can infect various cells of the retina when administered subretinally, but the retinal detachment accompanying this injection induces changes that negatively impact the microenvironment and survival of retinal neurons. Intravitreal administration could circumvent this problem, but only AAV2 can infect retinal cells from the vitreous, and transduction is limited to the inner retina. We therefore sought to investigate and reduce barriers to transduction from the vitreous. We fluorescently labeled several AAV serotype capsids and followed their retinal distribution after intravitreal injection. AAV2, 8, and 9 accumulate at the vitreoretinal junction. AAV1 and 5 show no accumulation, indicating a lack of appropriate receptors at the inner limiting membrane (ILM). Importantly, mild digestion of the ILM with a non-specific protease enabled substantially enhanced transduction of multiple retinal cell types from the vitreous, with AAV5 mediating particularly remarkable expression in all retinal layers. This protease treatment has no effect on retinal function as shown by electroretinogram and visual cortex cell population responses. These findings may help avoid limitations, risks, and damage associated with subretinal injections currently necessary for clinical gene therapy.

Introduction

Adeno-associated virus (AAV) has become the most promising ocular gene delivery vehicle over the past ten years (Hauswirth *et al.,* 2008; Lebherz *et al.,* 2008; Mueller and Flotte, 2008). Its low immunogenicity, ability to infect the majority of retinal cells, and long term transgene expression following a single treatment make the virus a very efficient gene delivery vector (Buning *et al.,* 2008). AAV is a nonpathogenic virus composed of a 4.7 kb single-stranded DNA genome enclosed within a 25 nm capsid (Goncalves *et al.,* 2005). In recombinant vectors, genes encoding replication (*rep*) and capsid (*cap*) proteins from the wild type AAV genome are replaced by a promoter and therapeutic transgene cassette flanked by the AAV inverted terminal repeats that are required for packaging and replication. To date, hundreds of AAV variants have been identified (Gao *et al.,* 2004; Wu *et al.,* 2006a), and their tissue tropism and transduction efficiency are controlled by the capsid, which mediates initial receptor attachment, cellular entry, and trafficking mechanisms and thereby determines selectivity for particular cells or tissues. In particular, receptor binding specificity is a key determinant of viral tropism. Specific glycan motifs have been identified as primary receptors for some AAV serotypes, and AAV2 uses heparan sulfate for cell recognition and entry whereas AAV1 and AAV5 bind to glycans with a terminal sialic acid (Wu *et al.,* 2006b). In addition, AAV2, 8, and 9 bind to the 32k laminin receptor (Akache *et al.,* 2006), likely as their secondary receptor.

AAV is particularly promising for gene therapy in the retina (Hauswirth *et al.,* 2008; Lebherz *et al.,* 2008; Mueller and Flotte, 2008), where mutations in genes

expressed in photoreceptors and retinal pigment epithelia (RPE) comprise the great majority of defects underlying inherited blindness. Since AAV is unable to reach these cells via intravitreal administration, the subretinal route of delivery is necessary. However, subretinal administration of AAV requires the surgeon to perform a vitrectomy, i.e. create a needle hole through the retina (retinotomy) and detach the photoreceptors from the RPE with the injection of fluid. This retinal detachment causes series of macromolecular and structural modifications that are damaging to visual processing (Fisher *et al.,* 2005). Also, in most retinal diseases, the degeneration is not uniform across the retina (Jacobson *et al.,* 2008a; Jacobson *et al.,* 2008b; Jacobson *et al.,* 2005), making identification of where to introduce the subretinal 'bleb' difficult. Furthermore, the degenerating retina is often extremely fragile and poses a high risk of creating a retinal tear or macular hole (Maguire *et al.,* 2008). Thus, in clinical settings it would be advantageous to introduce AAV vectors capable of outer retinal transduction from the vitreous.

It has been shown that after intravitreal injection, the AAV transduction profile of retinal cells differs significantly between neonatal and adult rats (Harvey *et al.,* 2002). Injection of AAV2 at P0 results in photoreceptor, amacrine, and bipolar cell transduction, whereas the vast majority of transduced cells in adults are RGCs (Harvey *et al.,* 2002). The inner limiting membrane (ILM) – a basement membrane that contains 10 distinct extracellular matrix proteins (Candiello *et al.,* 2007) and histologically defines the border between the retina and the vitreous humor (Halfter *et al.,* 2008)– may pose a barrier for penetration of AAV into the retina from the vitreous in adults, whereas a less differentiated ILM or increased extracellular space may results in fewer barriers in

the developing retina. Importantly, the ILM is essential for normal eye development (Halfter, 1998; Semina *et al.,* 2006); however, it is dispensable in adults, and its removal is considered beneficial for patients undergoing macular hole surgery (Mester and Kuhn, 2000).

We have investigated the localization and retinal transgene expression profile of five relevant AAV serotypes following intravitreal administration. In addition, we identified the ILM as a barrier to AAV-mediated retinal transduction by digesting it with Pronase E, a group of proteolytic enzymes from *Streptomyces griseus* previously shown to digest monkey ILM (Heegaard *et al.,* 1986). Specifically, co-administration of Pronase and AAV into the vitreous resulted in high efficiency transduction of several retinal cell types, including photoreceptors and RPE. We anticipate this finding may greatly enhance AAV-mediated retinal gene therapy with intravitreal administration.

Experimental Methods

Generation of rAAV vectors:

AAV vectors containing sm.CBA promoter (which has the shortened hybrid chicken ß–actin/rabbit ß–globin intron) followed by hGFP were produced by plasmid co-transfection into 293 cells (Grieger *et al.,* 2006). The resulting clarified cell lysate was subjected to iodixanol density gradient purification, and the interface between the 54% and 40% iodixanol fraction, along with the lower three-quarters of the 40% iodixanol fraction, were extracted after ultracentrifugation and diluted with an equal volume of PBS with 0.001% Tween20. An Amicon Ultra-15 Centrifugal Filter Unit was pre-incubated with 5% Tween in PBS for 20 minutes, then washed once with PBS+0.001% Tween. The diluted iodixanol fractions were loaded onto the centrifugal buffer exchange unit and spun until 250 µl of concentrated vector remained. Fifteen milliliters of sterile PBS+0.001% Tween was added, and the concentration step was repeated three times with fresh sterile PBS+ 0.001% Tween. A final viral concentrate of about 200 µl, devoid of iodixanol, was ultimately obtained. The vector was then titered for DNase-resistant vector genomes by quantative PCR using diluted plasmid DNA as a standard. Finally, the purity of the vector was validated by silver-stained SDS-PAGE gel electrophoresis.

Cy3 labeling of rAAV vectors:

Purified and concentrated rAAV was labeled as previously described (Bartlett *et al.,* 2000). Briefly, amine reactive Cy3 dye (GE Healthcare) was resuspended in a 0.2 M

$NaCO_3/NaHCO_3$ buffer at pH 9.3. Viral stock was mixed 1:1 with the dye suspension to a total volume of 400 µl. The reaction was allowed to take place for two hours at room temperature and quenched by the addition of 4 µl 1 M TrisHCl at pH 8.0. Buffer exchange and concentration was then conducted using Amicon Ultra-5 Centrifugal Filter Units (Millipore).

Intraocular administration routes:

Adult wild type Sprague Dawley rats were used for all studies, and animal procedures were conducted according to the ARVO Statement for the Use of Animals and NIH guidelines for the use of laboratory animals, as approved by the Office of Laboratory Animal Care at University of California Berkeley. Before vector administration, rats were anesthetized with ketamine (72 mg/kg) and xylazine (64 mg/kg) by intraperitoneal injection. An ultrafine 30 1/2-gauge disposable needle was passed through the sclera, at the equator and next to the limbus, into the vitreous cavity. Injections were made with direct observation of the needle in the center of the vitreous cavity. The total volume delivered was 5 µl, containing 2-5x10^{12} vg/ml of AAV-Cy3. In addition, where indicated, 5x10^{12} vg/ml of AAV encoding eGFP driven by the ubiquitous chicken b-actin (CBA) promoter was mixed at a ratio of 4:1 with 0.001% Pronase E and injected.

Fundus photography:

In vivo retinal imaging was performed two to four weeks after injections with a fundus camera (RetCam II; Clarity Medical Systems Inc., Pleasanton, CA) equipped

with a wide angle 130° retinopathy of prematurity (ROP) lens to monitor eGFP expression in live, anesthetized rats. Pupils were dilated before imaging with tropicamide (1%).

Electroretinography:

Sprague Dawley rats (n=6) were injected with 5 µl of AAV5 encoding eGFP mixed at a ratio of 4:1 with 0.001% Pronase E in the vitreous of one eye and five microliters of PBS in the contralateral eye, n=8. This was repeated with the middle-dose (0.001%, final concentration, n=6) and high-dose (0.002%, final concentration, n=8) Pronase E concentrations. One-week post-injection, animals were dark-adapted for four hours and anesthetized, and their pupils were then dilated. Animals were placed on a heating pad, and contact lenses were positioned on the cornea. Reference electrodes were inserted subcutaneously in the cheeks, and a ground electrode was inserted in the tail. Electroretinograms were recorded (Espion ERG system; Diagnosys LLC, Littleton, MA) in response to seven light flash intensities from 0.0001-3.16 (cd-s)/m^2 presented in series of three. Light flash intensity and timing were elicited from a computer-controlled Ganzfeld flash unit. Data were analyzed with MatLab (v7.7; Mathworks, Natick, MA). After correction for oscillatory potentials, scotopic a-wave values were measured from the baseline to the minimum ERG peak while scotopic b-waves were measured from the minimum to maximum ERG peaks. Statistical differences between Pronase E and PBS injected eyes were calculated using paired Student t-test.

Cryosections:

Two to four weeks after vector injection, rats were humanely euthanized, the eyes were enucleated, a hole was made in the cornea, and tissue was fixed with 10% neutral buffered formalin for 2-3 hours. The cornea and lens were removed. The eyecups were washed in PBS followed by 30% sucrose in PBS overnight. Eyes were then embedded in optimal cutting temperature embedding compound (OCT; Miles Diagnostics, Elkhart, IN) and oriented for 5-10 μm thick transverse retinal sections.

Immunolabeling and histological analysis:

Tissue sections were rehydrated in PBS for 5 minutes followed by incubation in a blocking solution of 1% BSA, 0.5%Triton X-100, and 2% normal donkey serum in PBS for 2-3 hours. Slides were incubated overnight at 4ºC with commercial mouse monoclonal antibodies against intact capsids of AAV1, 2, or 5 (ARP American Research Products, Inc., Belmont, MA) at 1:100, rabbit monoclonal antibody raised against the green fluorescent protein (Invitrogen, Carlsbad, CA) at 1:400, or in anti-laminin antibody (Sigma, L9393) at 1:100 in blocking solution. The sections were then incubated with Alexa488-conjugated secondary anti-rabbit antibody (Molecular Probes) at 1:1000 in blocking solution for 2 hours at room temperature. The results were analyzed by fluorescence microscopy using an Axiophot microscope (Zeiss, Thornwood, NY) equipped with X-cite PC200 light source and QCapturePro camera, or by confocal microscopy (LSM5; Carl Zeiss Microimaging).

Visually Evoked Potentials:

All experiments were approved by the Animal Care and Use Committee at the

University of California, Berkeley**.** A week prior to recordings, Sprague Dawley rats were injected $5x10^{13}$ vg/ml of AAV5 mixed at a ratio of 4:1 with 0.001% Pronase E (n=6) or $5x10^{13}$ vg/ml of AAV5 mixed at a ratio of 4:1 with 0.01% Pronase E (n=6) and injected in the vitreous of one eye and 5µl of PBS in the contralateral eye. One week post-injection, animals were anesthetized using ketamine (72mg/kg i.p.) and xylazine (64mg/kg i.p) and pupils dilated. Animals were restrained in a stereotaxic apparatus (David Kopf Instruments, Tujunga, CA) and body temperature was maintained at 36°-37°C via a heating blanket (Harvard Apparatus, Holliston, MA). Anesthesia was supplemented with 0.5-1% isofluorane as needed during the recordings. A small craniotomy and durotomy (~$1mm^2$) were performed over the primary visual cortex (2-3mm lateral to the midline, 1mm anterior to lambda). A glass micropipette (resistance ~0.5-3MΩ) containing saline solution was lowered to 0.5-0.6 mm below the surface of the cortex and contralateral to the side of the stimulated eye. Visual stimulation consisted of 10 ms pulses of light (white LED, 1cm from eye) presented at 0.2Hz for 40-50 repeats. Sweeps were filtered at 2 kHz, sampled at 10 kHz by a 12 bit digital acquisition board (National Instruments, Austin, TX), and analyzed with custom software running in Matlab (The Mathworks, Natick, MA).

Transmission Electron Microscopy:

A generic processing protocol was used to prepare samples for TEM. Briefly, gluteraldehyde- fixed, osmocated retinas were treated with uranyl acetate at 4ºC overnight. Samples were then dehydrated with 35 to 100% water /acetone steps on ice. After Epon Araldite resin infiltration, samples were left in a polymerization oven for 2

days. 70 to 100 nm thick sections were cut from Epon Araldite resin-embedded samples with a Reichert-Jung Ultra E microtome (Leica, Heerbrugg, Switzerland). They were collected on 0.6% Formvar-coated slot grids and post- stained in 2% aqueous uranyl acetate and Reynold's lead citrate. Sections were imaged on a FEI Tecnai 12 TEM (FEI, Eindhoven, The Netherlands) with an Ultrascan 1000 CCD camera (Gatan, Pleasanton, CA).

Results

Labeling and characterization of AAV Serotypes 1, 2, 5, 8, and 9:

To assess the localization of viral particles in the retina after intravitreal injection, we labeled each AAV serotype by covalently linking a Cy3 amine-reactive dye to lysine residues exposed on the viral capsid surface (Bartlett *et al.,* 2000). Labeled virus was incubated with 293T cells to visualize particle localization before proceeding with in vivo studies (Figure 2a.1). To confirm that fluorescent signal observed at the cell surface and in endosomal/lysosomal compartments was associated with intact viral particles, we employed immunocytochemistry. Antibodies against AAV1, 2, and 5 colocalized with the Cy3 dye (Figure 2a.1), confirming Cy3 labeling is an appropriate means of monitoring viral dispersion in and among cells.

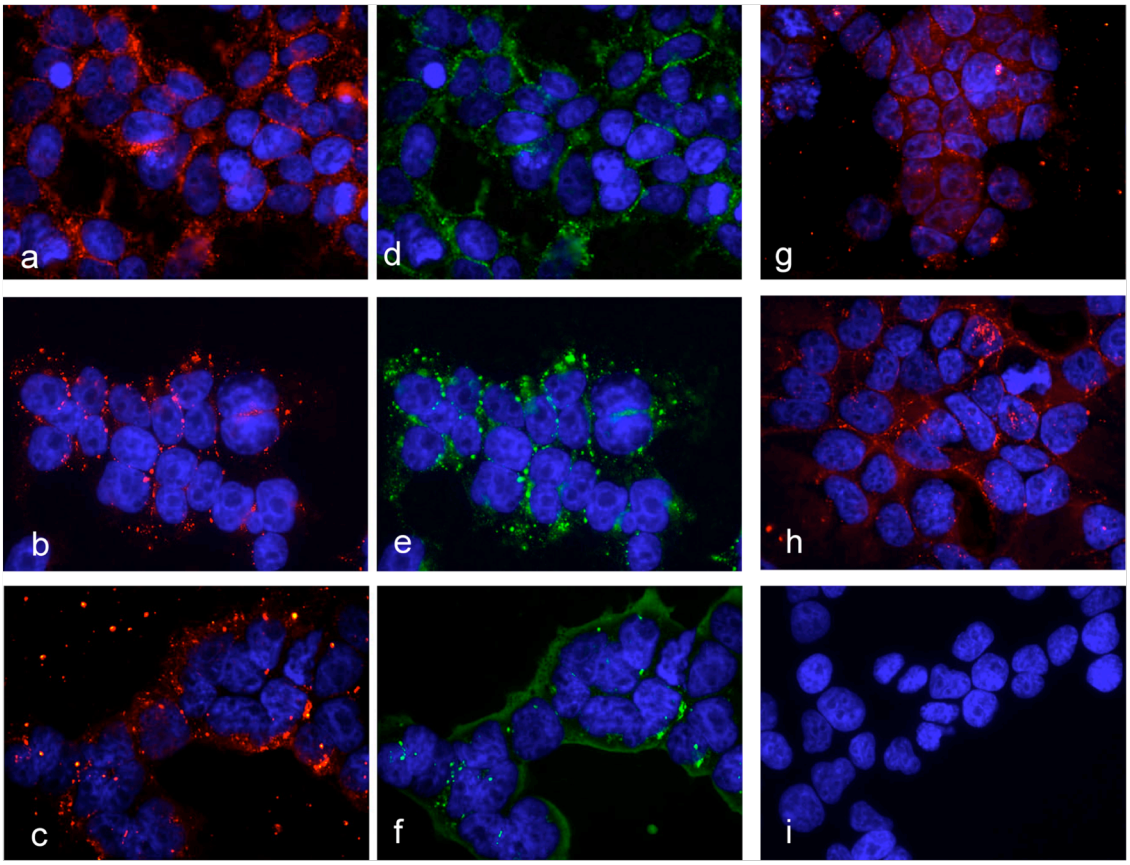

Figure 2a.1. Cy3-labeled AAV particles at a MOI of 10^4 were observed at the cell surface and in the endosomal/lysosomal compartments after a 20 min incubation with cells at 37ºC: a) AAV1-Cy3 b) AAV2-Cy3 c) AAV5-Cy3. In parallel, the Cy3-labeled viral particles were immunostained with antibodies directed against conformational epitopes of intact AAV capsids: d) AAV1-Cy3 with anti-AAV1 (green), e) AAV2-Cy3 with anti-AAV2 (green) f) AAV5-Cy3 with anti-AAV5 (green), g) AAV8-Cy3, h) AAV9-Cy3, and i) an equivalent quantity of unconjugated Cy3 dye.

Retinal penetration of Cy3-labeled viral particles following intravitreal injection:

Localization of the different AAV serotypes after intravitreal injection was assessed by visualization of direct fluorescence resulting from the labeled capsids (Figure 2a.2 b,e,h,k,m), and by immunostaining the same cryosections with anti-AAV capsid antibodies when available (Figure 2a.2 c,f,i). The cryosections of retinas treated with AAV1-Cy3 did not exhibit any significant fluorescence (Figure 2a.2 b,c). AAV5-Cy3 showed only very localized signal in displaced ganglion cells. To confirm that these results were not due to the difficulty of visualizing the Cy3 capsid label over tissue autofluorescence, AAV5-Cy3 was injected subretinally, and robust fluorescence was observed in the RPE and photoreceptors at the region of injection (Figure 2a.3). Cy3-AAV2 and 9 injected retinas showed viral accumulation at the vitreoretinal junction (Figure 2a.2 e.m), as shown by punctate fluorescence on the ILM, at the RGCs, on the nerve fibers associated with RGCs, and at the Müller cell endfeet. AAV8 could also be detected at the vitreoretinal junction, though to a lesser extent (Figure 2a.2 k).

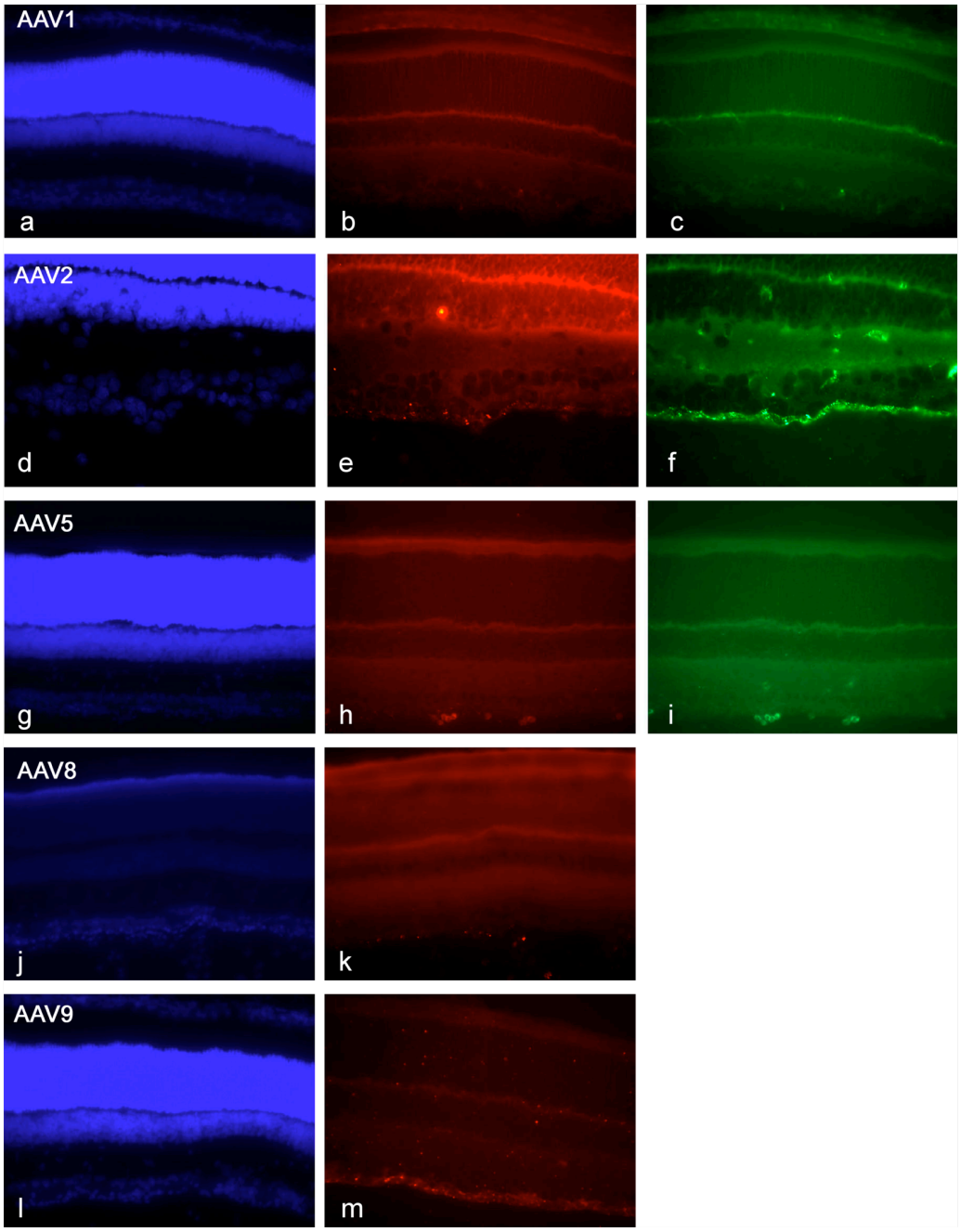

Figure 2a.2. Localization of Cy3-labeled AAV particles in the retina of p30 rats. DAPI fluorescence (left panel), Cy3 fluorescence corresponding to the viral particles (middle panel), and green immunofluorescence (right panel) from anti-AAV intact capsid antibodies against AAV1, AAV2 and AAV5 capsids (c, f, and i).

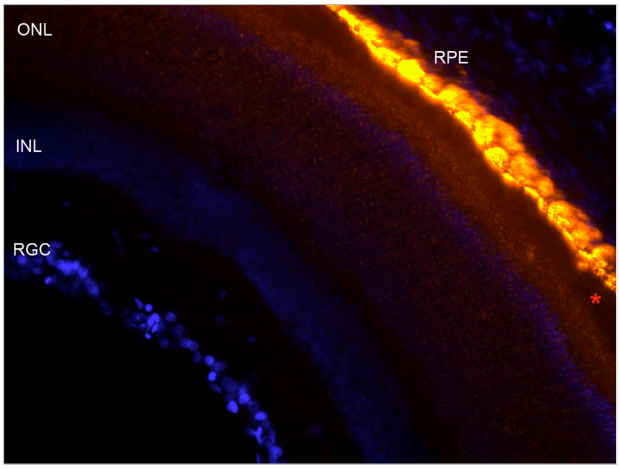

Figure 2a.3. Retinal cryosection showing spreading of Cy3-labeled AAV5 particles following subretinal injection. * indicates the site of subretinal injection.

Although AAV2 and 9 showed strikingly similar localization patterns, only AAV2 resulted in GFP expression in the retina one month after intravitreal injection (Figure 2a.4), consistent with prior reports with AAV2.

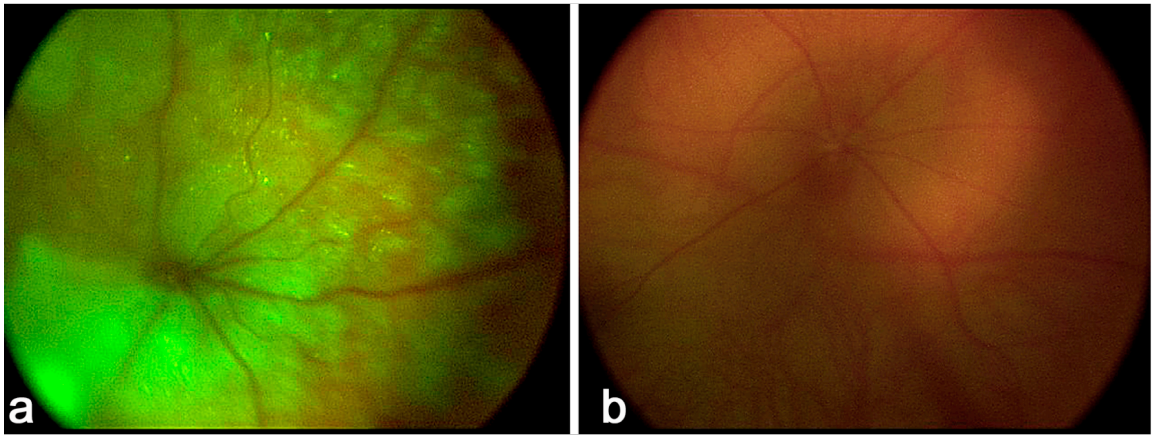

Figure 2a.4. Representative fundus image of eyes injected with a) AAV2.smCBA.hGFP and b) AAV9.smCBA.hGFP.

Mild digestion of the ILM with Pronase E, a non-specific protease:

The localization of AAV2 and AAV9 at the vitreoretinal junction, where the ILM separates the vitreous from the retina, suggests that this anatomical feature may play a major role in initial viral attachment and subsequent penetration into the retina. It had been shown by Hegaard et al. that various enzymes can be used to disrupt the macaque monkey ILM (Heegaard *et al.,* 1986). After testing multiple glycosaminoglycases and proteases, the non-specific protease, Pronase E, was shown to be the most successful agent in digesting the ILM. Pronase is a mixture of at least 10 proteases, including serine-type proteases, zinc endopeptidases, zinc leucine aminopeptidases, and a zinc carboxypeptidase (Jurasek *et al.,* 1971). We hypothesized that using Pronase E would disrupt the ILM, thereby enabling vector access to receptor binding sites and potentially cells that were previously unavailable to viral serotypes such as AAV1 and AAV5.

AAV is resistant to digestion by enzymes such as trypsin (McCarty, 2008), but we first confirmed that the AAV serotypes we used are also resistant to pronase by performing *in vitro* tests. AAV was incubated with 0.01% and 0.05% Pronase E at 37ºC overnight, and DNase resistant viral genomes were then quantified by qPCR. We found that Pronase treatment did not degrade the viral capsid at the concentrations relevant for intraocular use (data not shown). Therefore, enzyme was mixed with AAV prior to all intravitreal injections to prevent the need for multiple injections into the same eye. As a control, virus was injected into the contralateral eye without the enzyme. Various doses of pronase were used to permeablize the ILM (0.01, 0.005, 0.001 and 0.0002% total). Dosages above 0.0002% are deleterious to the retina, as shown by a reduction in ERG

A-wave and B-wave amplitudes (Figure 2a.5). In addition, at high doses, the disruptive effect of the enzyme on the ILM could be readily visualized by anti-laminin inmmunohistochemistry on cryosections of treated retinas (Figure 2a.6).

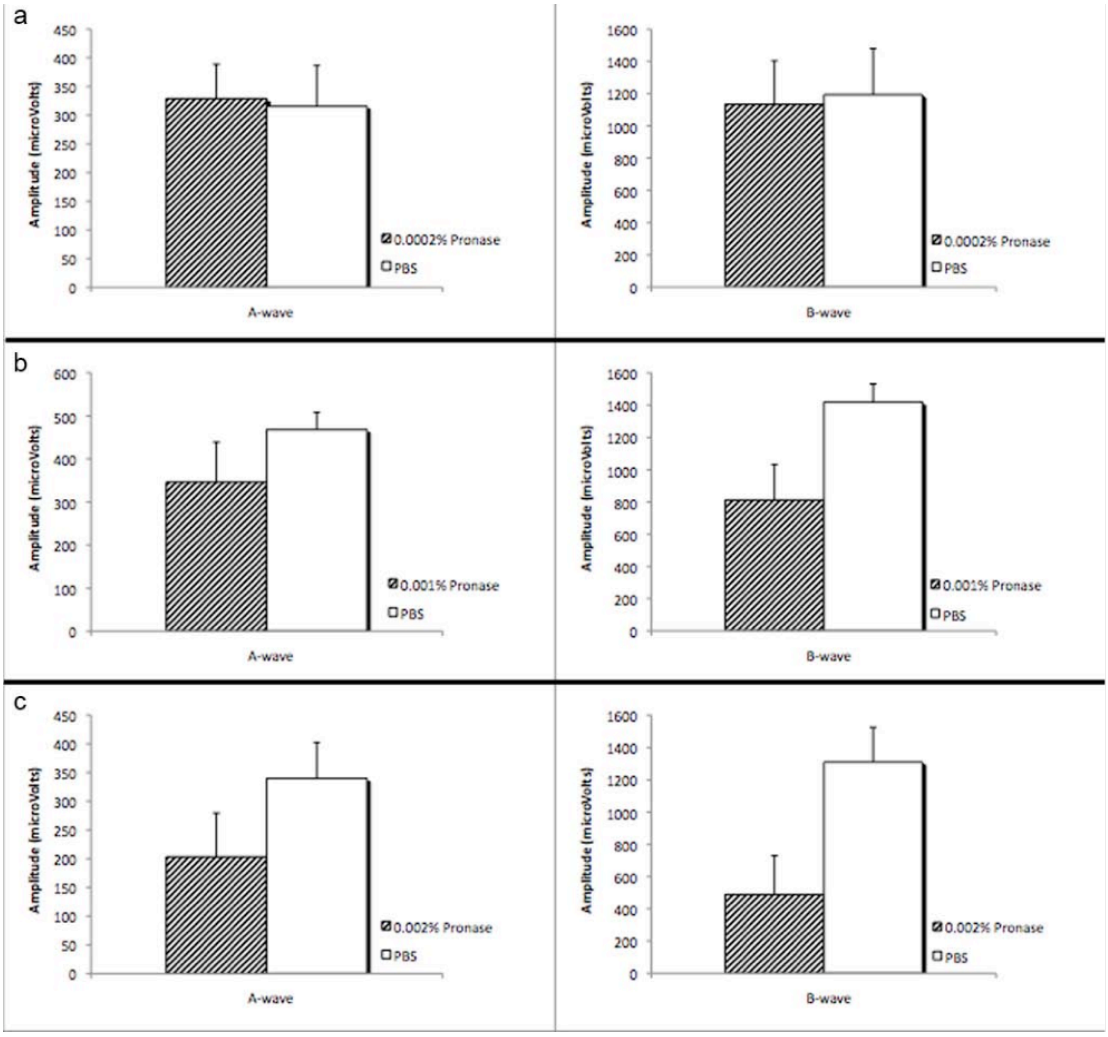

Figure 2a.5. The electroretinogram of animals injected with 0.0002% (n=8), 0.001% (n=6) and 0.002% (n=8) Pronase E was analyzed to assess toxicity of mild enzymatic cleavage of the ILM. Each animal was injected with the enzyme in the vitreous of one eye and PBS in the contralateral eye. Pronase E injection exhibited no significant change

in a- or b-wave amplitude compared to control PBS injected eyes. Statistical differences between PronaseE and PBS injected eyes were calculated by Student's t-test.

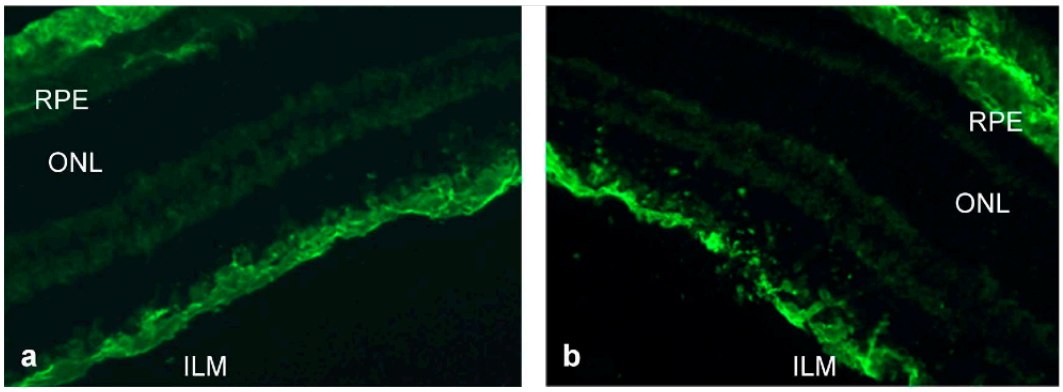

Figure 2a.6. Disruptive effect of Pronase E on the ILM a) Untreated retina stained with anti-laminin antibody show immunoreactivity at the ILM and at the choroid, whereas b) laminin immunolabeling after treatment with 0.01% Pronase E exhibits a disintegrated ILM structure.

As Pronase E is a non-selective protease, once it had disrupted the ILM, it likely perturbed the underlying nerve fiber layer and RGCs, which are essential components for vision. In contrast, at lower doses (0.001% and below) the effect of the enzyme on laminin immunohistochemistry was not pronounced. Interestingly, we have observed some changes in the pronase-treated ILM using TEM (Figure 2a.7), where retinas treated with pronase showed a reduction in loose collagen fibrils and the appearance of dark aggregates along the ILM, which we hypothesize to be degraded proteins that have aggregated after enzymatic digestion.

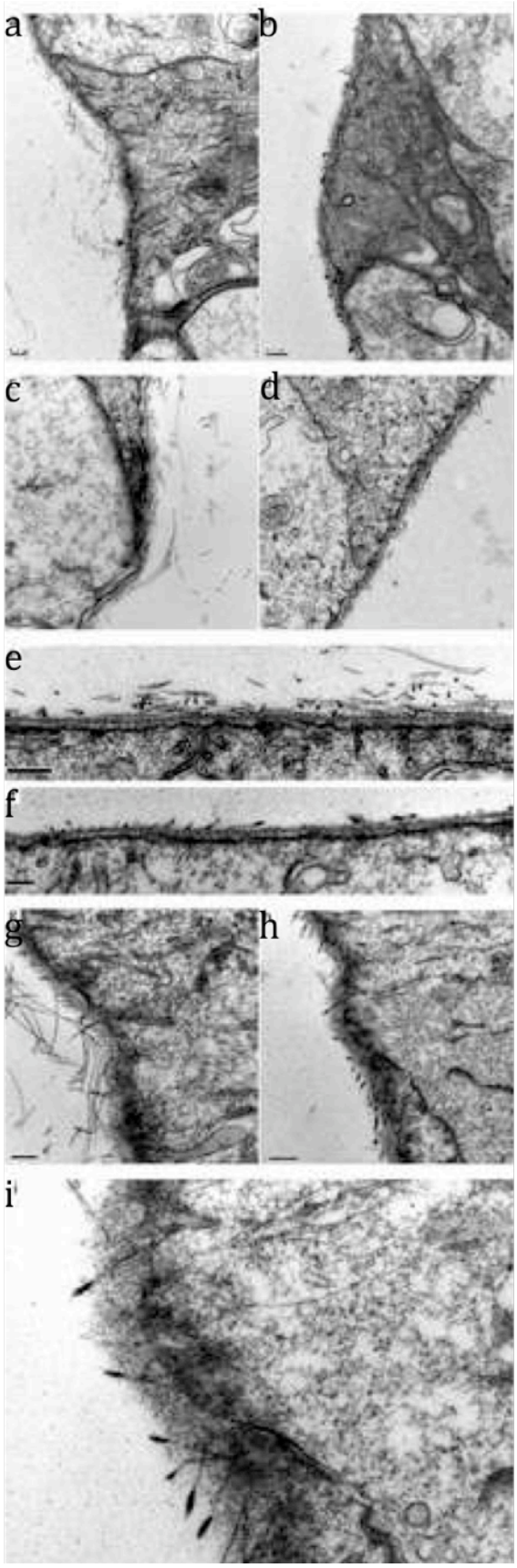
a
b
c
d
e
f
g
h
i

Figure 2a.7. Comparative images of naïve and Pronase-treated retinas by TEM. a,c) non-treated and b,d) 0.002% A Pronase-treated rat retina cross section comparing ILM structure at the Müller cell endfoot. Scale bars are 200 nm. A stretch of ILM from c) non-treated and d) 0.002% Pronase treated retinas. Scale bars are 200 nm. Higher magnification image of g) non-treated and h) 0.002% Pronase treated retinal ILM. Scale bars are 200 nm and 500 nm respectively. i) Further magnification of h), where the scale bar is 200 nm.

We next analyzed whether these morphological changes corresponded to retinal functional changes and found that pronase doses of 0.0002% and below did not alter ERGs compared to the untreated eye (Figure 2a.5). However, considering that only radial currents and not retinal ganglion cell activity are reflected in the ERG, we also recorded local field potential responses in V1 in animals treated with pronase. These animals were only treated with enzyme in one eye, allowing the contralateral eye visual input to serve as an internal control. Interestingly, our data shows that VEPs are more robust to enzymatic treatment compared to ERGs (Figure 2a.8). A reduction was observed only at the highest concentration (Figure 2a.8, right panel), yet this was not statistically significant (n=4 out of 6). It is thus likely that the cortex is compensating for the reduction in signal.

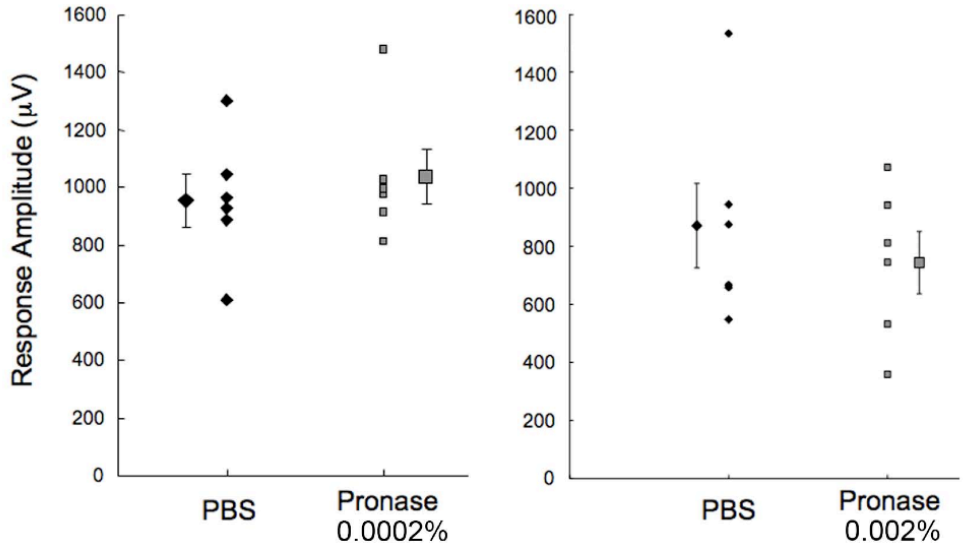

Figure 2a.8. Peak amplitude of visually evoked potentials in response to full-field stimulation of eyes injected with PBS (black diamonds) or Pronase (gray squares) at the low dose, n=6, and high dose, n=6. Recordings were performed on the contralateral visual cortex. Means for each data set are showed laterally displaced. Error bars indicate SEM. The two data sets for each dose were not significantly different (n=6, p>0.6, Wilcoxon signed-rank test).

GFP expression following AAV/Pronase E co-injection:

All AAV serotypes injected intravitreally with pronase (0.0002%) showed robust GFP expression in various cell types throughout the retina 3 weeks after injection (Figure 2a.9 a-d). In stark contrast, when AAV alone was injected intravitreally, only AAV2 led to gene expression in the inner retina, consistent with prior reports (Surace and Auricchio, 2008). The strongest transduction was achieved with pronase and AAV5 (Figure 2a.9 e-h), which mediated strong GFP expression in RGCs, Müller cells, photoreceptors, and RPE. The proportion of cells transduced varied throughout the

extent of the retina (Figure 2a.9 f-h), potentially due to non-homogeneous diffusion of the enzyme through the vitreous and a resulting higher concentration of the enzyme at the site of injection.

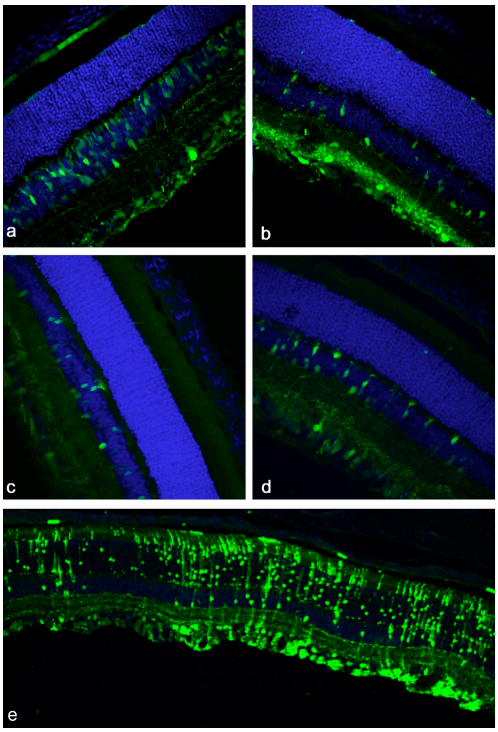

Figure 2a.9. GFP expression in cryosections of rat retina after intravitreal delivery of 10^{11} vector genomes of AAV vectors carrying smCBA.hGFP in the presence of 0.0002% pronase, 3 weeks after injection. Nuclei are stained with DAPI, shown in blue. a) AAV1, b) AAV2, c) AAV8, d) AAV9, e-h) AAV5. A representative area shows robust GFP fluorescence in all retinal layers in e). The proportion of transduced cells shows variability from one part to the other (n=6) with strong expression in RGCs and Müller cells in f) and predominantly photoreceptors with weaker RGC with some expression in the RPE in g). An entire cryoslice is shown in h).

Discussion

AAV vectors traverse a complex pathway during the process of gene delivery. At the cellular level, viral binding to cell surface receptors, internalization, nuclear accumulation, capsid uncoating, and single to double stranded genome conversion can all represent barriers to gene transfer (McCarty, 2008; Schultz and Chamberlain, 2008). For in vivo delivery, however, the virus-host interaction begins at the site of administration, and the virus needs to bypass extracellular barriers such as basal membranes before reaching the target tissue and cells.

The tropism of AAV serotypes 1 through 9 has previously been studied in the retina (Allocca *et al.,* 2007; Auricchio *et al.,* 2001). Following subretinal delivery, AAV serotypes 1 and 4 primarily infect and mediate expression in RPE cells (Auricchio *et al.,* 2001; Weber *et al.,* 2003); AAV2, 5, 7, 8, and 9 transduce RPE and photoreceptors (Allocca *et al.,* 2007); and AAV 8 and 9 also infect Müller glia. Interestingly, AAV5, 7, 8, and 9 also exhibit more efficient transduction and faster transgene expression than type 2 after subretinal injection. However, only AAV2 has been found to efficiently transduce the inner retina after intravitreal injection (Surace and Auricchio, 2008), indicating that the vitreoretinal junction represents a tissue barrier to AAV gene delivery. Studies showing that physically larger viruses like Pseudorabies Virus are capable of RGC transduction from the vitreous (Pickard *et al.,* 2002) seem to indicate that the nature or this barrier is not diffusional or purely physical. In rodents, this feature of the retina is relatively thin and homogeneous; however, in larger animals such as dogs and monkeys, the ILM is significantly thicker and varies in thickness from one region of the retina to the other. This may have important consequences for translational studies

relying on the intravitreal delivery of AAV.

In the present study, we investigated and sought to overcome this barrier. After fluorescently labeling several relevant AAV serotype capsids, we visualized their localization in retinal tissue upon intravitreal injection. Serotypes 2, 8, and 9 were able to find attachment sites at the ILM and accumulate to various degrees at the vitreoretinal junction, and AAV2 and 9 in particular exhibited very similar localization patterns. However, the highly interdigitated nature of the components of the vitreoretinal junction (Figure 2a.10) prevented us from clearly identifying the specific site viral particles had bound and accumulated.

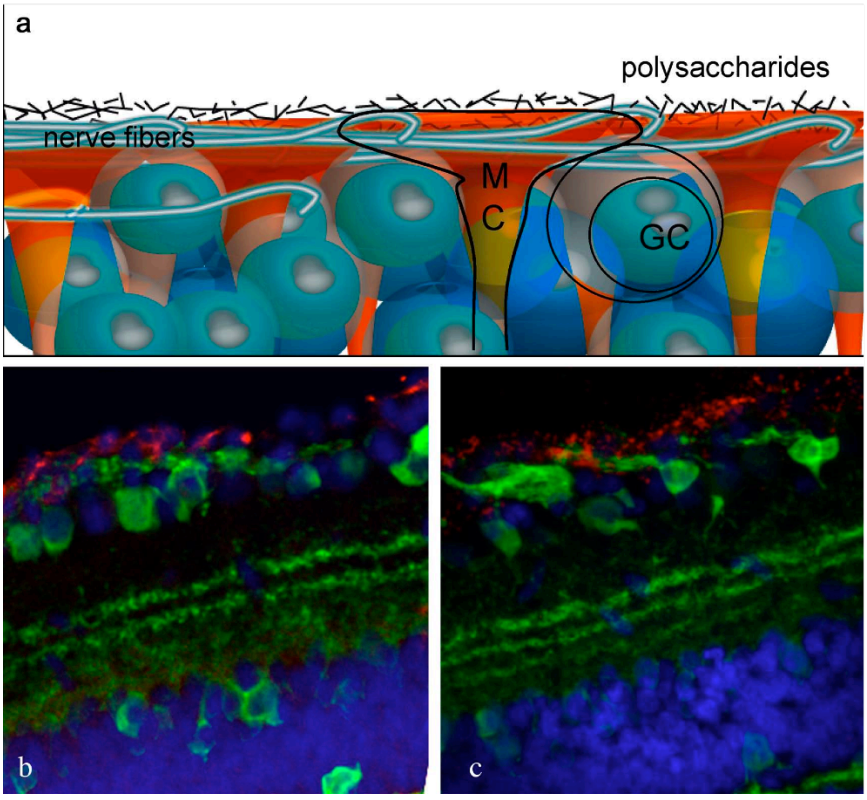

Figure 2a.10. a) Schematic representation of the overlapping structures of the vitreoretinal junction. b) Confocal image of AAV2-Cy3 and c) AAV9-Cy3 accumulation

at the vitreoretinal junction (red). The cryosections are counterstained with an antibody against calbindin (green), which labels the retinal neurons.

AAV8 showed a weaker fluorescent signal at the ILM, indicating less robust attachment. It has been shown that the laminin receptor is involved in viral transduction by all three serotypes and could thus partially account for the attachment observed at the ILM, as laminin receptors are abundant at the vitreoretinal junction, the Müller cell endfeet, and RGCs (Chai and Morris, 1999). AAV2 binds to heparan sulfate proteoglycan, also present at the ILM (Chai and Morris, 1994). This binding may assist in viral accumulation at the ILM and thereby contribute to the intravitreal permissivity of this serotype. Interestingly, AAV2 and 9 seemed to show very similar fluorescent localization and signal intensity, yet AAV9 leads to no detectable expression after intravitreal injection (Figure 2a.4). Cell surface and intracellular trafficking barriers are likely to be responsible for this difference. A recent discovery shows that phosphorylation of surface-exposed capsid tyrosines target the AAV viral particles for ubiquitination and proteasome-mediated degradation, and mutations of these tyrosine residues lead to substantially increased vector transduction (Zhong *et al.,* 2008). This finding has been used successfully to manipulate AAV retinal transduction profiles, and mutant AAV2, 8, and 9 displayed strong and widespread transgene expression in the inner retina after intravitreal delivery compared to their wild-type counterparts (Petrs-Silva *et al.,* 2008). This finding, together with our localization results, clearly indicates that AAV serotypes 2, 8, and 9 are all able to bind to the vitreoretinal junction, but subsequent cellular barriers limit the transduction of inner retinal cells by AAV8 and 9.

In contrast to AAV2, 8, and 9, we find that AAV serotypes 1 and 5 are unable to find attachment sites at the vitreoretinal junction. It is known that both serotypes depend on sialic acid (Kaludov *et al.,* 2001) for initial binding and that this monosaccharide is absent at the ILM (Cho *et al.,* 2002). Disruption of the ILM, a dispensable structure for the adult retina, using a non-specific protease apparently resolves the access barrier to retinal transduction by sialic acid-dependent AAV serotypes 1 and 5 (Wu *et al.,* 2006b). In particular, our results show that intravitreal injection of AAV5 in combination with Pronase E leads to robust gene expression in various cells of the retina, including the RPE and photoreceptors. To our knowledge, this is the first time RPE transduction has been achieved by an intravitreally injected AAV vector. Interestingly, AAV5 is apparently the only serotype to date that is capable of packaging genomes larger that 4700 nucleotides; therefore, ILM digestion in conjunction with AAV5 delivery may allow for targeting of outer retinal cells without the need for subretinal injection and offers the capacity to deliver large genes to these cells (Alloca *et al.,* 2008). Finally, a cell specific promoter can be used to limit and control levels of transgene expression in a cell type of choice.

Collectively, our data point to the importance of both extracellular and intracellular determinants of viral transduction in the retina. For intravitreal injections, viral binding and accumulation at an intact ILM may be necessary for virus to access and infect the retina. By contrast, viral particles that lack binding sites at the ILM do not undergo concentration at this site, remain diffuse within the vitreous humor, and do not lead to gene expression. The ILM thus represents an important barrier to retinal gene delivery from the vitreous.

Chapter 2b

Changes to AAV Mediated Retinal Transduction Profile in the Diseased Retina: An Important Consideration for Ocular Gene Therapy Vector Design

Preface: This work was conducted in collaboration with Dr. Deniz Dalkara and Dr. Karen Guerin. Professor Bill Merigan and Dr. Lu Yin conducted all primate work. The laboratory technician, Meike Visel, and undergraduate students, Richard Kow, and Natalie Hoffman provided technical assistance. This manuscript has been submitted to the journal Human Gene Therapy and is under review.

Abstract

Gene therapies for retinal degeneration have relied on subretinal delivery of viral vectors carrying therapeutic DNA. The subretinal injection is clearly not ideal as it limits the viral transduction profile to a focal region at the injection site and negatively affects the neural retina by detaching it from the supportive epithelium (RPE). We assessed changes in adeno-associated virus (AAV) dispersion and transduction in the degenerating rat retina following intravitreal delivery. We observed a significant increase in AAV mediated gene transfer in the diseased compared to normal retina, the extent of which depends upon the AAV serotype injected. We also identified key structural changes that correspond to increased viral infectivity. Particle diffusion and transgene accumulation in normal and diseased retina was monitored via fluorescent labeling of viral capsids and quantitative PCR. Viral particles were observed to accumulate at the vitreoretinal junction in normal retina, whereas particles spread into the outer retina and RPE in degenerated tissue. Immunohistochemistry illustrates remarkable changes in the architecture of the inner limiting membrane (ILM), which may underlie the increased viral transduction in diseased retina.

We found analogous changes in AAV dispersion in the degenerating monkey retina and similar changes at the ILM as seen in the diseased rat. These data highlight the importance of characterizing gene delivery vectors in diseased tissue as structural and biochemical changes can alter viral vector transduction patterns. Furthermore, these results indicate that gene delivery to the outer nuclear layer may be achieved by non-invasive intravitreal AAV administration in the diseased state.

Introduction

Recent successes in the clinical application of adeno-associated virus (AAV) mediated gene therapy for Leber's congenital amaurosis, an inherited blinding disease, has established 'proof of concept' for this mode of treatment (Bainbridge *et al*., 2008; Cideciyan *et al*., 2008; Hauswirth *et al*., 2008; Maguire *et al*., 2008). All three clinical trials utilize very similar methodology, a single subretinal injection of a therapeutic AAV2 vector. Although the remarkable clinical success in correcting the disease phenotype demonstrates that this method is very effective, the methodology for these trials may be too invasive to be applied to advanced retinal disease states. In many cases, the risk of tearing the retina is too high to attempt a subretinal injection. Moreover, retinal detachment causes dramatic alterations in retinal cell morphology and survival (Arroyo *et al*., 2005; Fisher and Lewis, 2003; Fisher *et al*., 2005; Lewis *et al*., 2003; Lewis *et al*., 2002; Wickham *et al*., 2006). The subretinal injection also restricts viral transduction to the region of detachment. Therefore, intravitreal delivery of AAV would provide a clinically safer and more efficacious approach to ocular gene therapy.

AAV is currently the most successful vector for gene therapy, with different serotypes capable of stably transducing multiple retinal cell types with minimal immunogenicity (Auricchio, 2003; Buning *et al*., 2008; Buch *et al*., 2008; Surace and Auricchio 2003). Presently, eight AAV serotypes distinguished by the amino acid sequence of the viral capsid have been evaluated for ocular use. The capsid determines initial receptor attachment, cellular entry, and trafficking (Choi *et al*., 2005). Expression profile studies in the wild type, adult, rodent retina have shown that AAV serotypes 1, 2, 5, 8, and 9 are extremely efficient at transducing RPE and photoreceptors following

subretinal delivery. Unfortunately, delivery of most AAV serotypes into the vitreous results in poor retinal transduction, with the exception of AAV2, which efficiently transduces retinal ganglion cells (RGCs) (Auricchio, 2003; Buch *et al*., 2008; Harvey *et al*., 2002; Lebherz *et al*., 2008; Martin *et al*., 2002; Rolling, 2004). The lack of infection from the vitreous is likely due to barriers to diffusion into the retina. Previous work from our lab has shown that AAV injected into the vitreous either binds and accumulates at the ILM (AAV2, 5, and 9) or diffuses away from the retina if binding sites are unavailable (AAV1 and 5) (Dalkara *et al.,* 2009). In addition, mild digestion of the ILM allows for enhanced AAV transduction of outer retinal cells from the vitreous (Dalkara *et al.,* 2009).

During degeneration, the retina undergoes dramatic physical changes (Marc and Jones, 2003; Marc *et al*., 2007, Marc *et al*., 2003). Photoreceptor outer segments shorten and Müller cells become hypertrophic (Marc *et al*., 2003). Remodeling events are consistent among various animal models of photoreceptor degeneration (Jones and Marc, 2005). We have also observed disorganization of the ILM, where AAV particles accumulate in the healthy retina (unpublished data, Dalkara *et al.,* 2009). We hypothesized that changes in the structural and biochemical makeup of the diseased retina, particularly at the ILM and extracellular matrix, would alter AAV transduction patterns and efficiency.

The purpose of this study was to explore changes in vector diffusion and infectivity in the diseased retina when virus is delivered from the vitreous and thereby identify key structural changes that correlate with variations in viral transduction. We characterized the onset of expression and transduction profile of AAV1, 2, 5, 8, and 9

after intravitreal injection at different stages of degeneration in the TgS334ter-3 rat model of autosomal dominant retinitis pigmentosa (Steinberg *et al.,* 1997). Our results clearly demonstrate that, unlike what is observed in the healthy retina, several AAV serotypes are capable of efficiently transducing Müller cells, photoreceptors, and RPE from the vitreous in diseased tissue. We also discovered enhanced AAV transduction of Müller glia and similar structural changes in a diseased adult macaque monkey retina marked by ganglion cell loss and demyelination of the RGC axons after cranial infection (Cowey *et al.,* 1999). Taken together, these results point to the importance of considering structural and biochemical changes in diseased tissue when developing gene targeting and vector engineering strategies.

Experimental Methods

Generation of rAAV vectors:

Adeno-associated virus was produced by the plasmid triple transfection of 293T cells (Grieger JC *et al.,* 2006). After ultracentrifugation, the interphase between the 54% and 40% iodixanol fraction, and the lower three-quarters of the 40% iodixanol fraction were extracted and diluted with equal volume of PBS+0.001% Tween20. Amicon Ultra-15 Centrifugal Filter Unit pre-incubated with 5% Tween in PBS and washed with PBS+ 0.001% Tween. The diluted iodixanol fractions were buffer-exchanged and concentrated to 250µl. Virus was washed three times with fifteen milliliters of sterile PBS+ 0.001% Tween. Vector was then titered for DNase-resistant vector genomes by Real-Time PCR relative to a standard. Finally, the purity of the vector was validated by silver-stained SDS-PAGE gel electrophoresis.

Cy3 labeling of rAAV vectors:

Purified and concentrated rAAV was labeled as described previously (Bartlett *et al.,* 2000). Amine-reactive Cy3 dye (GE Healthcare) was re-suspended in 0.2M $NaCO_3/NaHCO_3$ buffer at pH 9.3. Viral stock was diluted 1:2 with the dye suspension in a total volume of 400µl. The reaction proceeded for two hours at room temperature and was quenched with 4µl of 1M TrisHCl at pH 8.0. Buffer exchange and concentration was done on Amicon Ultra-5 Centrifugal Filter Units (Millipore).

Intraocular administration:

Adult wild type Sprague-Dawley or TgS334ter-3 rats were used. All animal procedures were conducted according to the ARVO Statement for the Use of Animals and the guidelines of the Office of Laboratory Animal Care at the University of California, Berkeley. Rats were anesthetized with ketamine (72mg/kg) and xylazine (64mg/kg) by intraperitoneal injection before ocular injection. Pupils were dilated with topicamide (1%). An ultrafine 30 1/2-gauge disposable needle was passed through the sclera into the vitreous cavity. Five microliters of $5x10^{12}$ vg/ml of Cy3 labeled (n=3/serotype) or unlabeled AAV (n=6/serotype/time point) was injected with a blunt end Hamilton syringe. The AAV transgene encodes for eGFP driven by the ubiquitous chicken beta actin (CBA) promoter.

Two young adult macaque monkeys weighing approximately 6 kg were used. All animal procedures were conducted according to the ARVO Statement for the Use of Animals and the guidelines of the Office of Laboratory Animal Care at the University of Rochester. The injection was done in the lightly anesthetized monkey. Before injection the cornea was anesthetized with Proparacaine drops and the pupils dilated with tropicamide/phenylephrine. Ketofen, a non-steroidal anti-inflammatory was administered to minimize any discomfort produced by the injection. Fifty percent strength betadine/saline was poured into the palpebral fissure (eye and lids) to disinfect the injection site and then flushed out after 8 seconds with copious amounts of sterile water. One dose of approximately 100 µl of the AAV vector was administered intravitreally through a 30 gauge needle. Finally, lubricating ointment was applied to the cornea.

Fundus Imaging:

In vivo retinal imaging of rats was performed five days to four weeks after injections with a fundus camera (Retcam II; Clarity Medical Systems Inc., Pleasanton, CA) equipped with a wide angle 130° retinopathy of prematurity (ROP) lens to monitor eGFP expression in live, anesthetized rats.

Fluorescence fundus images of green fluorescent protein (GFP) expression in macaque retina were obtained approximately every two weeks after intravitreal injections on an EHV Topcon fundus camera equipped with excitation and barrier filters optimized for detection of GFP (Semrock, 472/30 excitation, 525/30 barrier).

Cryosections:

One day (for studies with labeled virus) to four weeks (for expression analysis) after vector injection, rats were humanely euthanized by CO_2 overdose and cervical dislocation. Eyes were enucleated, a hole was made in the cornea and eyes were fixed with 10% neutral buffered formalin overnight. The eyecups were washed in PBS and the cornea and lens were removed. The cups were then placed in 30% sucrose in PBS overnight. Eyes were then embedded in optimal cutting temperature embedding compound (OCT; Miles Diagnostics, Elkhart, IN) and oriented for 5-10μm thick transverse retinal sections.

Non-human Primate Histology:

Approximately 12 weeks following AAV injection each macaque was euthanized

with an overdose of thiopental. Eyes were enucleated, the cornea and lens were removed, and the eyecups immersion fixed in 4% paraformaldehyde for four hours. The retina and pigment epithelium were then removed and fixed in 4% paraformaldehyde overnight. The retinas were then washed and paced in phosphate buffered saline until they were prepared as wholemounts for microscopic examination. Selected regions of the retina were then cut out of the wholemount, embedded in optimal cutting temperature embedding compound (OCT; Miles Diagnostics, Elkhart, IN) and oriented for 5-10μm thick transverse retinal sections.

Immunolabeling and histological analysis:

Tissue sections were rehydrated in PBS for five minutes and then incubated in blocking solution (1% BSA, 0.5%TritonX-100 and 2% normal donkey serum in PBS) for 2-3 hours. Slides were then incubated with commercial rabbit monoclonal antibody raised against the green-fluorescent protein (Invitrogen, Molecular Probes, Carlsbad, CA), rabbit monoclonal antibodies against laminin (Sigma, L9393) at 1:100 in blocking solution, or mouse monoclonal antibody raised against vimentin (Dako, Cambridgeshire, UK) at 1:1000 in blocking buffer for 24 hours at 4ºC. Then tissue was washed in 2 changes of PBS for 3 hours and secondary antibodies (1:100 in blocking buffer) (Anti-mouse-Alexa488 (Molecular Probes) overnight at 4ºC. The tissue was washed with PBS before mounting in Vectashield mounting medium with DAPI. The results were examined by fluorescence microscopy using an Axiophot microscope (Zeiss, Thornwood, NY) equipped with X-cite PC200 light source and QCapturePro camera or by confocal microscopy (LSM5; Carl Zeiss Microimaging). Images were prepared using

Bitplane Imaris image processing and manipulation software (Bitplane Inc., St. Paul, MN).

Quantitative PCR:

Five microliters of AAV5 ($5x10^{12}$ vg/mL) was injected into the vitreous of anesthetized WT (n=10) or TgS334-3 animals (n=10). Five days post-injection, eyes were enucleated and fixed overnight. The cornea and lens were removed and retina was dissected away from the RPE. The RPE was then scraped away from the choroid. Separate, autoclaved tools were used for each retina and RPE dissection to avoid contamination. Total DNA was extracted from tissue (Qiagen DNEASY kit). QPCR was used to quantify total transgene number in the RPE and retina of WT and TgS334-3 animals compared to uninjected controls.

Results

Changes in viral transduction profile in the degenerating rodent retina:

Wildtype (WT) Sprague-Dawley and S334ter transgenic rats overexpressing a rhodopsin mutant causing autosomal dominant retinitis pigmentosa and subsequently photoreceptor degeneration (http://www.ucsfeye.net/mlavailRDratmodels.shtml) were injected into the vitreous with AAV1, 2, 5, 8 and 9 vectors carrying eGFP cDNA under control of the ubiquitous CAG promoter. Intraocular injections were performed at three ages corresponding to three different stages of degeneration: P20 (early), P30 (intermediate), and P60 (advanced). As previously described, intravitreal injection of AAV1, 5, 8, and 9, at all ages tested, results in no measurable transgene expression in healthy rat retina, whereas AAV2 leads to robust gene expression in the inner retina three weeks post-injection (Auricchio 2003; Ali *et al.,* 1998; Buch *et al.,* 2008; Lebherz *et al.,* 2008, Harvey *et al.,* 2002). GFP expression begins rapidly in the TgS334ter retina (five days post injection) for all serotypes except AAV2, which gave visible expression after three weeks. AAV2, 5, 8, and 9 lead to GFP expression after injection at P20 and all later time points, while AAV1 expression was not seen until later stages of degeneration (P60). Strong transgene expression was evident in RPE, Müller glia, and remaining photoreceptors for all serotypes (Table 1). AAV5 and AAV1 exhibited the greatest level of expression (Figure 1, a-d) while AAV8 and 9 mediated transgene expression was limited to sporadic RPE, photoreceptors, and retinal Müller cells around the optic nerve head (data not shown). AAV2 expression was evident in inner retinal neurons similar to the expression exhibited in the WT retina; however, Müller cell transduction was greatly increased in diseased tissue.

AAV serotype	P20	P30	P60
AAV1	-	-	MC, INL, RPE
AAV2	RGC, MC	RGC, MC, some INL, some RPE	RGC, MC, some INL, some RPE
AAV5	MC, PR, RPE	MC, PR, RPE	MC, PR, RPE
AAV8	MC, PR	MC, PR	MC, PR
AAV9	MC, PR	MC, PR	MC, PR, some RPE

Table *2b.1*. AAV transduction patterns (AAV1, 2, 5, 8, and 9) when injected at P20, P30, and P60. Expression was seen primarily in Müller cells (MC), photoreceptors (PR), and retinal pigment epithelium (RPE), with some inner nuclear layer (INL) and retinal ganglion cell (RGC) transduction.

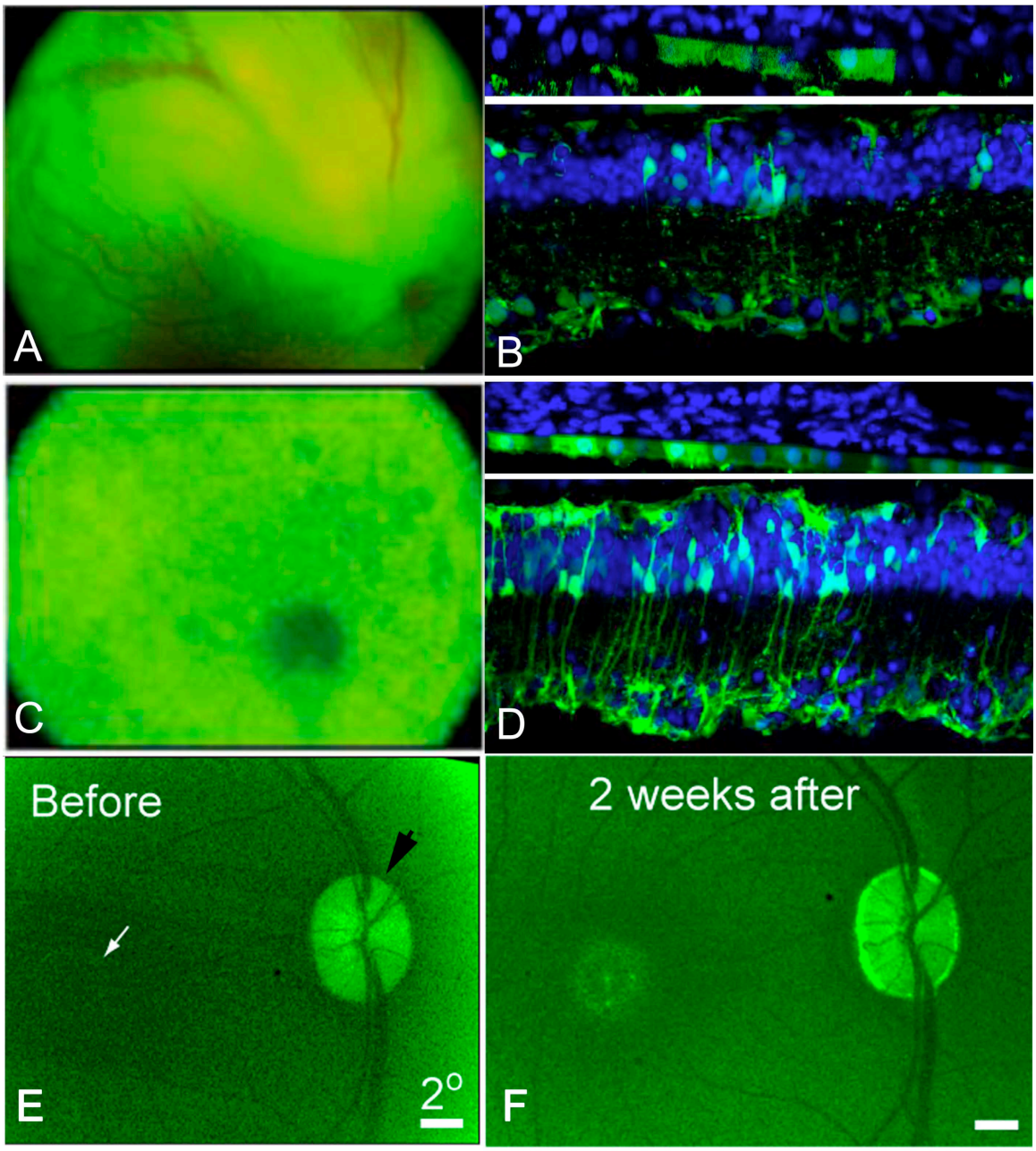

Figure 2b.1. AAV-mediated GFP expression in the inner retina after intravitreal administration into S334-3 rat eyes (A-D). Fundus images and histological cross sections (45x) of AAV1 (A, B) and AAV5 (C, D). AAV1 and AAV5 exhibited the most robust expression profile of all serotypes in the degenerated retina (n=10/serotype/time point). Both vectors transduced RPE, photoreceptors, and retinal Müller glia. In addition, GFP

expression was seen in the fundus of the diseased monkey two weeks after intravitreal delivery (E, F). Images were taken two (monkey) or three (rat) weeks post injection, though expression was seen as early as five days post-injection in the rat.

Viral particle migration through the retina is altered during degeneration:

AAV viral capsids were labeled with Cy3 to allow for the visualization of their movement into and throughout the retina 24 hours after intravitreal injection. In the WT rat retina, AAV2, 8, and 9 accumulate at the vitreoretinal junction while labeled AAV1 and 5 particles are not visible, which is likely due to absence of primary receptors at the vitreoretinal junction (Figure 2b.2 A) (Dalkara *et al.,* 2009). However, in TgS334ter animals, viral particles from all serotypes tested (AAV1, 2, 5, 8, and 9) were visible throughout all layers of the retina, reaching the outer nuclear layer and RPE (Figure 2b.2 B). The retina is a heterogeneous mixture of neurons, glia, blood vessels arranged in a laminar structure. We observed the Cy3-AAV distribution pattern to be primarily radial, suggesting that the capsids traverse the retina along Müller cell processes.

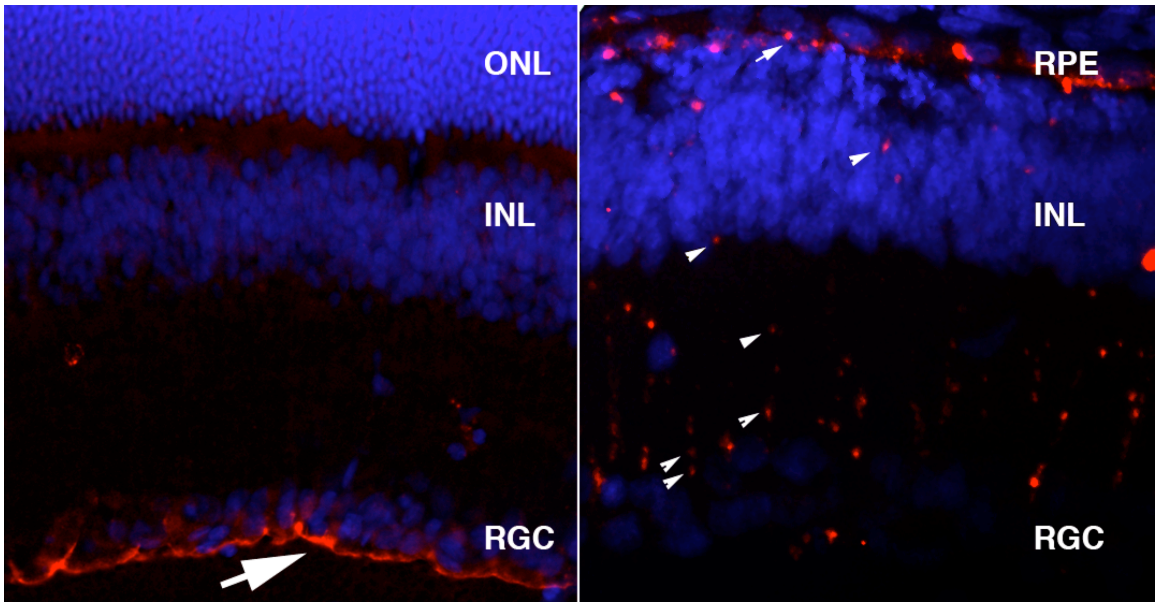

Figure 2b.2. Cy3 labeled virus dispersion in the P30 WT and degenerated retina. AAV9-Cy3 accumulation at the vitreoretinal junction in the WT retina after intravitreal injection (left). AAV9-Cy3 dispersion throughout the retina and into the inner retina and RPE when injected into the vitreous of P30 TgS334 rats (right). Eyes were taken 24 hours post-injection.

We employed quantitative PCR to quantify viral movement and infectivity in the retina and RPE. We showed that vector genom levels in the degenerated retinal tissue and RPE is significantly enhanced compared to the WT (Figure 2b.3). In fact, transgene number is approximately three log units greater in the retina and two and a half log units greater in the RPE.

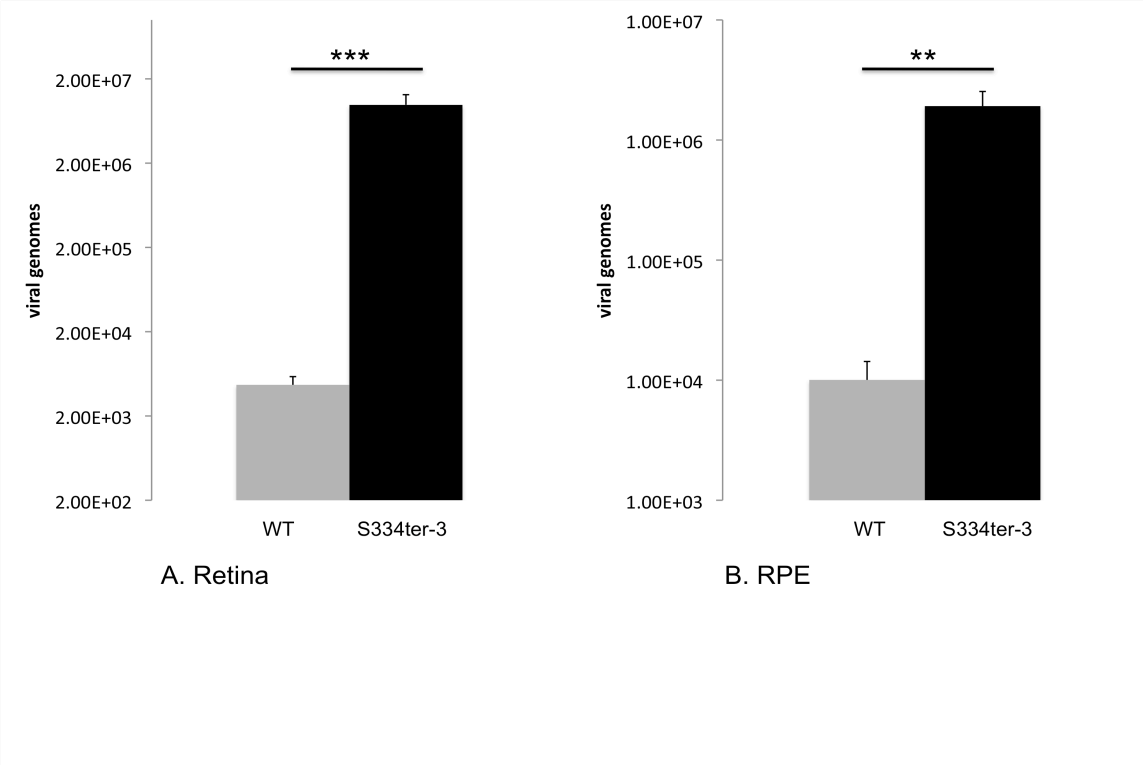

Figure 2b.3. Quantitative PCR demonstrates an increase in AAV transduction of the RPE and retina in degenerating tissue. AAV transgene copy number is significantly greater in the retina (A) and RPE (B) of TgS334-3 animals five days post intravitreal AAV5 injection (n=10). Values are average copy number normalized to uninjected control retina or RPE as genomic DNA elicits some background amplification.

Structural changes at the inner limiting membrane in the transgenic rat retina:

ILM disorganization during degeneration was visualized by immunostaining for laminin and vimentin in P30 TgS334-3 animals (Halfter *et al.,* 2008). To account for changes in ILM structure within the retina, the regularity and thickness of the ILM matrix was examined by anti-laminin immunohistochemistry at comparable retinal

eccentricities. The staining patterns observed were visibly different when contrasting the healthy and degenerated retina (Figure 2b.4 and 2b.5), and such changes were similar in later stages of degeneration (P60) (data not shown). In addition to laminin, co-staining for vimentin, a marker that exclusively labels intermediate filaments in Müller cells, showed substantial gliosis that results in the migration of Müller endfeet into and throughout the plane of the glycoconjugate layer of the ILM in TgS334-3 retinas (Figure 2b.5).

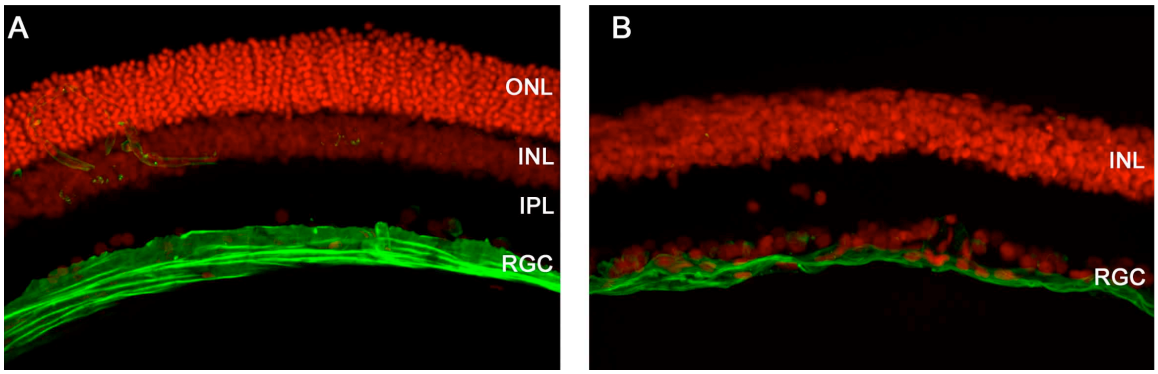

Figure 2b.4. Agarose sections of WT (A) and TgS334-3 retina (B) stained for laminin (green) show disorganization of the inner limiting membrane in degenerated tissue. Animals were P30 at time of sacrifice, though disorganization was visible at all stages of degeneration (data not shown) (25x).

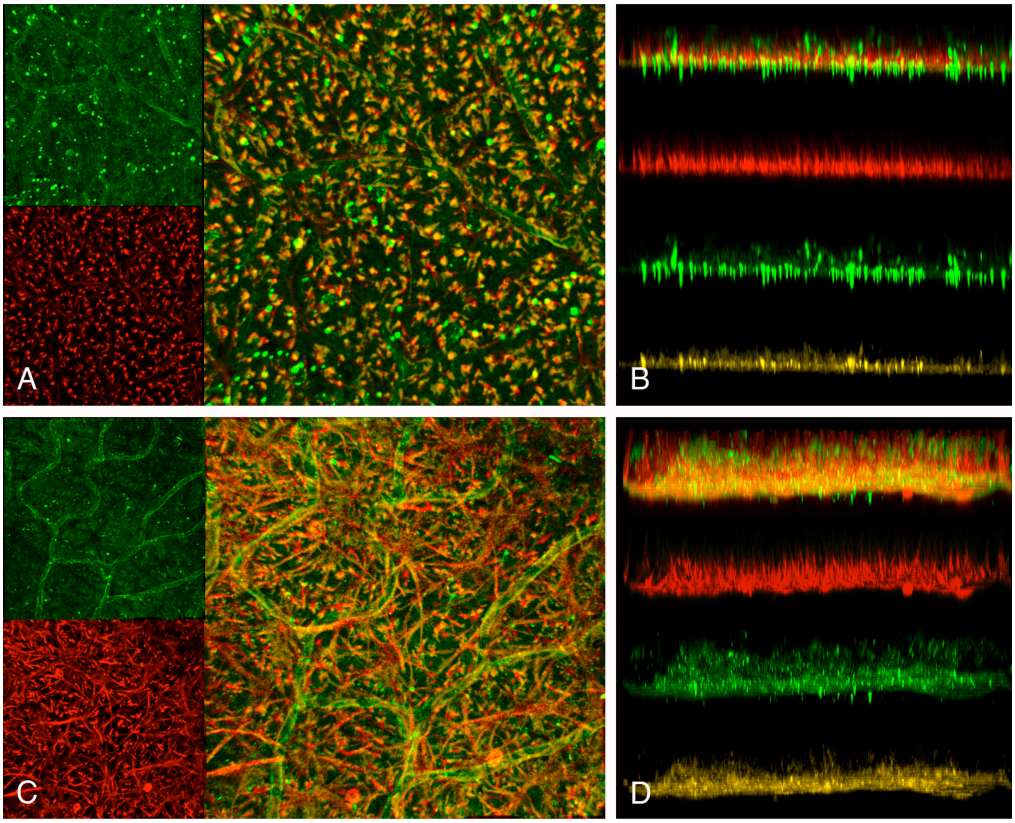

Figure 2b.5. WT (A) and TgS334-3 (C) flatmount retina stained for laminin (green) and vimentin (red). Z-stack projections of WT (B) and TgS334-3 retina (D) show the depth of Müller cell hypertrophy/ILM disorganization.

AAV transduction is enhanced in the diseased monkey retina:

To assess whether the changes in viral transduction profile seen in the degenerated rodent retina extend to the primate, we assessed AAV5 expression after intravitreal injection in the diseased and normal macaque monkey retina. The diseased monkey in this study had suffered from a cranial infection that resulted in severe retinal ganglion cell loss as assessed by optical coherence tomography (Zeiss Cirrus) (Cowey *et al.,* 1999). We discovered GFP expression in retinal Müller cells in the central retina +/-

10 degrees (approximately 2.5 - 3 mm) from the fovea less than two weeks post injection (Figure 2b.6). Intravitreal injection of AAV5 in a healthy, adult monkey resulted in no transgene expression as of three months post-injection.

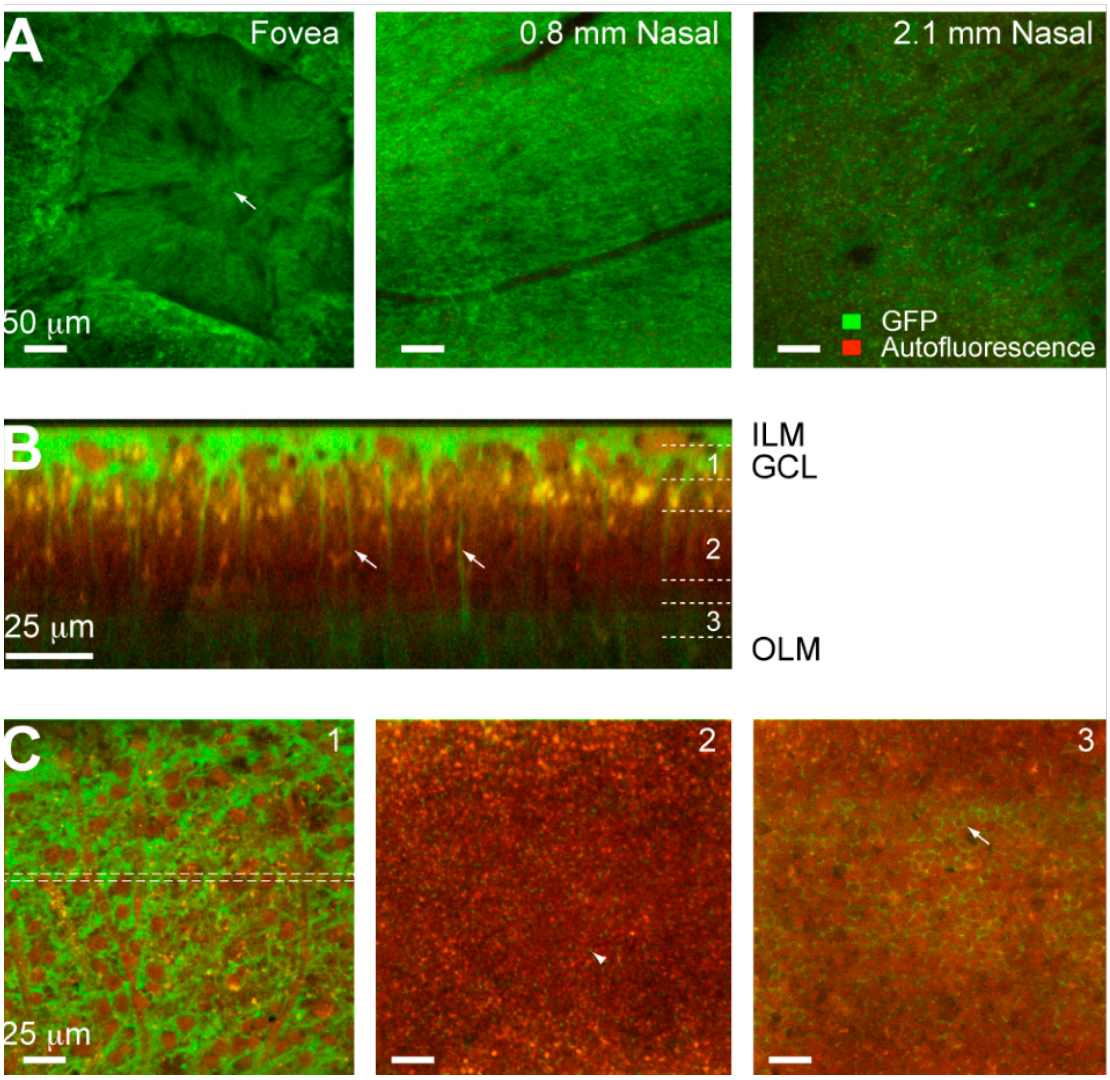

Figure 2b.6. Fundus images and confocal Z-stack image of diseased monkey retina shows GFP expression throughout retinal Müller glia around the fovea (A,B,C). Section 1, 2, and 3 are shown in flatmount view at different depths of the retina (C).

Structural changes at the ILM in the monkey retina:

We assessed ILM integrity in diseased and normal macaque monkey retina to explore whether the structural changes identified during rodent retinal degeneration that parallel changes in viral transduction patterns, also occur in the non-human primate. Indeed, vimentin immuno-labeling shows massive Müller cell end-feet hypertrophy and resulting disorganization within the plane of the ILM (Figure 2b.7).

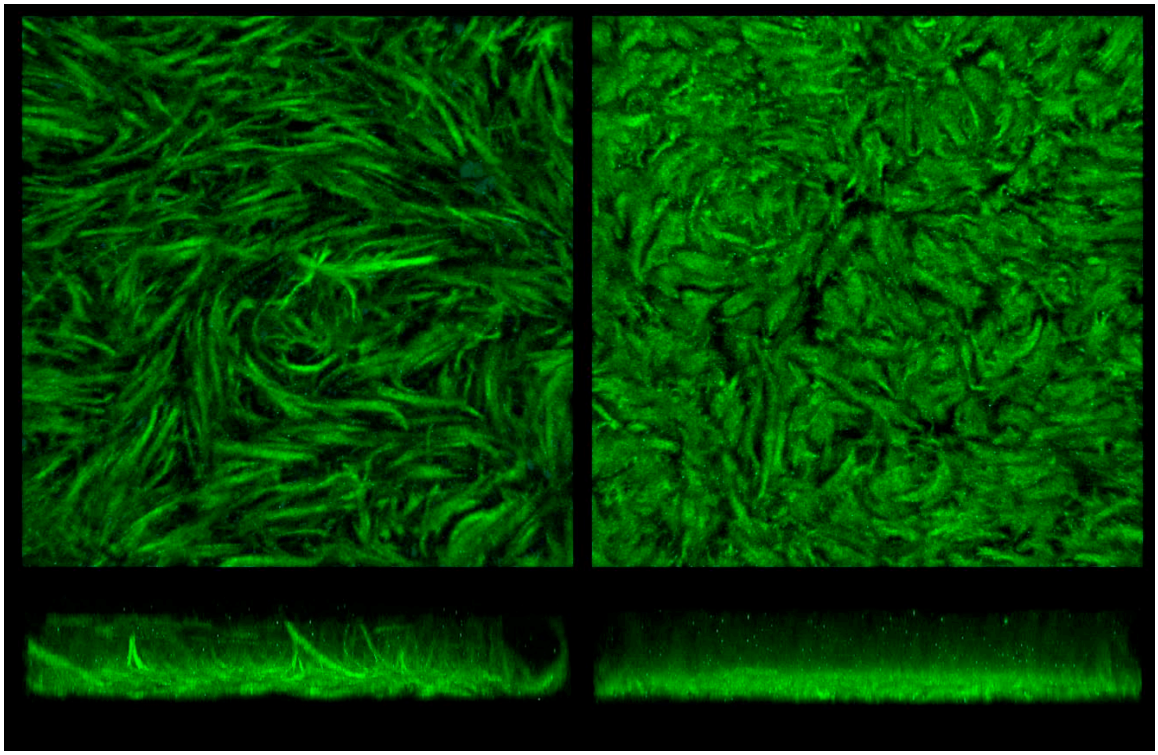

Figure 2b.7. Müller cell hypertrophy in the diseased monkey retina as shown by vimentin immunohistochemistry (green) (Right). Top: flatmount, bottom: z-projection. The control, healthy primate retina shows regular and organized Müller cell distribution in flatmount (top) and z-projection views (bottom) (left) (65x).

Discussion

Because the subretinal injection poses a significant risk of retinal damage and limits the efficacy and extent of ocular gene therapy, we explored enhancement of AAV retinal transduction from the vitreous in a monkey and in rodents with disease associated retinal degeneration. We hypothesized that changes in the structural and biochemical composition of the retina that occur during degeneration may allow for alterations in vector penetration and infection (Marc and Jones, 2003).

Previous work has shown that the enzymatic disruption of the inter-photoreceptor matrix (Grüter *et al*., 2005) enhances viral infectivity. In another study, the viral transduction profile of AAV8 was shown to dramatically improve in a mouse model of retinoschisin (Colosi *et al.,* 2009), a disease characterized by retinal tears arising due to the lack of schisin protein in the extracellular matrix. Similar changes take place during retinal degeneration. More specifically, extracellular matrix proteolysis occurs during neurite extension and Müller glia hypertrophy (Marc *et al*., 2003). As in the aforementioned studies, these changes in the ECM may contribute to the observed increase in AAV transduction in the degenerating retina.

We also reasoned that, like in the developing retina (Harvey *et al*., 2002), changes in the structural integrity and make-up of the inner limiting membrane could open access to previously masked AAV receptors. The ILM is a basement membrane that histologically defines the border between the retina and the vitreous humor and consists of 10 distinct extracellular matrix proteins including laminin, as well as Müller cell endfeet (Candiello *et al*., 2007). Recent data from our lab shows that the specific

enzymatic digestion of the inner limiting membrane allows for AAV mediated expression in the outer retina and RPE (Dalkara *et al.,* 2009). Studies have shown that active matrix metalloproteinase-9 (MMP-9) levels are elevated in the retina during degeneration (Ahuja *et al*., 2006), causing laminin degradation at the ganglion cell layer/ILM (Zhang *et al*., 2004). These studies suggest that the ILM is a barrier to AAV infection and a region of the retina that could undergo great changes during retinal degeneration, perhaps opening access to deeper AAV penetration and transduction.

Laminin receptors - found at the vitreoretinal junction, Müller cell endfeet, and RGCs - are known to mediate viral transduction of AAV2, 8, and 9 (Akache *et al*., 2006). Also, AAV2 binds heparin sulfate proteoglycan as a primary receptor, which is found at the ILM (Chai and Morris, 1994; Chai and Morris, 1999; Summerford and Samulski, 1998), as well as the fibroblast growth factor receptor1 (FGFR1) as a secondary receptor (Qing *et al*., 1999). AAV1 and 5 bind sialic acid, which is not present at the WT ILM (Chen *et al*., 2006; Cho *et al*., 2002; Kaludov *et al*., 2001; Walters *et al*., 2001). In the degenerating retina, viral particles that would otherwise accumulate in receptor reservoirs at the ILM (AAV2, 8, and 9) or diffuse away into the vitreous when no receptors are present (AAV1 and 5) may now be recruited deeper into the retinal tissue by interacting with previously masked binding sites (Figure 2b.2) (Dalkara *et al.,* 2009). For example, the increase in surface area and movement of Müller cell end feet into and throughout the glycosaminoglycan layer of the ILM during gliosis is likely to expose receptors, like the 32 kD laminin receptor (a receptor for AAV2, 8, and 9), at the site of vector administration (Akache *et al*., 2006; Halfter *et al*., 2008) (Figures 2b.5 and 2b.7).

Up-regulation of AAV receptors throughout the retina could also assist in recruitment of viral particles. Fibroblast growth factor receptor 1 (FGFR1) has been shown to be up-regulated during degeneration or after retinal stress due to injury or detachment, particularly in Müller glia (Guillonneau *et al*., 1998; Ozaki *et al*., 2000; Wen *et al*., 1995). Heparin sulfate proteoglycan expression also increases in the retina during degeneration (Landers *et al*., 1994). However, as the localization and identity of many receptors and co-receptors for specific AAV serotypes remain unknown, it is difficult to discern exactly how receptor recruitment of AAV changes in the degenerating retina and whether these changes are due to macroscopic structural changes and/or alterations in receptor expression patterns.

To apply our current data to improve ocular gene therapy in the clinic, it is necessary to identify consistent patterns of vector transduction and associated retinal changes during disease across species and pathologies. To this end, we studied changes in vector diffusion and infectivity after intravitreal injection in a monkey suffering from retinal ganglion cell loss and demyelination of axons after a cranial infection. Though the nature of retinal degeneration is different from our rodent model of autosomal dominant retinitis pigmentosa, we observed strikingly similar changes at the inner limiting membrane (disorganized architecture and hypertrophied Müller cells). After injection of AAV5 into the vitreous of the diseased monkey, transgene expression initiated rapidly (within two weeks) in the Müller glia around the fovea. One natural function of Müller cells is to protect photoreceptors during degeneration or retinal stress by modulating neurotrophin expression (Harada *et al*., 2000, Zack, 2000). Therefore, targeting Müller glia from the vitreous with AAV carrying trophic factor cDNA is a

promising method of improving ocular gene therapy for retinal diseases (Dorrell *et al*., 2009, Chapter 3).

These data highlight the need to consider changes in the degenerating retina when developing therapeutic interventions for retinal diseases. This is particularly important, as patients who may benefit from gene therapy are likely to have undergone a degree of retinal degeneration before treatment is sought. Future experiments will be necessary to determine whether such dramatic changes in AAV transduction profiles are consistent across multiple retinal disease models. Identifying putative barriers to intravitreal introduction of AAV to the outer retina is the first step toward developing a safer and more efficacious approach to gene delivery.

Chapter 3

Restricted, High Efficiency Müller Cell Expression of hGDNF in an Animal Model of Autosomal Dominant Retinitis Pigmentosa

Preface: This work was conducted in collaboration with Dr. Karen Guerin, Dr. Deniz Dalkara, and Ph.D. student, Ryan Klimczak. The laboratory technician, Meike Visel, and undergraduate students, Richard Kow, and Natalie Hoffman provided technical assistance.

Abstract

The purpose of the present study was to achieve sustained secretion of human glial cell line-derived neurotrophic factor (hGDNF) from Müller glia and subsequently slow degeneration in a rodent model of retinitis pigmentosa. Retinal Müller cells (RMCs) span the entire retina and provide trophic support by secreting survival factors. Thus, we hypothesized that hGDNF gene transfer to retinal glia will enhance the protective affects of RMCs in the diseased retina and slow degeneration. Furthermore, targeting hGDNF to RMCs will alleviate photoreceptor stress caused by direct gene transfer to cells that are undergoing apoptosis. By manipulating vector capsid/envelope proteins, promoter, and delivery route we were able to optimize gene transfer to RMCs. During this process, we observed surprising toxic effects caused by specific combinations of promoter and vector that have implications for ocular gene therapy strategies in general. We determined that an engineered AAV vector that specifically and efficiently infects RMCs from the vitreous is the optimal method to deliver hGDNF cDNA to RMCs. A ubiquitous promoter effectively drives hGDNF expression and secretion at therapeutic levels. We have also observed the beginnings of functional rescue with this method of targeted hGDNF expression. However, we are still in the process of correlating functional rescue with morphological preservation and hGDNF production levels. In summary, we have developed a non-invasive RMC targeted gene delivery strategy that shows promise as a general therapy for progressive retinal degenerative diseases.

Introduction

Therapies that have been developed for inherited blinding diseases typically rely on the viral delivery of DNA encoding for replacement genes or trophic factors (Rolling, 2004). Retinitis pigmentosa is a genetically heterogeneous retinal degenerative disease caused by mutations in important phototransduction, structural, metabolic, or maintenance proteins that are primarily found in the RPE and photoreceptors (Travis, 1998).

Because of the enormous variability in the genetic make-up and disease progression of retinitis pigmentosa patients, it would be ideal to tailor a therapeutic approach that could be applied to all cases of progressive photoreceptor degeneration (Travis, 1998). To this end, we aimed to harness the natural support character of retinal Müller glia (RMC) by restrictively transducing RMCs with a therapeutic vector carrying a transgene that encodes for the pro-survival protein, human glial derived neurotrophic factor (hGDNF). We hypothesized that regulated expression and secretion of hGDNF from the retinal Müller cells will enhance the natural protective character of RMCs and slow retinal degeneration in an animal model of retinitis pigmentosa.

Previous studies have shown that hGDNF has anti-apoptotic and pro-survival effects on retinal neurons during disease or damage (Andrieu-Soler *et al.,* 2005; Frasson *et al.,* 1999; McGee Sanftner *et al.,* 2001; Wu *et al.,* 2002). More specifically, viral delivery of hGDNF to the photoreceptors has been shown to slow the disease progression of the S334-ter rat model of autosomal dominant retinitis pigmentosa, as demonstrated by functional (ERG) and histological rescue (McGee Sanftner *et al.,*

2001). However, because the photoreceptors are undergoing the bulk of the stress during retinal degeneration, vector transduction and protein production provides an additional workload for the already damaged cells. Moreover, at later stages of disease progression, hGDNF production will become compromised as photoreceptor cells die. Thus, we expected that targeting Müller cells with the therapeutic vector would enhance rescue and avoid the extra burden placed on photoreceptors by direct transduction.

Müller glia are the major support and maintenance cells of the retina (Bringmann *et al.,* 2006; Bringmann and Reichenbach, 2001; Newman and Reichenbach, 1996). Müller cells span the entire width of the retina and ensheath all cell types and their processes. This close physical relationship allows RMCs to be intimately involved in neuronal function and the preservation of the physical integrity of the retina. More specifically, RMCs maintain homeostastis in the extracellular matrix by removing metabolic waste, controlling ion and neurotransmitter concentrations, and regulating osmotic pressure and pH (Bringmann *et al.,* 2006; Bringmann and Reichenbach, 2001; Newman and Reichenbach, 1996). Postnatal death of Müller glia results in photoreceptor apoptosis which progresses to complete retinal degeneration (Dubois-Dauphin *et al.,* 2000). RMCs are activated in disease states. This activation (gliosis) refers to RMC hypertrophy, proliferation, and upregulation of the intermediate filament proteins vimentin and GFAP (glial fibrillary acidic protein). Müller cell activation during stress can either be beneficial or detrimental to the survival of retinal tissue. RMCs secrete the pro-survival trophic factors, basic fibroblast growth factor (bFGF) and CNTF when activated, take up and degrade excess glutamate that can cause neuronal excitoxicity, and secrete the antioxidant glutathione (Bringmann and Reichenbach, 2001). However,

nerve growth factor binding to p75 receptors on RMCs decreases bFGF secretion, which in turn increases photoreceptor apoptosis (Harada *et al.,* 2000). In addition, RMCs increase nitric oxide synthetase activity and enhance nitric oxide (NO) release in animal models of retinitis pigmentosa (de Kozak *et al.,* 1997; Travis, 1998). The release of NO has been shown to contribute to the progression of photoreceptor degeneration (Becquet *et al.,* 1994). Therefore, the correct balance of RMCs many functions is necessary for the cells to carry out support functions in disease states.

Crucial to the present study, RMCs play an important role in trophic factor production and signaling in the retina. Early work by LaVail and colleagues explored the effects of different survival factors including bFGF, BDNF, and CNTF in combination and alone on eight animal models of retinal degeneration (LaVail *et al.,* 1998; LaVail *et al.,* 1992). These experiments showed that certain factors slow photoreceptor death depending on the model and species. This work has been followed by the optimization of trophic factor delivery and careful assessment of functional and morphological rescue in animal models of retinal disease by specific survival proteins, namely CNTF, bFGF, and GDNF (Frasson *et al.,* 1999; Green *et al.,* 2001; Lau *et al.,* 2000; Liang *et al.,* 2001; McGee-Santfner *et al.,* 2001; Wu *et al.,* 2002).

Though the exact role retinal Müller glia play in mediating the effects of trophic factors is not entirely elucidated, it is widely accepted that RMCs are integral to the success of neurotrophin therapy in the retina (Harada *et al.,* 2000; Whalin *et al.,* 2000; Zack, 2000). GDNF, a member of the TGF-β superfamily, signals through binding and activation of the GFRα-1 and RET receptors (Airaksinen and Saarma, 2002). Recent work in the porcine retina has shown that GFRα-1 and RET receptors (among other

GDNF family receptors) are expressed on RMCs but not photoreceptors (Hauck *et al.,* 2006). Furthermore, GDNF triggers multiple intracellular signaling cascades in isolated RMCs. It also induces signaling in RMCs of intact retina as shown by localized ERK phosphorylation. *In vitro* studies by Hauck and colleagues demonstrated that GDNF induced intracellular RMC signaling initiates bFGF upregulation that in turn promotes photoreceptor survival (Hauck *et al.,* 2006). Therefore, it is likely, that GDNF's pro-survival effects are, at least in part, mediated through RMC activity and subsequent enhanced bFGF production (Lau *et al.,* 2000; Raymond *et al.,* 1992; Ozaki *et al.,* 2000; Valter *et al.,* 2002).

In the present study we utilized viral vectors to restrictively target and express human GDNF from RMCs with the aim of functional and morphological rescue in the TgS334-4 animal model of autosomal dominant retinitis pigmentosa. Viral vectors can be non-pathogenic, infect non-dividing cells, and gene transfer results in sustained transgene expression (Kay *et al.,* 2001). Until recently, there was little data characterizing a gene delivery vehicle that stably and efficiently transduces retinal Müller cells. The route of vector administration determines proximity of virus to receptors. The capsid or envelope of a virus controls initial receptor attachment, cellular entry, and trafficking within the cell. And finally, the promoter drives expression once infection has taken place.

By manipulating the aforementioned three properties of a gene transfer vehicle, recent studies have developed methods to efficiently target retinal Müller cells (Alloca *et al.,* 2007; Greenberg *et al.,* 2007). More specifically, Greenberg and colleagues utilized lentivirus pseudotyped with either VSV-G (vesicular stomatitis virus glycoprotein)

envelope or gliotropic RRV (Ross River virus) envelope to direct RMC infection *in vitro* (Greenberg *et al.,* 2007). In vivo work showed that VSV-G mediates higher RMC transduction then RRV via a subretinal delivery while intravitreal delivery yields no discernable RMC transduction from either vector. Furthermore, Müller cell specific promoters (CD44, GFAP, and Vimentin) proved to be crucial for directing specific and robust vector transgene expression as ubiquitous promoters drive expression only in the RPE (Greenberg *et al.,* 2007). In addition, recently isolated adeno-associated virus serotypes 8 and 9 have now been shown to efficiently transduce RMCs when delivered to the subretinal space (Alloca *et al.,* 2007; Surace and Auricchio 2008). In light of these studies, we assessed the efficiency of the two vector systems to deliver hGDNF cDNA to RMCs. In both of these systems the viral vector required subretinal delivery in order to lead to RMC transduction. This delivery route proved to be a pitfall for the long-term goals of this project. To overcome this obstacle, in collaboration with the Schaffer lab, we engineered a novel AAV capsid variant for enhanced transduction of RMCs from the vitreous (Klimczak et al., 2009, *under review*).

In summary, by manipulating virus/serotype, route of delivery, and promoters we optimized Müller cell transduction and hGDNF expression in TgS334-4 rats as measured by ELISA, RT-PCR, and microscopy. We are now assessing functional and morphological rescue in the aforementioned animal model of autosomal dominant retinitis pigmentosa using this optimized gene delivery vehicle. Preliminary results are promising; however, highly variable ERG responses of treated (and untreated) animals require further optimization of the ERG setup. We are in the process of correlating the

functional rescue results with GDNF production and preservation of the photoreceptor layer in treated animals.

Experimental Methods

Lentivirus vector construction:

pFmGFAP.G.W and pFCD44.G.W were generously provided by Dr. Kenneth Greenberg (Greenberg *et al.,* 2007). Human GDNF was removed from pTR-UFwGDNF with HindIII and NsiI and digest sites were blunt ended with Klenow. GFP was removed from the pFmGFAP(FL)GW plasmid with Xba1. The backbone vector was blunt ended and phophatased. GDNF was then ligated into the pFmGFAP backbone (3:1 molar insert: vector ratio) using the Roche Rapid Ligation Kit for 1 hour to create pFmGFAP(FL)-hGDNFW. All clones were digest-checked and sequenced. mGFAP(FL)-hGDNF was also subcloned into a bicistronic miniCMV.GFP LV vector (Amendola *et al.,* 2005).

To clone pFmCD44mGFAP-hGDNFW, pFmGFAP(FL)-hGDNFW was digested with XbaI and XhoI to isolate the hGDNF cDNA.WPRE (1285 bp fragment). An XbaI and XhoI double digest was used to release the backbone of pFmCD44(FL)GW (no GFP.W:9154 bp). The 1285 bp insert and 9154 bp vector were ligated together (3:1 molar insert: vector ratio) using the Roche Rapid Ligation Kit to create pFmCD44(FL)-hGDNFW. All clones were digest-checked and sequenced.

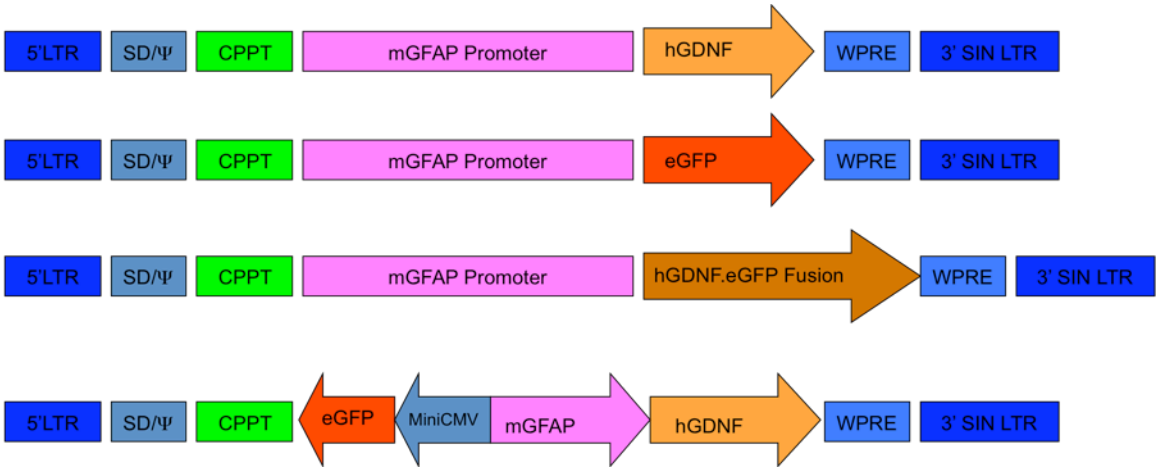

Figure 3.1. Lentivirus transgene vectors were constructed by subcloning hGDNF into a LV transfer vector containing mGFAP or mCD44 promoters and the WPRE enhancer element.

AAV vector construction:

mGFAP.GFP and mGFAP.GDNF were removed from pTR lentivirus backbone with HindIII and ligated into pAAV-6p1-TB (AAV2 vector backbone containing terminal repeats and poly A tail). The backbone vector was phophatased before ligation. All clones were digest checked for directionality of insert and to ensure minimal recombination (SmaI digest).

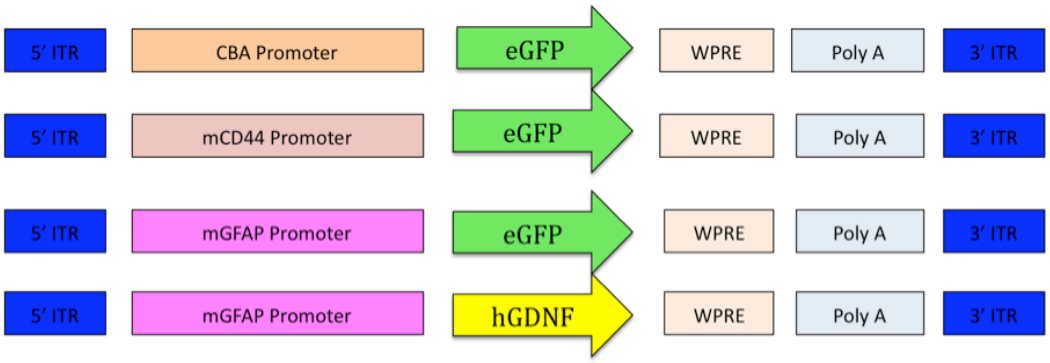

Figure 3.2. Adeno-associated viral transgenes were constructed by subcloning mGFAP or CD44 promoters and hGDNF or eGFP into an AAV2 transfer vector containing the WPRE enhancer element, and inverted terminal repeats (ITRs).

Lentivirus production

VSV-G pseudotyped virus was produced by the transient transfection of pMDLg/pRRE(gag/pol), pRSV-REV(reverse transcriptase), pmDG (vsvg), and transfer vector as described in *Greenberg et al.,* 2007. Virus was purified by sucrose gradient ultracentrifugation at 24,000 and 24,800 RPM. Pelleted virus was resuspended in cold PBS and flash frozen for storage at -80°C. Virus was used within two months of preparation. To try to improve the purity of the virus we tried adding the viral pellet (resuspended in lactose buffer) to an anion exchange column (Toyopearl DEAE-650C). The virus was washed and eluted with PBS in 1-4 ml fractions. The eluted virus was then concentrated by ultracentrifugation and the pellet was resuspended in 100µl sterile lactose buffer. To improve viral purity further we also attempted utilizing the His tagged

VSV-G envelope to allow for column purification as described by Yu and Schaffer, 2006.

Adeno-associated-virus production (AAV9, AAV8, and Shh10 evolved virus)

AAV-2/9 or 8 viruses were produced by triple transfection of 293T cells as previously described (Grieger *et al.,* 2006). A plasmid encoding for AAV9, AAV8, or Shh10 (AAV6 mutant) capsid proteins were used to pseudotype the vector. Cells were harvested 72 hours after transfection, lysed and treated with benzonase. The resulting clarified cell lysate was subjected to iodixanol density gradient purification. After ultracentrifugation, the interphase between the 54% and 40% iodixanol fraction, and the lower three-quarters of the 40% iodixanol fraction were extracted and diluted with equal volume of PBS+0.001% Tween20. Amicon Ultra-15 Centrifugal Filter Unit pre-incubated with 5% Tween in PBS and washed with PBS+ 0.001% Tween. The diluted iodixanol fractions were buffer-exchanged and concentrated to 250µl. Virus was washed three times with fifteen milliliters of sterile PBS+ 0.001% Tween. Vector was then titered for DNase-resistant vector genomes by Real-Time PCR relative to a standard. Finally, the purity of the vector was validated by silver-stained SDS-PAGE gel electrophoresis.

Virus titering

Functional titering of lentivirus was conducted as previously described (Satstry *et al*. 2002). In summary, 100,000 293T cells were infected with serial dilution of concentrated lentivirus. Four days post-infection, total DNA was harvested from infected

cells. The cells are counted before harvesting. Quantitative PCR of viral genomes was conducted to quantify functional viral transduction. WPRE primers were used for QPCR:

"WPRE F2" 5' CTGCTTTAATGCCTTTGTATCATGCTAT3'

"WPRE R2" 5' CAACTCCTCATAAAGAGACAGCAACCA 3'

Transducing units/mL were calculated as follows: (Copy #)/5 (μl in QPCR) x50ul (total volume in DNA prep)/10 (10x more cells were harvested than infected). Virus used in experiments displayed a functional titer on the order of $1x10^9$ to $1x10^{10}$ TU/mL.

Ocular Injections:

TgS334-4 rats at age p15 were used for all experiments. Before vector administration, animals were anesthetized with ketamine (72mg/kg) and xylazine (64mg/kg) by intraperitoneal injection. An ultrafine 30 1/2-gauge disposable needle was passed through the sclera, just below the ora serrata, into the vitreous cavity until the needle stopped at the retina. Three microliters of $5x10^{12}$ -$5x10^{13}$ vg/ml of AAV or $1x10^9$ to $1x10^{10}$ TU/mL of lentivirus was injected into the subretinal space with a blunt end Hamilton syringe. The subretinal injection was confirmed by the visualization of a retinal detachment through the surgical microscope.

Fundus Imaging:

In vivo retinal imaging was performed five days to four weeks after injections with a fundus camera (Retcam II; Clarity Medical Systems Inc., Pleasanton, CA)

equipped with a wide angle 130° retinopathy of prematurity (ROP) lens to monitor eGFP expression in live, anesthetized rats.

Cryosections:

Animals were humanely euthanized by CO_2 or isofluorene overdose and cervical dislocation. Eyes were enucleated, a hole was made in the cornea and eyes were fixed with 10% neutral buffered formalin overnight. The eyecups were washed in PBS and the cornea and lens were removed and then placed in 30% sucrose in PBS overnight. Eyes were then embedded in optimal cutting temperature embedding compound (OCT; Miles Diagnostics, Elkhart, IN) and oriented for 5-10μm thick transverse retinal sections.

Immunohistochemistry:

Tissue sections were rehydrated in PBS for five minutes and then incubated in blocking solution (1% BSA, 0.5%TritonX-100 and 2% normal donkey serum in PBS) for 2-3 hours. Slides were then incubated with commercial rabbit monoclonal antibody raised against the green-fluorescent protein (Invitrogen, Molecular Probes, Carlsbad, CA), rabbit monoclonal antibodies against GFAP (Sigma, L9393) at 1:1000 in blocking solution, or mouse monoclonal antibody raised against vimentin (Dako, Cambridgeshire, UK) at 1:1000 in blocking buffer overnight at 4ºC. The results were examined by fluorescence microscopy using an Axiophot microscope (Zeiss, Thornwood, NY) equipped with X-cite PC200 light source and QCapturePro camera or by confocal microscopy (LSM5; Carl Zeiss Microimaging). Images were prepared using Bitplane

Imaris image processing and manipulation software (Bitplane Inc., St. Paul, MN).

RT-PCR:

Retinas were quickly harvested and total RNA was extracted using RNeasy Kit (Qiagen). RNA was eluted in 30µl of DEPC-treated water followed by DNase treatment with Invitrogen DNase I, Amplification Grade. cDNA was synthesized with the Invitrogen ThermoScript RT-PCR kit. The primers used for PCR amplification were:

hGDNF Forward 5' - ATGAAGTTATGGGATGTCGT-3'

hGDNF Reverse 5' - TCACCAGCCTTCTATTTCTG-3'

ELISA:

Protein isolation buffer (50mM Tris-acetate, 65mM NaCl, 2mM MgCl2, 2mM EDTA, 1% protease inhibitors cocktail) and brief sonication was used to homogenize retinas or vitreous from treated and control animals. ELISA was performed using the DuoSet Kit for human GDNF (R&D Systems). A 96-wells plate was coated overnight with the capture antibody diluted in PBS. After incubation, wells were washed 3 times in wash buffer (0.05% Tween-20 in PBS) then blocked for 3 hours at room temperature with 1% BSA in PBS. After 3 rinses, samples and standard were added in duplicate for 2 hours. Samples were washed and then incubated with the detection antibody. After the last series of washes, the substrate solution was added for 20 minutes. At the end of the incubation stop solution was directly added to the wells. The optical density of each well

was determined immediately using a microplate reader set to 450nm. To correct for optical imperfections in the plate, 540 nm readings were subtracted from the readings at 450 nm. The amount of GDNF present in samples was calculated from a hGDNF standard curve. Results are the average of duplicates.

Electroretinography:

Transgenic S334 line-3 rats at ages P45, P60, or P100 were dark-adapted for four hours, anesthetized, and pupils dilated. Animals were placed on a heating pat and contact lenses were positioned on the cornea of both eyes. Reference electrodes were inserted subcutaneously in the cheeks and a ground electrode was inserted in the tail. Electroretinograms were recorded (Espion ERG stystem; Diagnosys LLC, Littleton, MA) in response to seven light flash intensities ranging from -4 (cds/m^2) to 1 cds/m^2. Each stimulus was presented in series of three. Light flash intensity and timing were elicited from a computer controlled Ganzfeld flash unit. Data were analyzed with MatLab (v7.7; Mathworks, Natick, MA). After correction for oscillatory potentials and heartbeat artifacts, scotopic a-wave values were measured from the baseline to the minimum ERG peak while scotopic b-waves were measured from the minimum to maximum ERG peaks. Data were analyzed using Student's *t* test.

Histology:

At P60, rats were euthanized by carbon dioxide overdose and cardiac perfusion with 2.5% glutaraldehyde and 2% formaldehyde in PBS. The superior cornea was marked for orientation. Eyes were enucleated and cornea and lens were removed.

Eyecups were further fixed in 1% osmium tetroxide, dehydrated by incubation in increased ethanol concentrations and a final incubation in 100% propylene oxide. The dehydrated samples were embedded in an epon-araldite resin and heated overnight at 65ºC. One-micrometer thin plastic sections of the eye were cut along the vertical meridian, through the optic nerve with a diamond blade. These sections were used to assess the thickness of the outer nuclear layer (ONL) (LaVail *et al.,* 1987). To account for variation in retinal degeneration in the TgS334 animal model, separate ONL measurements were taken of the superior and inferior retina (Green *et al.,* 2000). Retinal thickness measurements were made with a digitizing tablet (Wacom Technology Corporation**,** Vancouver, WA), a light microscope with camera lucida drawing tube and no-cost Axiovision morphometry software (http://www.zeiss.com/). Measurements from each region were averaged to obtain the mean ONL thickness. Data were analyzed with paired student's *t* test.

Results

1. Lentivirus mediated Gene Delivery Experiments

Lentivirus transgene expression profile after subretinal injection

VSV-G pseudotyped lentivirus infects Müller glia as shown by the observed reporter gene, GFP, expression in RMCs one week post subretinal injection. We chose to use the mGFAP promoter as GFAP expression is upregulated in the diseased retina, allowing for enhanced GDNF expression as disease progresses (Eisenfeld *et al.,* 1984). The mGFAP promoter restricts expression to the Müller cells (Figure 3.3). However, expression was weak and punctate with only sporadic Müller cells showing strong GFP. Furthermore, as a subretinal injection restricts the diffusion of viral particles, thus expression was limited to the area of detachment.

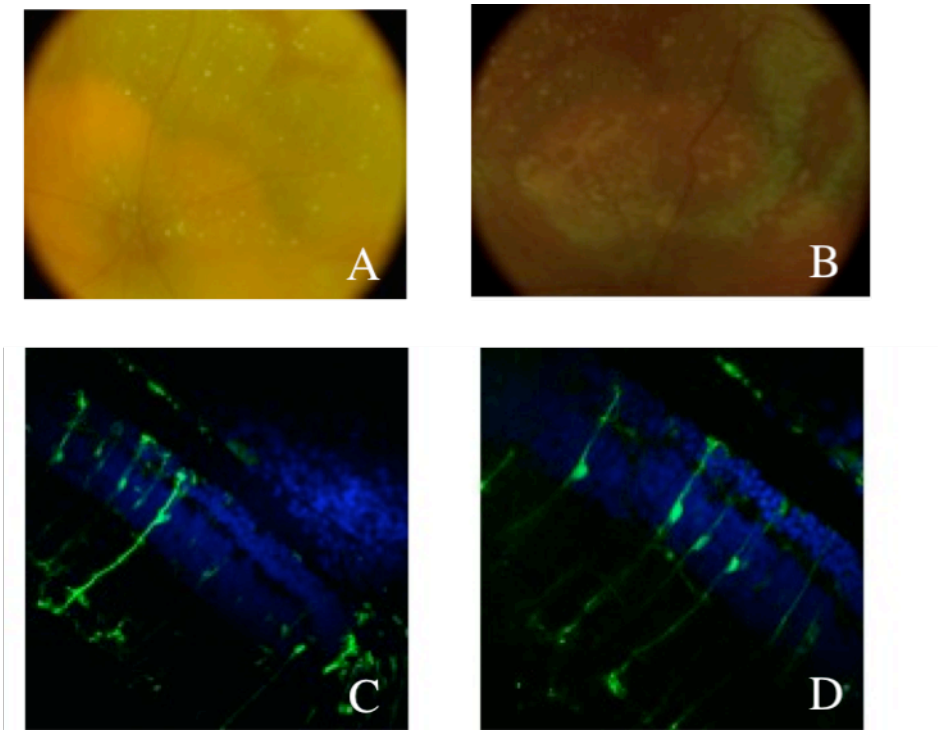

Figure 3.3. LV mGFAP.GFP vector drives weak expression in Müller glia one week after a subretinl injection of virus. Fundus imaging of miniCMV.eGFP-mGFAP.GDNF bicistronic LV vector 10 DPI (A) and mGFAP.GFP 10DPI (B). Cryosections show GFP expression from miniCMV.eGFP-mGFAP.GDNF (C) and mGFAP.GFP is specific to Müller glia (D).

Though the reporter gene, GFP, expression indicates that the GDNF should be expressed after hGDNF vector administration, we confirmed cDNA transcription by RT-PCR (Figure 3.4) and protein expression by ELISA in vivo one week post injection. hGDNF mRNA production in injected retinas was confirmed for all vectors.

Marker GDNF Plasmid GFP cDNA GFP No RT GDNF cDNA GDNF No RT Bicistronic cDNA Bicistronic No RT Fusion cDNA Fusion no RT

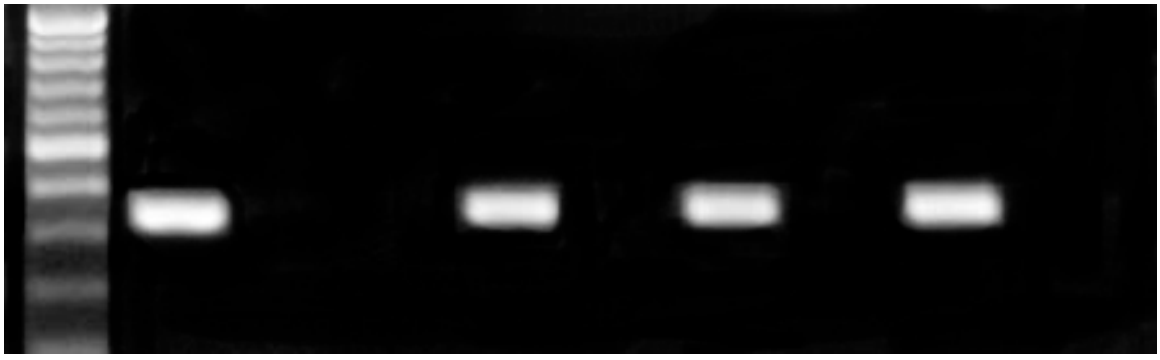

Figure 3.4. RT-PCR confirms that hGDNF mRNA is made only in retinas injected with hGDNF LV vectors.

The maximum concentration of hGDNF after LVmGFAP.hGDNF injection in retinal lysate as detected by ELISA was 64pg/ml. As this concentration is low by therapeutic standards, we repeated the experiment at different time points after injection and with multiple animals, however, we never detected larger concentrations of hGDNF. 293T cells infected with LV.mGFAP.hGDNF for 5 days produced 2ng/ml of hGDNF (a 30-fold increase when compared to in vivo data).

Functional and morphological rescue in TgS334ter-4 animals injected with LV mGFAP.GDNF

To determine the effects of Müller cell specific over-expression of hGDNF on photoreceptor survival in the S334ter-4 rat, we assessed functional and histological rescue. We obtained scotopic ERG recordings from P60 animals (n=9) injected with LV.mGFAP.eGFP in the left eye and LV.mGFAP.hGDNF in the right eye, 45 days post injection (Figure 3.5). We observed no significant difference in the a-wave amplitude after GDNF treatment. The average maximum a-wave amplitude was -61.22 ± 4.79 μvolts in GFP-injected eyes vs. -68.56 ± 8.04 μvolts in GDNF-injected eyes. However, the average maximum b-wave amplitude was significantly larger in the GDNF- injected eye (426.92 ± 47.10μvolts vs. 338.65 ± 28.25μvolts). At P60 the ERG was equal

between the treated and untreated eyes, therefore the minimal therapeutic effect was only temporary.

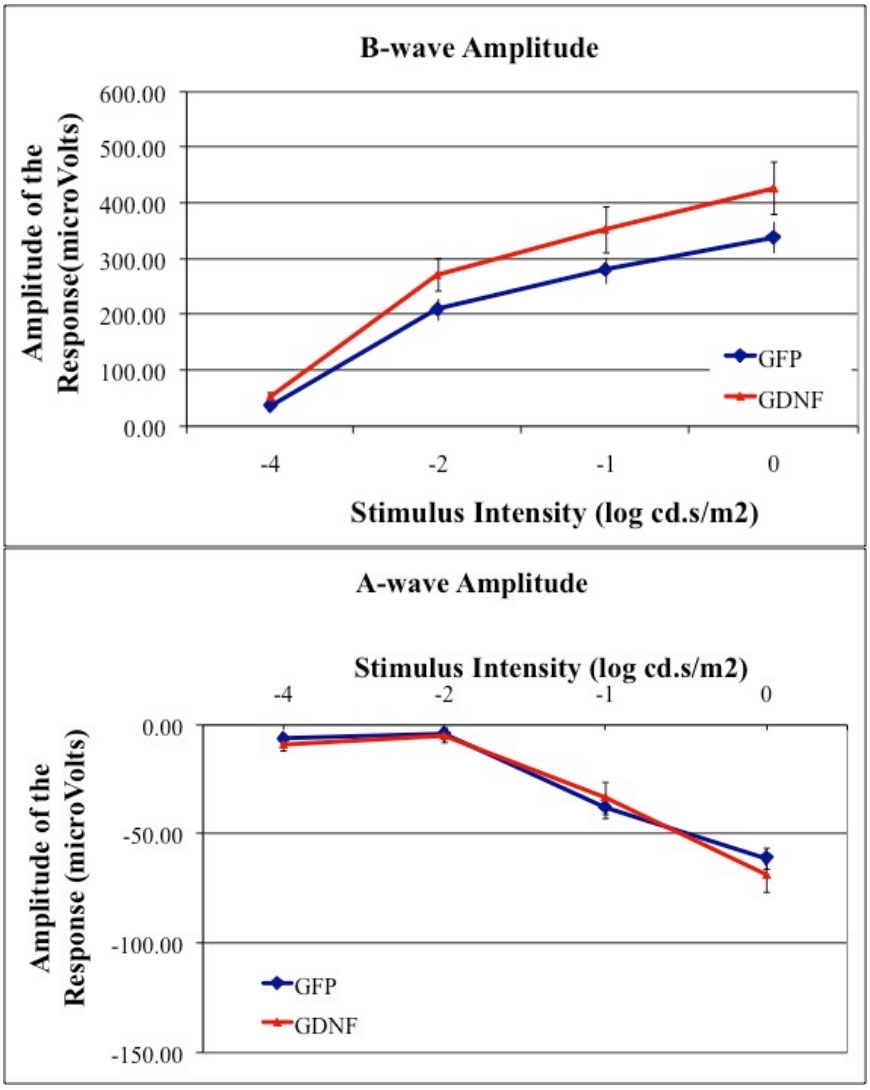

Figure 3.5. A and b-wave amplitudes at various light intensities from the S334ter-4 rats treated with LV.mGFAP.eGFP (blue line) and LV.mGFAP.hGDNF (red line). No significant difference in the a-wave amplitude was observed (bottom). However, the

average maximum b-wave amplitude was significantly larger in the GDNF-treated group (top) (n=9). ERGs were recorded 45 days post injection.

Morphological analysis of treated and control superior retinas showed no difference in ONL thickness (LV.mGFAP.GDNF-19.60 ± 4.13µm and LV.mGFAP.GFP control-19.09 ± 3.29µm) (Figure 3.6). On average, all retinas maintained 4 rows of nuclei. Similarly, analysis of the inferior retina showed no difference in retinal morphology between GDNF treated and untreated eyes (GDNF 25.14 ± 2.43µm *vs* GFP 26.85 ± 2.12µm). These data suggest that hGDNF treatment at the levels produced is not sufficient to slow photoreceptor apoptosis. These data are consistent with the lack of observed ERG a-wave improvement in treated eyes.

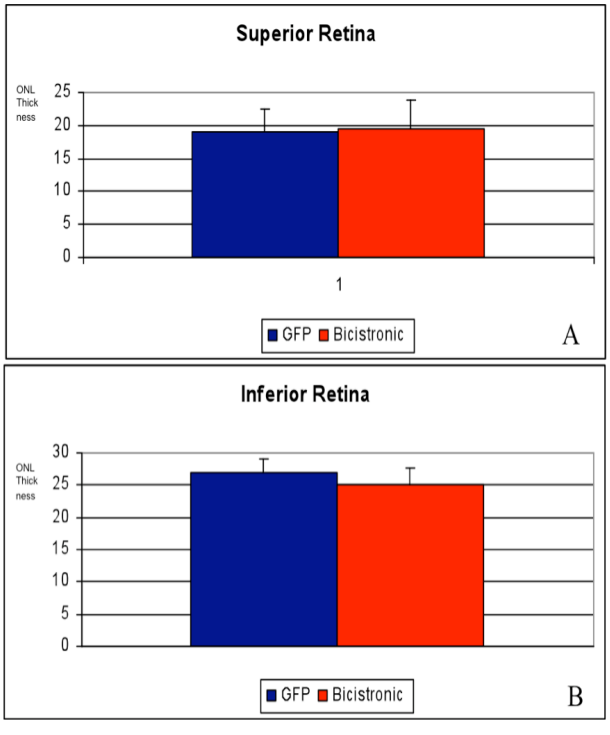

Figure 3.6. Histological analysis of remaining ONL in treated (red) and control (blue) P60 TgS334-4 eyes. No difference in ONL thickness was apparent for either the superior (top) or inferior retina (bottom) (n=9).

Targeted lentivirus transgene expression in Müllers Cells results in photoreceptor apoptosis

As LV mGFAP.hGDNF did not prove to successfully rescue photoreceptor degeneration, we decided to try an alternate promoter with the goal of enhancing transgene expression. Recent work by Greenberg and colleagues showed that the CD44 promoter drove the highest level of transgene expression when compared to the mGFAP and Vimentin promoters (Greenberg *et al.,* 2007). We thus replicated all experiments using lentivirus carrying the GDNF transgene driven by the CD44 promoter. Surprisingly, when this virus was injected subretinally, we observed both GFP expression (in LV CD44.GFP injected eyes) and massive auto-fluorescence (in LV CD44.GFP and GDNF eyes) (Figure 3.7). Morphological analysis showed complete photoreceptor loss in regions of auto-fluorescence. Photoreceptor loss and auto-fluorescence was restricted to the bleb where virus was delivered during the injection. Upon further analysis, we also observed some thinning of the ONL in animals injected with LV.mGFAP vectors. To further characterize this unexpected result, we decided to attempt GDNF delivery with an alternate vector, AAV. AAV viral preparation results in more pure virus, therefore we hoped to avoid possible contamination in the lentivirus preparation as well as any toxic effects of the LV infection.

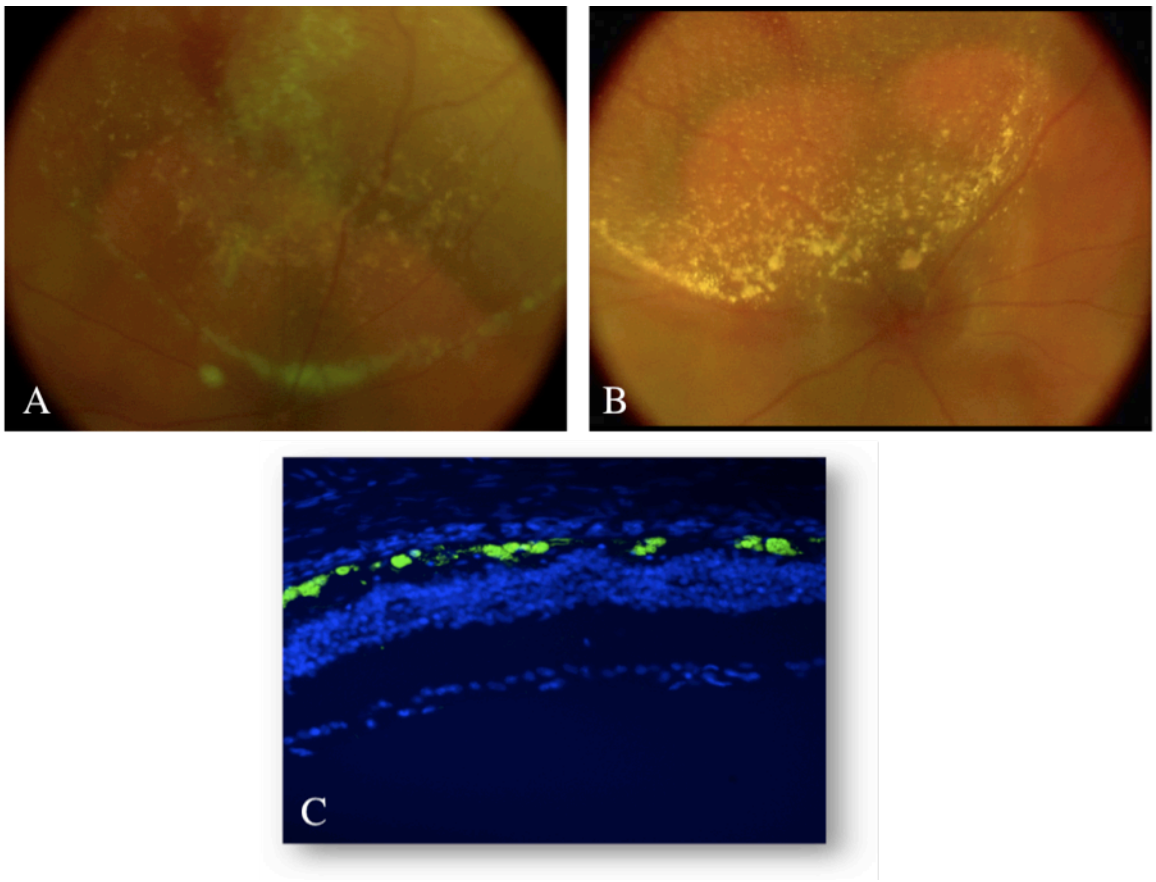

Figure 3.7. Fundus images of eyes injected in the subretinal space with 3 µl of LV.mCD44.GFP (A) or LV.mCD44.GDNF (B) at 10 days post-injection. Both GFP (A) and auto-fluorescence is visible (A, B). The cross-section of retina injected with LV.mCD44.GDNF seen in (A) shows an absence of ONL and auto-fluorescent aggregates (green) accumulated between the INL and RPE.

2) AAV Mediated Gene Delivery Experiments

High efficiency targeting of retinal Müller cells with AAV vectors

Recent studies have shown that AAV8 and 9 are capable of high efficiency infection and transgene expression in RMCs when delivered to the subretinal space (Allocca *et al.,* 2007). In these studies a ubiquitous promoter was utilized, resulting in transgene expression in photoreceptors, RMCs, and RPE. Therefore, we assessed the ability of AAV8 and 9 to drive restricted hGDNF expression in RMCs with the aforementioned glial specific promoters, mGFAP and CD44. We reasoned that enhancing hGDNF expression could improve functional rescue. Furthermore, if lentivirus infection or lack of purity of the LV preparation causes the observed retinal toxicity, the cleaner and well-characterized AAV preparations would likely avoid such damaging effects on the retina. Initial experiments comparing CBA promoter driven GFP expression with AAV8 and 9 indicated that AAV9 mediated the strongest infection of RMCs, therefore subsequent experiments were conducted with AAV9 (Figure 3.8).

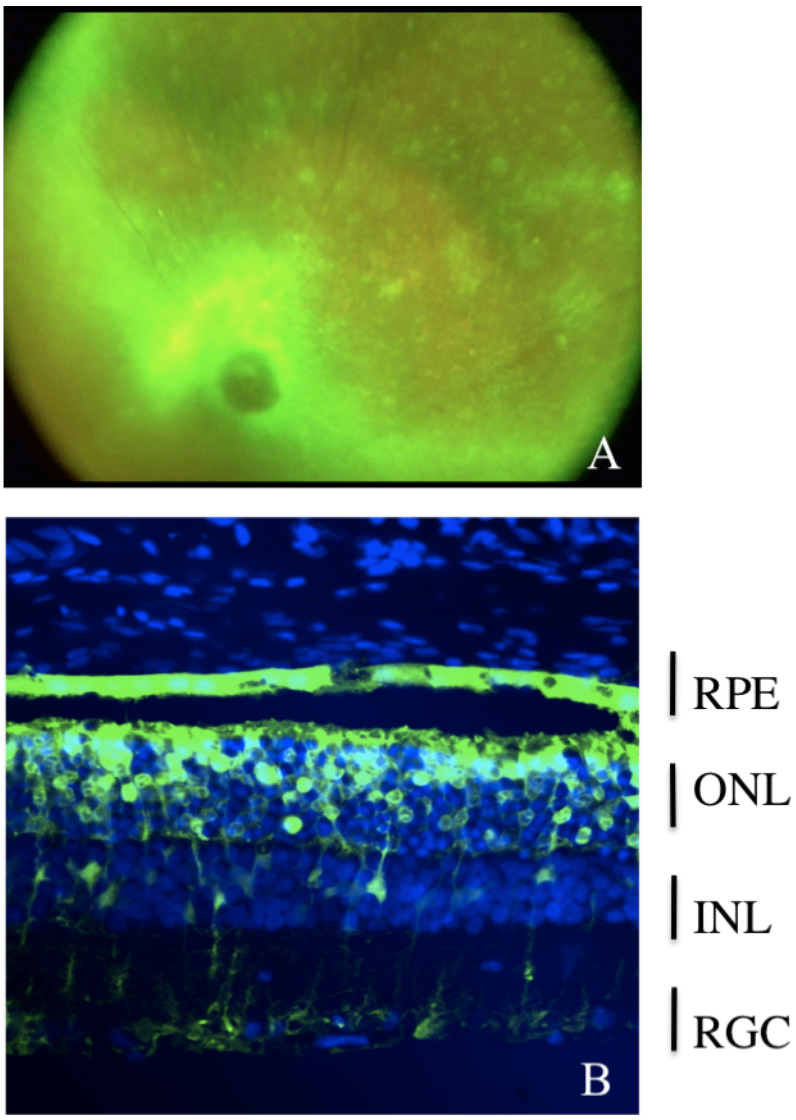

Figure 3.8. Subretinal injection of 3µl of AAV2/9 CBA.GFP results in early onset expression (3 days post injection) in photoreceptors and outer segments, RPE, and Müller cells. Nuclei are stained with DAPI. Fundus image taken one-week post injection (A). Retinal cross section of retina (B) (40x).

Surprisingly, when the CBA promoter was switched to the CD44 promoter (Müller cell specific promoter; Greenberg *et al.,* 2007), we observed minimal Müller cell transduction. GFP expression was most notable in photoreceptors and RPE.

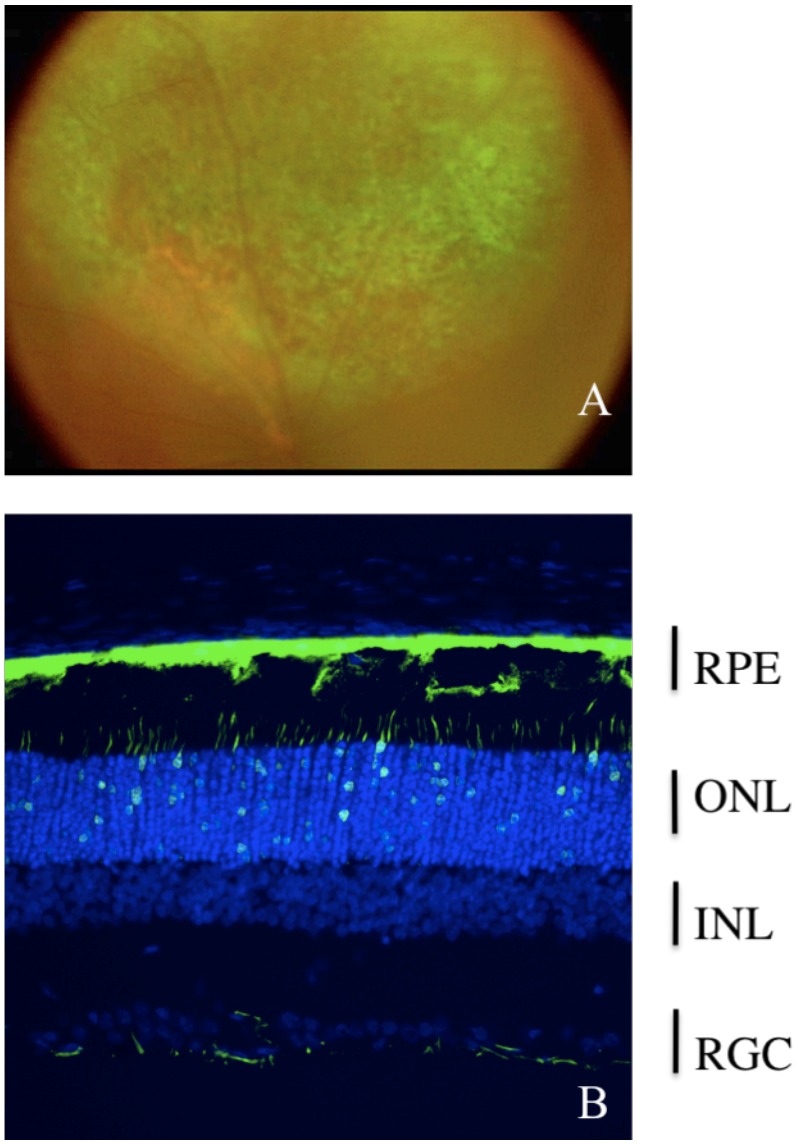

Figure 3.9. Subretinal injection of 3µl of AAV9 CD44.GFP results in early onset expression (3 days post injection) primarily in photoreceptors and RPE. Nuclei are

stained with DAPI. AAV2/9 mCD44.GFP fundus image (A) and retinal cross section (B).

However, the mGFAP promoter did drive restricted expression in RMCs when delivered with AAV9 (Figure 3.10). These data showed the most promising combination of vector and promoter as reporter gene expression was restricted to RMCs and expression was by far the most robust compared to the other promoters used (also compared to AAV8, data not shown). Therefore, all subsequent rescue experiments utilized AAV9 and the mGFAP promoter.

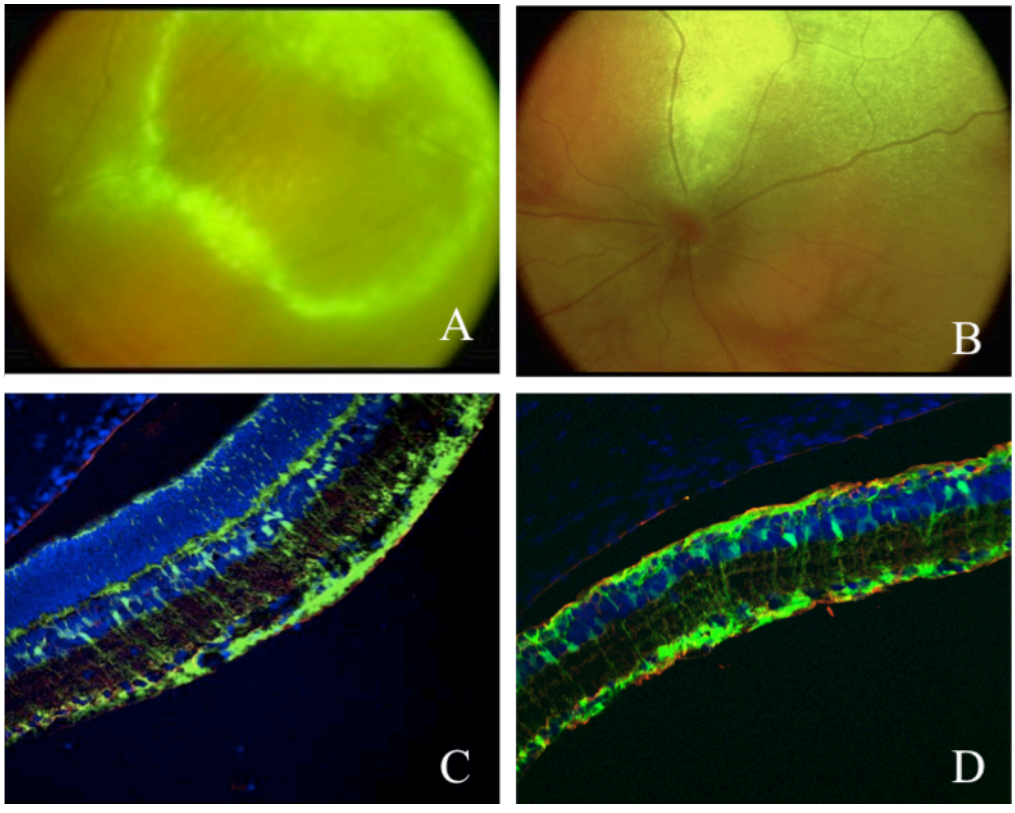

Figure 3.10. Subretinal injection of 3µl of AAV9mGFAP.GFP results in expression as early as three days post injection that is restricted to Müller cells. AAV9 mGFAP.GFP fundus images (A) WT (B) S334-4. WT retinal cross section (C). S334-4 retinal cross section stained with Glutamine Synthetase (Cy-3) (D) (25x). Nuclei are stained with DAPI.

hGDNF production and therapeutic value of AAV9 hGDNF delivery in S334ter rats

The observed level of Müller cell GFP expression in animals injected with AAV9 mGFAP.GFP indicated that this combination of delivery route, promoter, and virus could be the optimal method of restricted delivery of hGDNF to the retina. To confirm that therapeutic levels of hGDNF were being produced and secreted in the retina, we measured protein concentration by ELISA in retinal homogenates and vitreous of injected animals (3.11). At 5 days post-injection hGDNF concentration in retinal homogenates was 500 ± 112 pg/ml, 7.8-fold higher than what we measured in retinal homogenates from animals injected with LVmGFAP.hGDNF (n=9). Twenty days post-injection, hGDNF concentration was measured to be 2ng/ml (n=7). hGDNF concentration was 250pg/ml in the vitreous, indicating that the protein was indeed secreted from transduced Müller cells. Furthermore, these levels of hGDNF are equal to or greater than that produced in previous studies that have achieved photoreceptor degeneration rescue through GDNF overproduction (Gregory-Evans *et al.,* 2009).

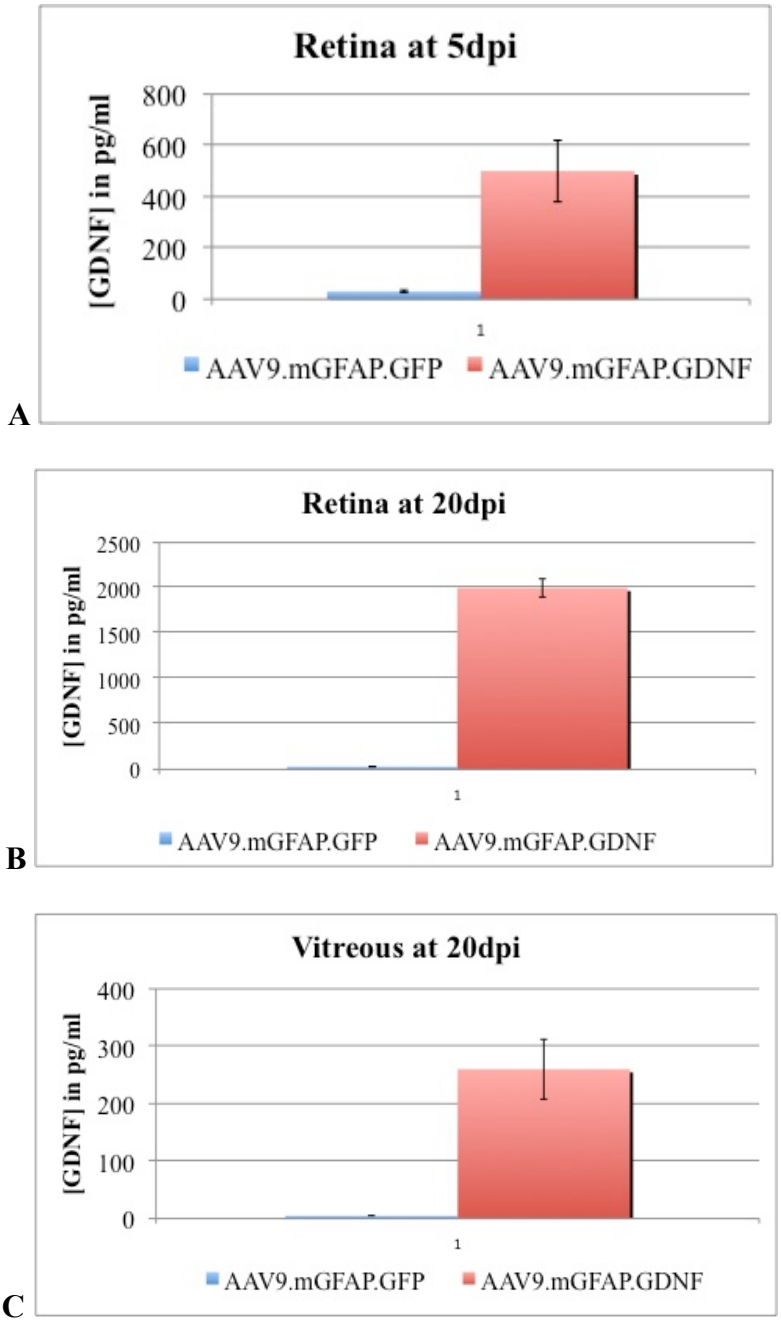

Figure 3.11. hGDNF protein expression levels were measured by ELISA 5 days (A) and 20 days (B) following sub-retinal delivery of AAV9.mGFAP.GDNF in the retina.

hGDNF secretion was also achieved as shown by ELISA measurements of GDNF in the vitreous (C).

As hGDNF production and targeted transgene expression showed very promising results, we assessed functional rescue. Thirty and forty-five days post AAV9 mGFAP.hGDNF injection into the subretinal space, ERGs were recorded. Treated eyes were compared to the internal untreated eyes of a litter of TgS334ter animals (n=12). Not only did we not observe functional rescue, the treated eye ERG a- and b-waves were reduced across animals (data not shown). To confirm the viral preps were not contaminated we performed silver stain analysis (Figure 3.12).

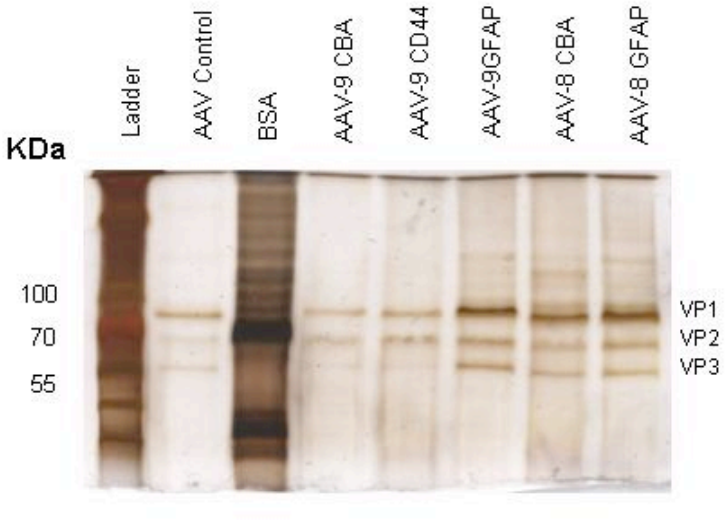

Figure 3.12. Silver stained gel of AAV vectors confirms purity of injected virus.

AAV9 mediated transgene expression in Müller Cells causes retinal toxicity

We were surprised to see a reduced ERG after AAV injection as AAV vectors are very well characterized and have not been shown to be toxic. Furthermore, AAV preparations are extremely pure, unlike the lentivirus preparations used in early experiments (Greenberg *et al.,* 2007; Grieger *et al.,* 2006). Since AAV, as well as lentivirus, displayed toxicity when transgene expression was limited to Müller glia, it appears unlikely that the nature of the viral infection itself was causing the damage. Could restricted transgene expression in Müller glia be toxic? To answer this question we developed an AAV vector with the serotype 2 backbone (like all other AAV vectors used), an mGFAP promoter followed by a scrambled, non-coding sequence. This vector was to test whether the transgene expression itself was causing the observed retinal toxicity. One-week post-injection, fundus images of treated animals were taken and ERGs were performed. Animals were injected with the AAV9 mGFAP.Empty vector in only one eye so that the contralateral eye could serve as a control. Fundus images displayed autofluorescene that indicated toxicity (Figure 3.13) and the ERG a and b-wave were both reduced (Figure 3.14). As the AAV9 CBA.GFP displayed no discernable toxicity, the ERG results suggest that the mGFAP promoter itself, perhaps in concert with the route of vector delivery is causing toxicity. The exact mechanism by which this damage is occurring is unknown.

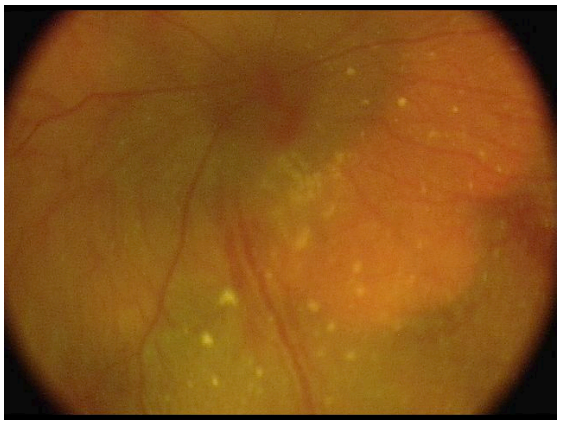

Figure 3.13. Fundus image of animal injected with AAV9mGFAP.Empty into the subretinal space, one-week post injection. Autofluorescence appears in yellow throughout the region of detachment.

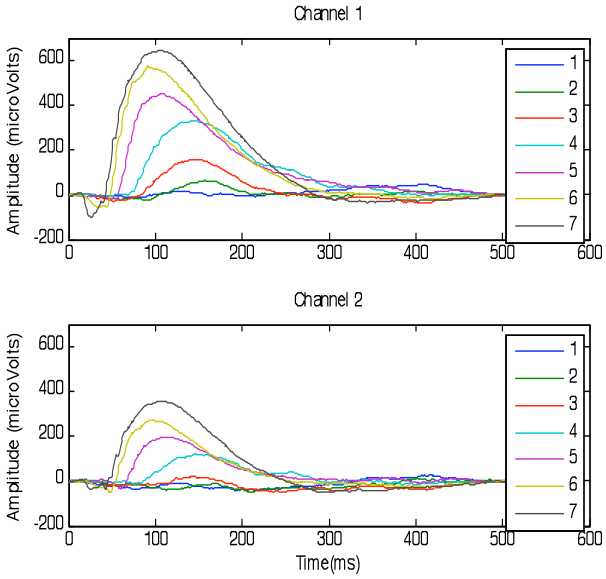

Figure 3.14. Average ERG traces of TgS334-4 animals one week post AAV9.mGFAP.Empty subretinal injection (channel 2, RE) and PBS (channel 1, LE) (n=6).

Evolved AAV vector, ShH10, shows restricted Müller cell transduction from the vitreous with the ubiquitous chicken-beta-actin promoter

The observed toxicity was concerning as it remains unknown why such damage is occurring. Our experiments suggest that the promoter and/or route of delivery are the most likely culprits for the observed damage. In parallel with the discussed work, in graduate student, Ryan Klimczak, in collaboration with members of Dr. Schaffer's Lab (JT Koerber) engineered an evolved AAV vector that restrictively and efficiently targets astrocytes. More specifically, large and diverse, AAV vector libraries were generated from DNA shuffling and error-prone PCR approaches (Maheshri *et al.,* 2006; Jang *et al.,* 2007). Each variant was subjected to positive selection by infecting specific glia (in vivo and *in vitro*) and vectors with enhanced permissivity to astrocytes were isolated (Koerber *et al.,* 2009 *under review*). One such variant efficiently and specifically transduced retinal Müller glia from the vitreous (Koerber *et al.,* 2009 *under review*; Klimczak *et al., under review*) (Figure 3.16). The Shh10 variant is most closely related to AAV6. Only four mutations separate Shh10 from AAV6. This small change in capsid amino acid sequence results in robust RMC transduction from the vitreous (3.15, 3.16). Shh10's transduction efficiency and specificity is superior to that of the naturally occurring AAV2, which is the best AAV vector for retinal transduction when delivered intravitreally (Figure 3.16). Furthermore, the capsid controls largely restricted infection of glia, therefore a cell-type specific promoter is no longer necessary. Therefore, by utilizing the engineered AAV vector we would avoid the possibly damaging effects of the subretinal delivery route and the cell-type specific promoter.

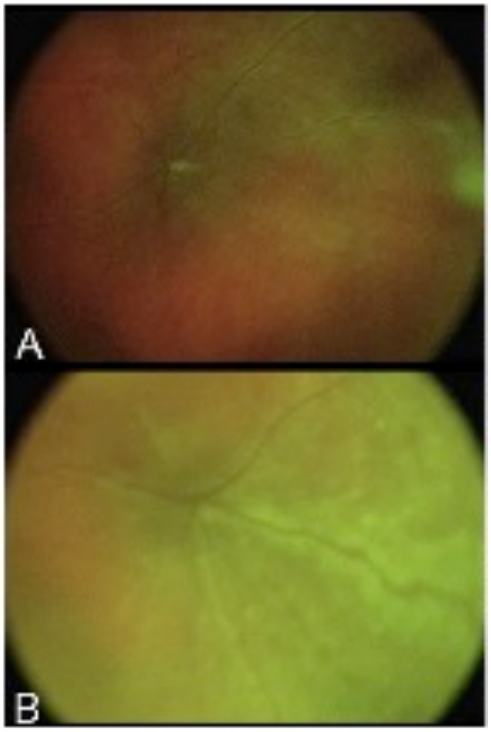

Figure 3.15. Fundus images of animals injected with Shh10 dsCAG.GFP, one-week post inejction (A). Expression increases three weeks post-injection (B).

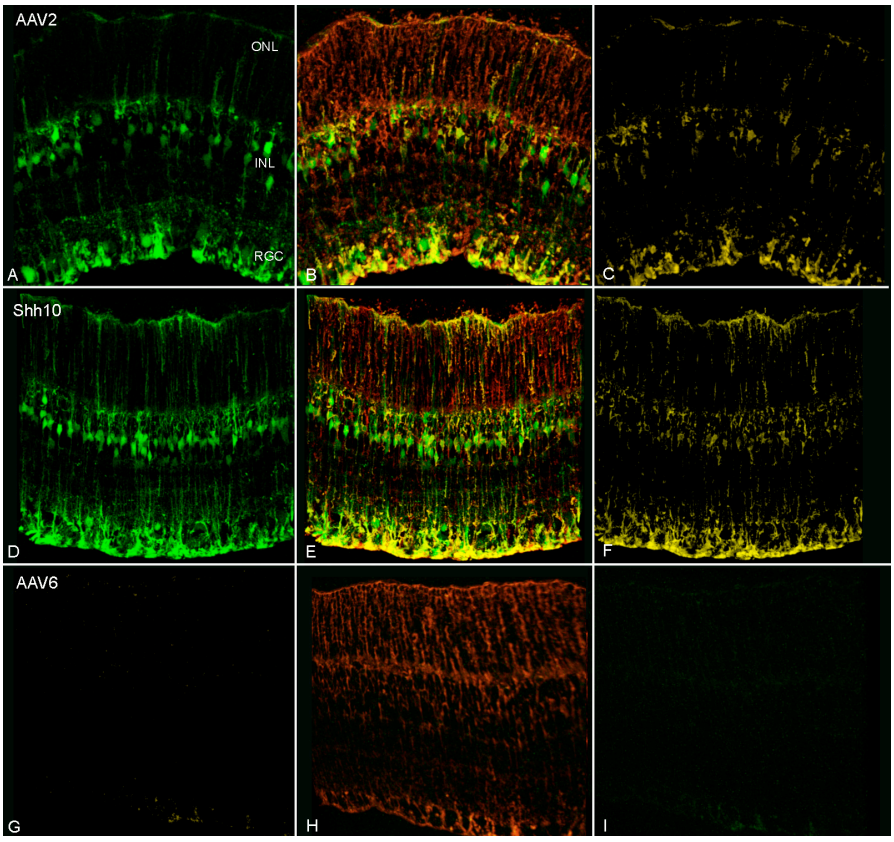

Figure 3.16. Directed Müller cell transduction when animals are injected into the vitreous with Shh10 dsCAG.GFP (D, E, F). Shh10 mediated transgene expression is more robust and specific than AAV2 transduction from the vitreous (A, B, C). RMCs are labelled with GFAP antibody (red) and yellow shows colocolization. Shh10 is a derivative of AAV6, which shows no Müller cell specific transduction when delivered from the vitreous (G, H, I) (45x).

Not only was transgene expression robust after Shh10 gene transfer, the spread was throughout the retinaas the intravitreal injection allows for greater vector diffusion and no auto-fluorescence was visible in the fundus images. Furthermore, ELISA data

showed high levels of hGDNF production in retinal homogenates of animals injected with Shh10 CAG.hGDNF (Figure 3.17).

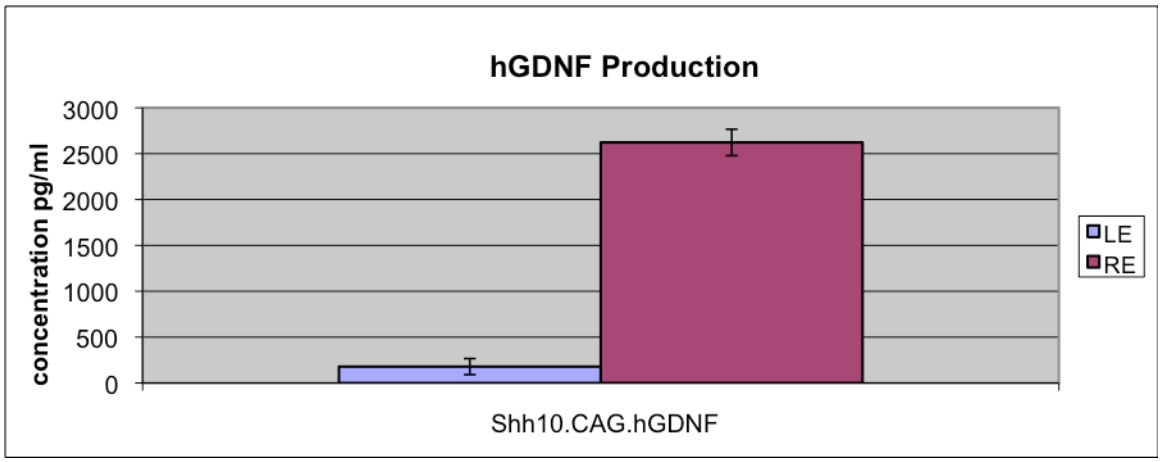

Figure 3.17. hGDNF protein expression levels were measured by ELISA 2 months following intravitreal delivery of Shh10 CAG.hGDNF (n=7). All animals received hGDNF vector treatment in the RE and no injection in the left eye.

While expression data is very promising, one-month post-injection of Shh10 CAG.hGDNF, no consistent functional rescue was observed by ERG analysis. However, recent data indicates that two and three months post injection there is a noticeable trend towards a and b-wave rescue (Figure 3.18, 3.19). Strong functional rescue was seen in five out of nine animals two months post injection and three out of six animals three months post injection. Furthermore, there is great variability in the ERG of the control eyes between animals. Thus, the difference in a and b wave values between treated and untreated eyes are not significant. Some differences between treated eyes may be caused

by the variability in the injection. Therefore, we are in the process of correlating ERG responses with hGDNF production and retinal morphology in individual animals.

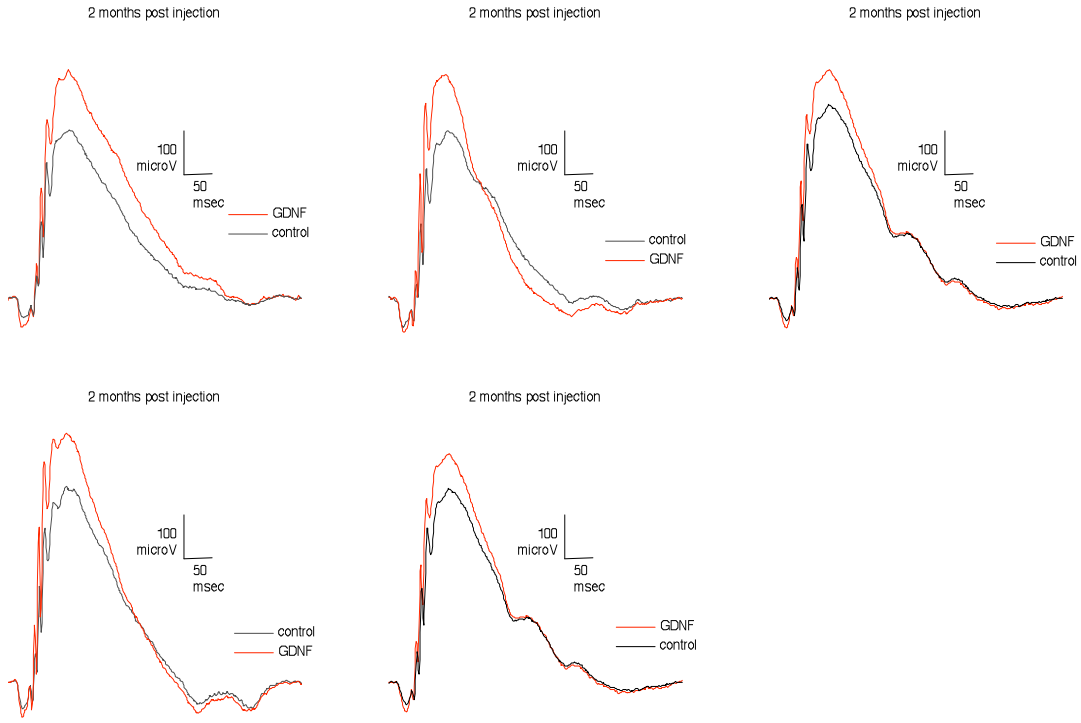

Figure 3.18. ERG responses to the highest light intensity from a litter of TgS334-4 animals injected with Shh10 CAG.hGDNF at age P15 (ERGs were taken two-months post injection) (n=5/9 injected). Animals were injected in the right eye (red traces) with the hGDNF vector and no injection was performed on the control left eye (black traces).

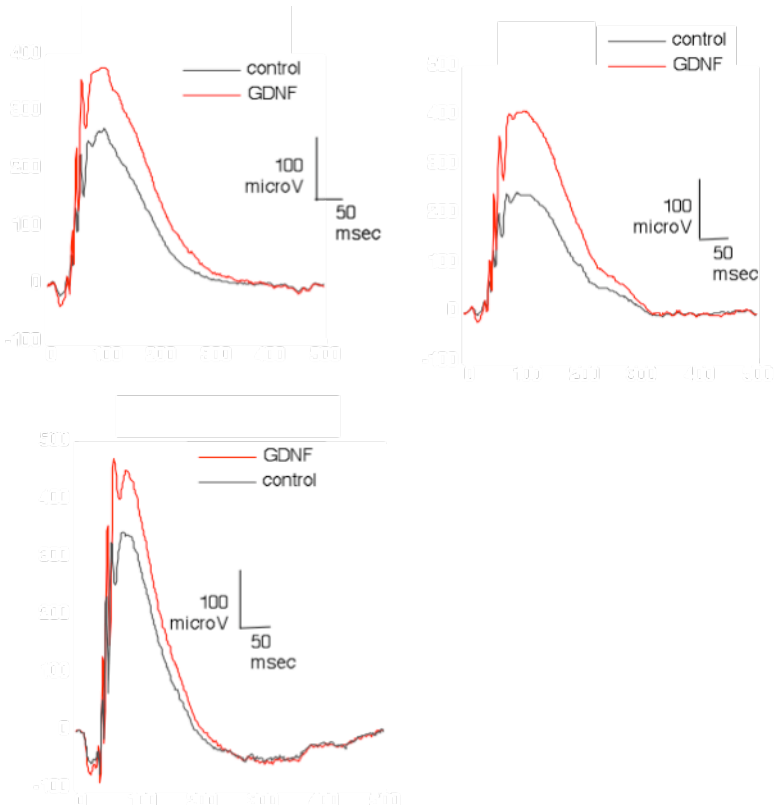

Figure 3.19. ERG responses to the highest light intensity from a litter of TgS334-4 animals injected with Shh10 CAG.hGDNF at age P15 (ERGs were taken three-months post injection) (n=3/6 injected). Animals were injected in the left eye (red traces) with the hGDNF vector and no injection was performed on the control right eye (black traces).

Discussion

In the current study, much effort was invested in the optimization of hGDNF gene transfer to retinal Müller cells in order to achieve long-term and maximal preservation of retinal function and structure in an animal model of retinitis pigmentosa. We did accomplish restricted and sustained hGDNF production in retinal Müller cells by optimizing gene delivery through vector, delivery route, and promoter manipulation. Trophic factor mediated rescue of retinal degeneration in an animal model of retinitis pigmentosa via Müller cell trasduction with a therapeutic vector remains a work in progress, though we have seen the beginnings of functional improvement. During this process surprising questions concerning the toxic side effects of subretinal gene delivery were raised.

Through lentiviral delivery of hGDNF (driven by the mGFAP promoter) to retinal Müller cells, we were able to preserve the b-wave of the ERG, but not the a-wave in an animal model of retinal degeneration. Morphological assessment showed no slowing of ONL thinning after treatment. One possible explanation for these results is that at the levels produced by LV gene delivery, hGDNF is acting not to slow photoreceptor apoptosis but enhancing photoreceptor-bipolar synaptic efficacy. Previous studies have shown that GDNF enhances dopaminergic neuron synaptic efficacy by increasing the number of functional synaptic terminals and enhancing dopamine and glutamate (co-transmitter) release (Bourque and Trudeau 2000; Pothos *et al.,* 1998). GDNF also modulates neuromuscular junction synaptic activity and induces hyper-innervation of the NMJ when over-expressed through development (Nguyen *et al.,* 1998; Wang *et al.,* 2001). Though the mechanism of GDNF's action on neural synapses is not

fully elucidated, the trophic factor has been shown to directly modulate glutamate release (Bourque and Trudeau, 2000). As glutamate is the primary neurotransmitter for photoreceptor-bipolar cell communication, it is possible that hGDNF expression is acting to modulate glutamate release, rather then specifically exerting its effects on photoreceptor survival.

Unfortunately, further experimentation not only showed no positive hGDNF effect on photoreceptor survival and function, but also suggested that either the virus, purification method, or transgene itself was toxic over time. Toxicity was shown by lipofuscin accumulation between the ONL and RPE and photoreceptor apoptosis when glial specific promoters drove transgene expression. Therefore, even if synaptic efficacy could be enhanced at the photoreceptor-bipolar cell synapse, this effect would be temporary as photoreceptor apoptosis was enhanced with this method. We hypothesized that the toxic effects are likely to be related to the purity of the lentiviral prep or transgene integration. As there is no column purification step in our protocol for lentiviral preparation, we attempted alternative protocols aimed to increase purity (His-tag VSV-G envelope for column purification; Yu and Schaffer, 2006) and even purchased our preparation from a company that produces clinical-grade virus with proprietary methods (Lentigen Co. Gathersburg, MD). Unfortunately, none of these attempts produced pure virus of a high enough functional titer to robustly transduce RMCs and express hGDNF at a therapeutic level.

One property of lentivirus is that in order to successfully function as a gene delivery vector, the transgene must integrate into chromosomal DNA (Naldini *et al.,* 1996). Depending on the integration site, insertional mutagenisis could be related to the

observed cytotoxicity. Recently, a non-integrating lentiviral vector was developed that could be used to avoid this risk (Philpott and Thrasher, 2007; Yáñez-Muñoz *et al.,* 2006).

The observed toxicity of lentiviral vectors in combination with low levels of hGDNF production provided the impetus for us to alter our method of gene delivery. By utilizing AAV2/9 to deliver hGDNF to the retina, we were able to greatly enhance hGDNF production and secretion. However, again, cytoxicity was observed in the form of photoreceptor death as well as depressed ERG. As AAV is well characterized as a non-toxic vehicle for gene delivery, it is unlikely that the virus itself is causing the response (Auricchio, 2003; Buning *et al*., 2008; Buch *et al*., 2008; Surace and Auricchio 2003). Further experimentation suggests that the promoter, mGFAP, is likely to initiate the toxic response, however the mechanism by which this is occurring is unknown (Figures 3.8, 3.13, 3.14).

Retinal stress induced by degeneration or detachment causes RMC activation and an increase in GFAP expression (Bringmann and Reichenbach, 2001; Eisenfeld *et al.,* 1984). However, an increased copy number of GFAP promoter DNA sequences (from the introduced transgene) may recruit and monopolize transcription factors necessary for this stress response. Without an appropriate GFAP infrastructure, axonal regeneration is delayed after peripheral nerve damage and the retina is more susceptible to mechanical damage (Lundvist *et al.,* 2004; Triolo *et al.,* 2006). In summary, a very theoretical explanation for our results is that a lack of appropriate glial activation due to mGFAP promoter presence could cause changes in retinal resistance to stress induced damage from the retinal detachment during injection and disease related degeneration.

We were finally able to achieve robust, non-toxic, hGDNF gene transfer and expression by utilizing the engineered AAV vector, Shh10. Employing a virus that specifically and robustly transduces glia allowed us to avoid the use of the mGFAP promoter that evidence suggests causes cytotoxicity. In addition, we were able to achieve therapeutic levels of hGDNF production and avoid the damaging subretinal injection. However, not until two months post-injection did we observe hints of retinal function preservation. In previous studies, AAV delivery of hGDNF to the photoreceptors achieved functional rescue 1.5 months after injection (McGee-Sanftner *et al.,* 2001). A major difference between the two methods of hGDNF delivery to the retina is the route of administration: subretinal vs. intravitreal delivery. The subretinal injection used by McGee-Sanftner and colleagues causes injury-related rescue by an increase in basic fibroblast growth factor production (Faktorovich *et al.,* 1992; Ozaki *et al.,* 2000). The non-invasive intravitreal injection we utilized in the current study does not induce the injury related burst in trophic factor secretion. Therefore, disease rescue will only be initiated once hGDNF has accumulated to appropriate levels at the correct location. In our present study, this threshold does not appear to be achieved until two months post injection. However, further functional and morphological assessments need to be made at different time points after therapeutic vector administration. These experiments need to be correlated with hGDNF production in treated animals to account for variability in vector delivery.

Finally, is hGDNF the optimal trophic factor for this method of inherited blinding disease therapy? As hGDNF has been described as a potent neurotrophic factor for ocular gene therapy, our first inclination was it is likely to be a very good option

(Andrieu-Soler *et al.,* 2005; Frasson *et al.,* 1999; McGee-Sanftner *et al.,* 2001; Wu *et al.,* 2002). However, as described by previous research, bFGF interacts directly with photoreceptors to exert pro-survival effects, is upregulated during retinal stress leading to the slowing of retinal degeneration, and it appears that hGDNF's (and other trophy factor's) pro-survival effects are mediated through the upregulation of bFGF (Faktorovich *et al.,* 1990; Faktorovich *et al.,* 1992; Fontaine *et al.,* 1998; Harada *et al.,* 2000; Hauck *et al.,* 2006; Ozaki *et al.,* 2000). In addition, *in vitro* studies have shown that bFGF induces an increase in endogenous bFGF production in RMCs (Cao *et al.,* 1997). Basic fibroblast growth factor transgene delivery to RMCs could both directly exert pro-survival effects on photoreceptors as well as initiate a positive feedback loop to increase RMC production of bFGF. Therefore, we are in the process of assessing the effects of bFGF transgene delivery to RMCs with the hope that this method of gene therapy will provide a more direct and subsequently more robust way of preserving photoreceptor structure and function in an animal model of retinitis pigmentosa.

Chapter 4

Engineered Light Activated Glutamate Receptor Drives Visual Responses in the Cortex of Blind Animals

Preface

This work was done in collaboration with Dr. Natalia Caporale, a postdoctoral fellow in Professor Yang Dan's lab at UC Berkeley. The foundational work (development of LiGluR) for this project was conducted in Professor Ehud Isacoff's lab at UC Berkeley (Volgraf et al. 2006; Gorostiza et al. 2007; Szobota et al. 2007). Tracy Huang, a graduate student in Dr. Richard Kramer's lab performed the multi-electrode array recordings. Meike Visel provided technical assistance.

Abstract

An alternative therapy for inherited blinding diseases such as retinitis pigmentosa is to confer light sensitivity on second and/or third order neurons in the retina. One benefit of this approach is it provides a treatment for late stages of retinal degeneration, where the majority of photoreceptors have already been lost. We have delivered an engineered light sensitive protein to retinal ganglion cells in animal models of photoreceptor degenerative diseases. This light sensitive protein is capable of mediating finely tuned control of single neuron activity in hippocampal cell culture (Szobota *et al.*, 2007). We utilized adeno-associated virus (serotype 2) to deliver LiGluR cDNA to retinal ganglion cells under the control of the human synapsin promoter. We show temporally precise and robust photo-activation in *in vitro* retinal tissue preparation. These recordings demonstrate cell ensemble photo-activation that requires AAV-2 introduced LiGluR expression in retinal ganglion cells and MAG photoswitch labeling. Though these recordings establish that light sensitivity can be re-introduced to and mediate electrophysiological activity in remaining neurons of the degenerating retina, our next step was to assess information transduction of LiGluR mediated retinal responses to the visual cortex. We recorded and characterized in vivo cell population responses (visually evoked potentials, VEPs) in V1 when visual input is limited to LiGluR induced activity in the retina. VEPs driven by LiGluR are approximately 50% of the amplitude of full field light flash driven responses in the wild type animal. We are now mapping LiGluR driven single cell receptive field and orientation tuning in V1 and

aim to assess LiGluR driven behavior in the same mouse model of severe retinal degeneration.

The naturally occurring light activated channel, channelrhodopsin, is an increasingly well-characterized tool for the re-introduction of light sensitivity to the degenerating retina. There are distinct differences between channelrhodopsin and LiGluR that include wavelength tuning, conductance and activation properties, and photoswitch requirements. Therefore, we wanted to compare LiGluR and channelrhodopsin driven visually evoked potentials in V1. Each channel was expressed in the retinal ganglion cells of rd1-/- animals by means of the same viral delivery vehicle (AAV-2) and under the control of the same promoter (human synapsin). We discovered that LiGluR mediated responses are at least three fold larger in amplitude when compared to channelrhodopsin2.

In summary, our initial characterization of LiGluR driven cortical responses in blind animals suggests that it is a promising therapy for restoring visual function in the late stages of retinal degeneration.

Introduction

There is a limited therapeutic window for patients suffering from retinal degenerative diseases who are seeking gene replacement or trophic factor treatment to slow or stop photoreceptor apoptosis. For example, Leber's Congenital Amaurosis is a disease characterized by very early onset and rapid photoreceptor degeneration, with severe cases resulting in an un-recordable ERG within the first two years of life and complete blindness by early teenage years (Hanein S *et al.,* 2004). Until recently, little work has been done to explore treatment options for end stage retinal disease. Some research has been conducted utilizing classical gene therapy methods during middle to late-stage degeneration. These groups were able to achieve a degree of histological maintenance with gene replacement or RNAi knockdown techniques in animal models of X-linked retinoschisis and autosomal dominant retinitis pigmentosa (P23H rat), respectively (Janssen *et al.,* 2008; LaVail *et al.,* 2000). However, functional rescue was either not attempted or not achieved as shown by electroretinogram analysis in these studies. Therefore, in cases of rapid retinal degeneration or for older patients who have received no viable treatment options during disease progression, a therapy to introduce light sensitivity to remaining, healthy cells, in the degenerated retina is a promising option. In the present study, we restored light sensitivity to the retina by viral delivery of an engineered, genetically encoded, light activated glutamate receptor (LiGluR). Once light sensitivity was re-established in retinal ganglion cells, we explored LiGluR mediated input to the visual cortex.

Currently, the most popular approaches to restoring visual responses in the retina after photoreceptor cell loss are conferring light sensitivity on second or third

order neurons by gene transfer of photosensitive proteins, employing stem cells to directly replace lost photoreceptors, or the implantation of an array of electrodes on the surface of the retina for direct stimulation (Lagali *et al.,* 2008; Weiland *et al.,* 2005; Yu and Silva, 2008). The use of retinal prosthetics has made significant headway as these "chips" have already been implanted in patients as a treatment for late stage retinal disease. The limitations of this approach include the low resolution of stimulation achieved with a restricted number of electrodes and the risk of damaging the retina during implantation. Furthermore, when the retina has been severely damaged during degeneration, the efficacy of stimulation is reduced (Weiland *et al.,* 2005).

A recent study elegantly showed that by injecting photoreceptor precursor cells isolated from an embryonic retina during photoreceptor genesis into an animal model of retinal degeneration, both molecular and functional rescue is achieved (MacLaren *et al.,* 2006). By immuno-staining for photoreceptor markers and crucial synaptic and phototransduction pathway proteins, the researchers demonstrated that stem cells properly differentiate and make synaptic contacts with bipolar cells. Retinal function improvements were found by measuring light-evoked extracellular field potentials in the retinal ganglion cell layer and pupillary reflexes. Though very promising, there remains much continued research to be done to make stem cell therapy for end-stage retinal diseases a real option in the clinic. Firstly, there is a limited window in which the retinal precursor cells can be harvested from the embryo. This window falls into the second trimester of human embryonic development, which poses ethical and technical limitations (Yu and Silva, 2008). Furthermore, retinal remodeling, particularly at the level of second order neurons, is prevalent during late stage degeneration (Marc *et*

al., 2003). Therefore, restoring photoreceptor input could result in substantially aberrant processing of visual information in the remodeled retina.

An alternative therapy for late stage disease is to override early stage retinal processing, or lack there of in the degenerating retina, and confer light sensitivity on retinal ganglion cells. Though there has been a recent burst of research in this general area, the idea of direct cellular photostimulation is not new. In 1971 Richard Fork utilized an intense beam of blue light to evoke action potentials in the abdominal ganglion of the Aplysia (Fork 1971). There are now multiple techniques by which photosensitivity can be introduced to neurons, including light mediated un-caging of neurotransmitters or the introduction of naturally occurring or engineered photosensitive proteins (Chambers and Kramer 2009; Zhang *et al.,* 2007; Zhang *et al.,* 2006). The nervous system performs on a millisecond time scale and each neurons activity, though shaped by the surrounding environment, operates in a unique fashion. Therefore, when considering different tools to photostimulate single or populations of neurons, one must take into account the temporal and spatial resolution of the technique.

Light mediated uncaging of neurotransmitters or stimulatory molecules allows for the selective alteration of membrane potential in a single neuron or large networks of neurons (Callaway and Katz 1993; Zhang *et al.,* 2006). The caged or inactive compound is converted to the active form upon one or two-photon stimulation. Neuronal activation has been achieved with ten-millisecond temporal resolution and 50μm spatial resolution (Callaway and Katz, 1993). Researchers frequently employ glutamate or other neurotransmitters as the caged compound to release upon photostimulation (Callaway and Yuste, 2002; Mayer and Heckel, 2006). Unfortunately,

the use of a single stimulatory molecule limits induced activity to regions expressing the necessary endogenous receptors. After uncaging, the stimulatory molecule is released and repeated activation requires the introduction of more caged substrate. In general, most uncaging techniques for neuronal activation is limited to *in vitro* preparations as it is difficult to deliver caged compounds deep into tissue (Callaway and Yuste, 2002).

The use of naturally occurring photosensitive proteins is a very attractive method for conferring light sensitivity on cells as it limits the need to introduce exogenous compounds that may be toxic and the proteins possess the added benefit of having undergone nature's rigorous selection and optimization process. Researchers employed proteins involved in the drosophila visual transduction cascade to confer light sensitivity on oocytes and cultured neurons (Zemelman *et al.,* 2002). The expression of drosophila phototransduction proteins arrestin, rhodopsin, and a heterochimeric G-protein, in cells allows for cellular depolarization by illumination. A major limitation to this work is that cellular activation is very slow with responses occurring only after seconds of illumination.

Microbial-type rhodopsins are photosensitive proteins used by the unicellular green alga, *Chlamydomonas reinhardtii,* to drive phototaxic and photophobic responses (Nagel *et al.,* 2005 (a); Kateriya *et al.,* 2004; Sineshchekov *et al.,* 2009). Channelrhodopsin 2 (ChR2), a seven transmembrane microbial-type rhodopsin that is non-selectively permeable to cations, is capable of driving temporally and spatially precise neuronal activity upon illumination (Boyden *et al.,* 2005). In light of the promise of ChR2 as a photostimulator, much effort has been taken to manipulate the properties of the channel, find variations of such naturally occurring microbial-rhodopsins, and use it

to treat diseases, modify behavior, or as a tool to probe the activity of single neurons and neural networks (Alilain *et al.,* 2008; Ayling *et al.,* 2009; Berndt *et al.,* 2008; Liewald *et al.,* 2008; Lin *et al.,* 2009; Nagel *et al.,* 2005 (b); Petreanu *et al.,* 2009; Zhang *et al.,* 2008; Zhang *et al.,* 2007 (a,b); Zhao *et al.,* 2008).

Of particular interest to the development of treatments for retinal diseases, ChR2 has been employed to re-establish light sensitivity in the retina after severe retinal degeneration (Bi *et al.,* 2006; Lagali *et al.,* 2008). Lagali and colleagues targeted ChR2 to ON retinal bipolar cells via electroporation in the adult rd1-/- mouse, an animal model of rapid degeneration due to a loss of function mutation in the PDE6β protein that is critical for progression of the visual transduction cascade (Pittler and Baehr, 1991). Targeting ChR2 to the ON bipolar cells was achieved using a fragment of the mGluR6 promoter to drive cell-type specific expression. Establishing light sensitivity in the ON-bipolar cells maintains amplification of signaling between second and third order neurons in the retina and a degree of retinal processing, as shown by recordings of excitatory inputs restricted to ON ganglion cells and inhibitory currents demonstrated in OFF retinal ganglion cells. In addition to the restoration of light sensitivity and a measure of processing in the retina, the authors showed that ChR2 expression in bipolar cells is capable of driving cortical response in the visual cortex and behavior demonstrating light sensitivity. This research confirms the promise of therapies establishing light sensitivity in residual neurons at late stages of degeneration. However, ChR2 possesses limitations that include low conductance and fast inactivation. Furthermore, one criticism of targeting bipolar cells in the retina is that they undergo dramatic remodeling, especially during late stages of disease, therefore re-establishing

retinal processing is likely to be limited (Marc *et al.,* 2003).

Proteins that have been manipulated to respond to illumination and subsequently mediate electrophysiological changes in cells present another, potentially more versatile, option for conferring photosensitivity on retinal neurons. The idea was first presented in 1980 when Lester and colleagues designed a choline analogue tether consisting of the photoisomerizable azobenze group that can be bound to the nictotinic achetocholine receptor. Illumination results in a conformational change of the azobenze group, subsequent ligand binding, and receptor activation (Lester *et al.,* 1980).

More recently, the synthetic photoisomerizable, azobenzene regulated K+ channel (SPARK) was developed (Banghart *et al.,* 2004; Chambers and Kramer, 2009). The SPARK channel is a genetically modified Shaker K+ channel that can be attached to the photo-isomerizable compound (azobenzene) through a reactive maleimide group that covalently binds to introduced cysteines on the surface of the channel. The azobenze is tethered on one side to the channel and on the other to the channel blocker, quaternary ammonium. The azobenzene-based attachment has been termed a "photoswitch". Upon illumination with short wavelength light (380nm), the channel is opened as the blocker is pulled out of the pore by the azobenzene linker. The channel is closed again upon illumination of longer wavelength light (500nm), when the azobenzene arm changes it confirmation back to the "trans" state, inserting the blocker in the channel pore. SPARK can drive potassium currents across the membrane in oocytes and turn on and off spiking in cultured hippocampal neurons and ganglion cells of flat-mount, *in vitro,* retina preparation (Banghart *et al.,* 2004; Borges & Greenberg unpublished data). The mechanism of photoswitch-mediated control of shaker K+ channels is currently being

explored in greater detail.

The light activated glutamate receptor (LiGluR) is another genetically engineered protein that employs a "photoswitch" (an azobenzene based chemical conjugate) attachment to induce light mediated activity (Volgraf *et al*., 2006). The ionotropic glutamate receptor is an attractive protein for engineering light sensitivity, as it is a major excitatory receptor in the central nervous system (Kandel *et al.,* 2000). Furthermore, the crystal structure of the ligand binding domain has been solved making structure based design of photoswitch attachment a realistic endeavor (Mayer *et al.,* 2005). The ionotropic glutamate receptor is made up of four subunits that tetramerize to create the ion channel pore through the membrane. Each subunit consists of an N-terminal domain, a ligand binding domain (LBD), and transmembrane domain.

Volgraf and colleagues used the structure of the ligand binding (LBD) domain to facilitate design of the light activated receptor. The LBD is distinctly shaped like a "clamshell". Introducing a cysteine to the top "lip" of the "clamshell" creates a photoswitch attachment site. The photoswitch consists of a maleimide group necessary for covalent attachment to the introduced cysteine, an azobenze group that changes confirmation when illuminated with specific wavelengths of light, and a glutamate analogue that when inserted into the LBD, activates the channel (Figure 4.1 and 4.2). The photoswitch was termed MAG (maleimide-azobenzene-glutamate). After screening potential sites for MAG attachment that had been identified based on the structure of the LBD and the length of the photoswitch in "cis" and "trans" form, a light activated glutamate receptor was successfully developed as shown by introduced photosensitivity in HEK293T cells (Volgraf *et al.,* 2006). The photoswitch binds to the lip of the

clamshell and when illuminated with short wavelength light (maximum activity at 380nm), the azobenzene moves into "cis" confirmation, introducing the glutamate analogue into the LBD, opening the cationic channel, and resulting in cell depolarization. When illuminated with 500nm light, azobenzene relaxes back into the "trans" confirmation, pulling glutamate out of the LBD and shutting off receptor activity (Figure 4.1). With this design, LiGluR mediates highly reproducible and reversible photocurrents as shown by calcium imaging in HEK cells (Gorostiza *et al.,* 2007; Volgrath *et al.,* 2006).

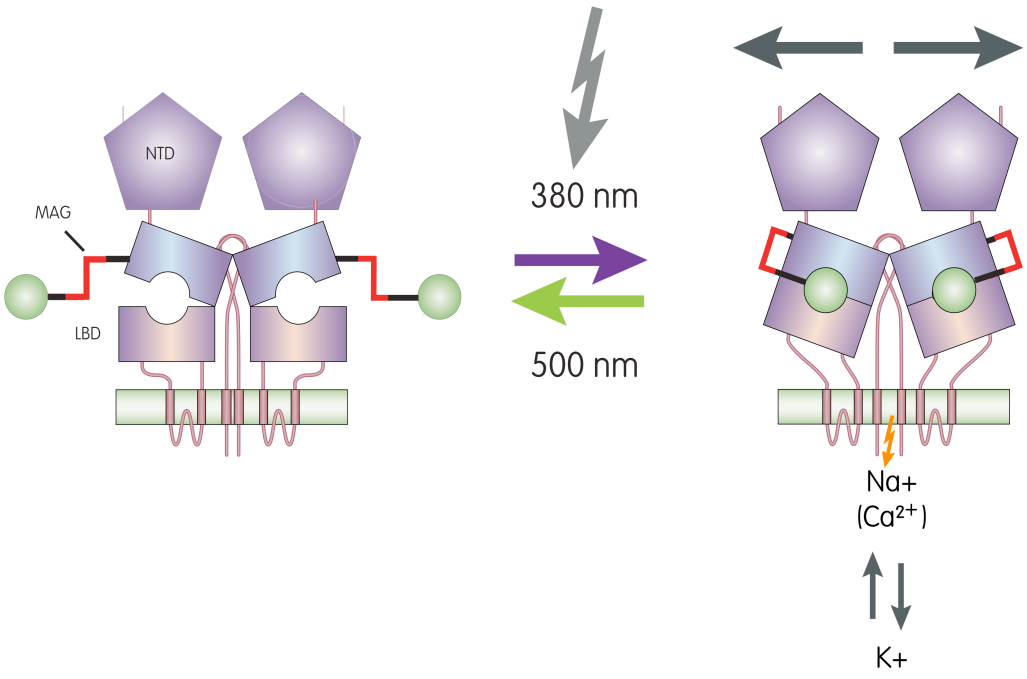

Figure 4.1. Schematic of light-activated glutamate receptor (LiGluR) activity (diagram courtesy of Dr. John Flannery). Upon illumination with short wavelength light, the MAG photoswitch changes confirmation from "trans" to "cis", inserting the glutamate analogue into the ligand binding domain of the receptor, causing the channel to open and the cell to depolarize. LiGluR activity is reversible when illuminated with 500nm light.

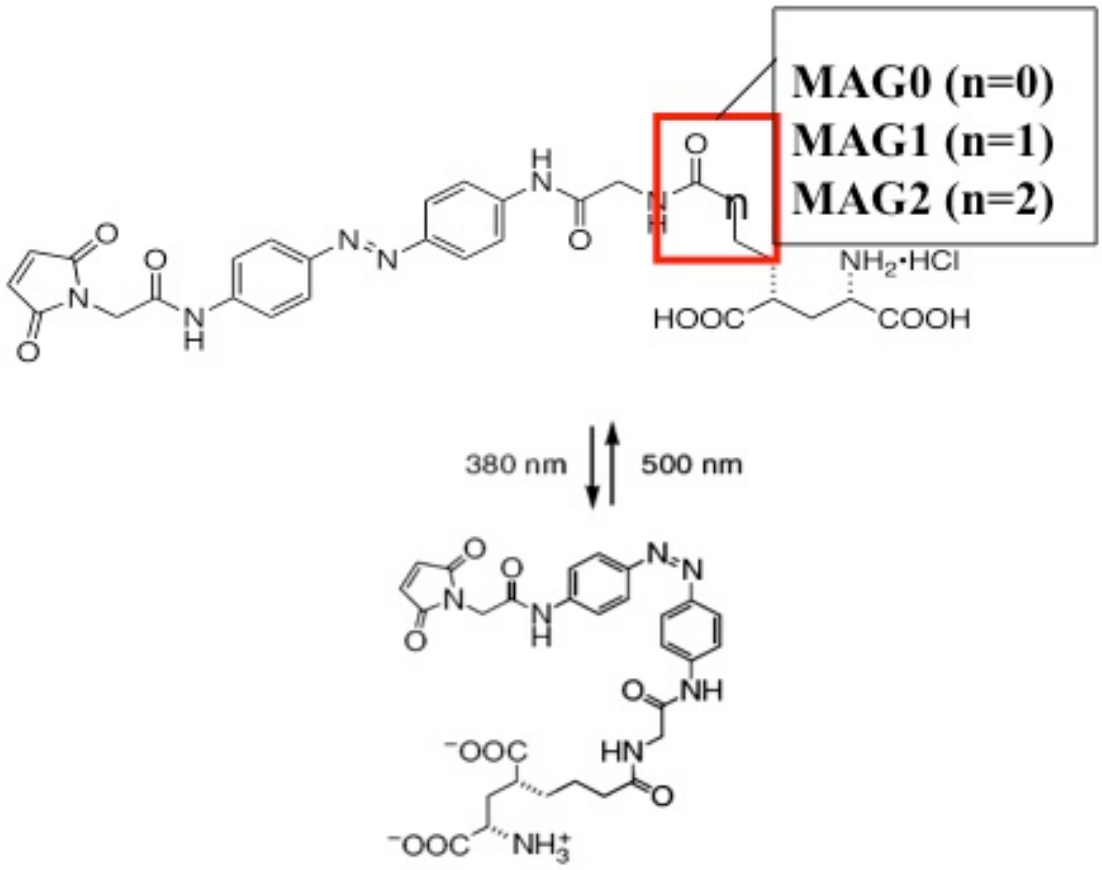

Figure 4.2. The LiGLuR photoswitch, MAG (Maleimide-Azobenzene-Glutamate) (b). There are currently three versions of MAG that vary with length. The various compounds determine different LiGluR response profiles (Numano *et al.,* 2009). For all cortical experiments, MAG0 was used.

Further investigation of LiGluR mediated activity in neurons *in vitro* and in vivo has shown that LiGluR can reversibly induce action potentials and membrane depolarization on a millisecond time scale and control escape behavior in the zebra fish (Szobota *et al.,* 2007). This work also highlights major advantages of LiGluR over

ChR2; LiGluR opening conducts far larger whole-cell current than channelrhodopsin2 and is bi-stable. Bi-stability refers to the fact that LiGLuR can be turned on and off by direct control of illumination and does not automatically revert to the OFF position after activation. The "cis" confirmation of LiGluR is highly stable, thus LiGLuR can drive action potentials or cellular depolarization for minutes after a short pulse of activating illumination, even in the dark (Gorostiza *et al.,* 2007). The control of activity via very short pulses of light, allows for more precise timing of cellular activity, a definitive advantage when attempting to restore single neuron or cortical network activity (Gorostiza and Isacoff, 2008; Wang *et al.,* 2007). Furthermore, brief illumination avoids photo-damage that could accompany high intensity, repetitive light stimulation. In summary, LiGluR is capable of driving neuronal activity at high temporal (millisecond scale) and spatial (less than a micron) resolution, characteristics that make it an attractive tool for restoring visual sensitivity in the degenerated retina.

The eye is an attractive organ to utilize photoswitches for the treatment of disease as it is readily accessible to light and extensive work has been done to optimize gene transfer to specific retinal cells (Aurrichio, 2003). LiGluR is an appealing tool for conferring light sensitivity on retinal cells as it provides precise control over neuronal activity. In the present study, our first aim was to reintroduce light sensitivity to the retina by employing viral delivery of LiGluR to retinal ganglion cells in an animal model of severe retinal degeneration. However, even if photo-sensitivity is restored in the retina, interpreting visual information requires appropriate input to and processing by the cortex. Therefore, we are also assessing properties of the recovered responses in rodent V1 at the single and population cell levels when visual input is limited to LiGluR

mediated activity in the retina. These properties include local field responses, orientation tuning, and receptive field mapping. Eventually we hope to target LiGluR to different subset of retinal cells to begin to restore retinal processing and use LiGLuR to mediate visually guided behaviors.

Experimental Methods

Animals

Initial cortical and electroretinography experiments were conducted on Sprague Dawley and transgenic S334 line-3 rats (courtesy of Dr. LaVail, UCSF). The TgS334-3 rat possesses a nonsense mutation in the introduced rhodopsin gene, resulting in rapid retinal degeneration and outer nuclear layer (ONL) thinning to 4μm by p20. After discovering that the TgS334-3 animals never completely loose photoreceptor responsiveness (as assessed by cortical recordings) we began utilizing the rd1-/- mouse (C3H/HeNCrl strain, Charles River Laboratories International Inc., CA). Wild type (C57/BL6 Charles River Laboratories International Inc., CA) mice were used for toxicity experiments.

All animal experiments were conducted according to the ARVO Statement for the Use of Animals and University of California, Berkeley Animal Care and Use Committee requirements designated for the Flannery Lab or Dan Lab.

Vector Construction

LiGluR cDNA was isolated by digestion with the restriction enzymes Nhe1 and BsrG1 from the pRK_iGLuR6 plasmid (prepared with the L439C mutation for MAG conjugation, provided by the Isacoff lab; Volgraf *et al.,* 2006). The 2.75kb DNA fragment was ligated into the pAAV.6p1.TB plasmid backbone to create an AAV-2 ITR construct with the human Synapsin promoter driving LiGLuR expression. A WPRE (woodchuck hepatitits post-transcriptional regulatory element) was inserted immediately after the LiGluR coding region to enhance expression (Klein *et al.,* 2006) (Figure 4.3).

Proper plasmid construction and maintenance of terminal repeats in the final product was confirmed by Sma1 digest check and sequencing.

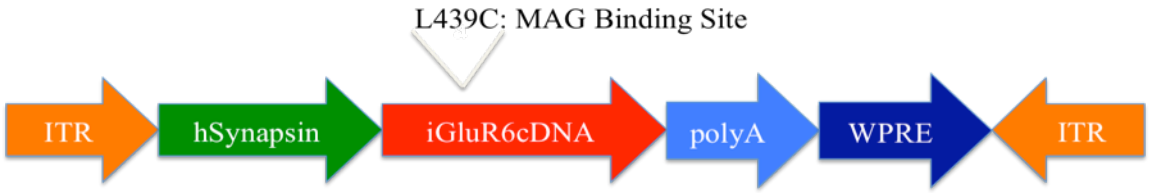

Figure 4.3. AAV ITR LiGluR6 plasmid construct. The inverted terminal repeats (TRs) flank the 5' and 3' end of the LiGluR transgene. The TRs serve to direct transgene packaging during rAAV preparation. The human synapsin promoter drives expression of LiGluR6. A point mutation in iGLuR6 cDNA was made to introduce a cysteine to the ligand binding domain of the receptor to allow for MAG binding.

Generation of rAAV-2 LiGLuR Vector:

Adeno-associated virus was produced by the triple transfection of LiGLuR transgene flanked by AAV2 inverted terminal repeats (ITRs), AAV serotype 2 *rep* and *cap* (pXX2), and Adenovirus helper plasmids (Grieger JC *et al.,* 2006). After ultracentrifugation, the interphase between the 54% and 40% iodixanol fraction was extracted and diluted with equal volume of PBS+0.001% Tween20. The isolated iodixanol fraction was purified on a Hi-Trap Heparin HP column (GE Healthcare Chalfont St. Giles, United Kingdom). To concentrate and buffer-exchange purified vector, Amicon Ultra-15 Centrifugal Filter Unit pre-incubated with 5% Tween in PBS and washed with PBS+ 0.001% Tween. The diluted iodixanol fractions were buffer-exchanged and concentrated to 250µl. Virus was washed three times with fifteen

milliliters of sterile PBS+ 0.001% Tween. Vector was then titered for DNase-resistant vector genomes by Real-Time PCR relative to a WPRE standard.

Ocular Injections:

Adult rd1-/- and WT (C57/BL6) mice were used. Before vector administration, animals were anesthetized with ketamine (72mg/kg) and xylazine (64mg/kg) by intraperitoneal injection. An ultrafine 30 1/2-gauge disposable needle was passed through the sclera, just below the ora serrata, into the vitreous cavity. Two microliters of PBS, MAG0 (see below for detailed description of preparation), DMSO, or $5x10^{12}$ - $5x10^{13}$ vg/ml of AAV-2 LiGluR was injected into the vitreous with a blunt end Hamilton syringe.

Flat mount and cryosection preparation:

Immediately after cortical recordings or at least one-month post LiGluR injection, animals were humanely euthanized by CO_2 or isofluorene overdose and cervical dislocation. Eyes were enucleated, a hole was made in the cornea and eyes were fixed with 10% neutral buffered formalin overnight. The eyecups were washed in PBS and the cornea and lens were removed and then placed in 30% sucrose in PBS overnight. Eyes were then embedded in optimal cutting temperature embedding compound (OCT; Miles Diagnostics, Elkhart, IN) and oriented for 5-10μm thick transverse retinal sections.

Retinal flatmounts were prepared by detaching the retina from the RPE by gently running micro-tweezers along the ora serrata, between the retina and the ciliary body. The retina was then floated away from the eye-cup in PBS using a small paintbrush.

Once the retina was removed, three or four small cuts were made perpendicular to the edge of the retina, running up to the optic nerve head. These cuts allow the retina to lay flat on the microscope slide.

Immunolabeling and histological analysis:

Tissue sections or flatmount retina were rehydrated in PBS for 5 minutes followed by incubation in a blocking solution of 1% BSA, 0.5%TritonX-100 and 2% normal donkey serum in PBS for 2-3 hours. Slides were incubated with commercial rabbit monoclonal antibody raised against the ionotropic glutamate receptors 6 and 7 (Upstate Cell Signaling Solutions (Millipore), Billerica MA) at 1:500 in blocking solution overnight at 4ºC. The sections were then incubated with the secondary anti-rabbit Alex-488 antibody (Molecular Probes) at 1:2000 in blocking solution for two hours at room temperature. Tissue was mounted on coverslips and nuclei stained with hard-set DAPI mounting media. The results were examined by fluorescence microscopy using an Axiophot microscope (Zeiss, Thornwood, NY) equipped with X-cite PC200 light source and QCapturePro camera or by confocal microscopy (LSM5; Carl Zeiss Microimaging). Images were prepared using Bitplane Imaris image processing and manipulation software (Bitplane Inc., St. Paul, MN).

Toxicity Experiments:

C57/Bl6 mice were injected with 2µl of PBS, Dimethyl Sulfoxide (diluted 1/100) in PBS), or 200µM MAG (see preparation description below). Animals were dark-adapted and ERGs were recorded on the day of injection (MAG, n=9; DMSO, n=9; PBS,

n=9), 24 hours post injection (MAG, n=7; DMSO, n=9; PBS, n=6), 48 hours post injection (MAG, n=5; DMSO, n=6; PBS, n=5), and one-week post injection (MAG, n=7; DMSO, n=6; PBS, n=10). Electroretinograms were also recorded from WT, uninjected c57/Bl6 mice to determine the baseline response profile (n=3). See below for description of ERG set-up.

Electroretinograms:

Sprague Dawley and transgenic S334 line-3 rats, or c57/BL6 mice were dark-adapted for four hours, anesthetized, and pupils dilated. Animals were placed on a heating pat and contact lenses were positioned on the cornea of both eyes (only one eye for mice). Reference electrodes were inserted subcutaneously in the cheeks and a ground electrode was inserted in the tail. Electroretinograms were recorded from TgS334-3 and WT rats (Espion ERG stystem; Diagnosys LLC, Littleton, MA) in response to ten light flash intensities from 0.0001-1250 (cd-s)/m^2 presented in series of three. For toxicity experiments, electroretinograms were recorded from c57/BL6 mice in response to eight light flash intensities from 0.0001-1(cd-s)/m^2 presented in series of three. Light flash intensity and timing were elicited from a computer controlled Ganzfeld flash unit. Data were analyzed with MatLab (v7.7; Mathworks, Natick, MA). After correction for oscillatory potentials and heartbeat artifacts, scotopic a-wave values were measured from the baseline to the minimum ERG peak while scotopic b-waves were measured from the minimum to maximum ERG peaks.

Photoswitch preparation:

Twenty millimolar MAG0 suspended in 100% DMSO (provided by Matt Volgraf, Trauner lab) was illuminated for 30 minutes in UV to facilitate labeling of LiGluR upon injection (Gorostiza *et al.,* 2007). MAG0 was then diluted 1/100 in sterile PBS and mixed thoroughly. Two microliters of 200µM MAG0 (1% DMSO) was immediately injected into the eye of an animal that had been injected with AAV2-LiGluR at least three weeks prior to experimentation. Cortical experiments were conducted six to 48 hours post MAG injection.

Multi-electrode array recordings:

Rd1-/- animals were sacrificed and eyes that were expressing LiGLuR or uninjected were enucleated and placed into a room temperature Ringer's solution bath (119mM NaCl, 2.5mM KCl, 1mM KH_2PO_4, 1.3mM $MgCl_2$, 2.5mM $CaCl_2$, 26.2mM $NaHCO_3$, 20mM D-glucose) bubbled with 95% O_2 and 5%CO_2. The retina was prepared as a flatmount as previously described, and gently placed, ganglion side down, on the surface of a 60-channel multi-electrode array (Multi-Channel Systems, Tubingen, Germany). The retina was secured in place with a piece of dialysis membrane attached to a weight, and continuously perfused with 37ºC Ringer's solution bubbled with 95% O_2 and 5% CO_2 at a rate of 1mL/min. Retinas expressing LiGluR were labeled with previously illuminated (UV) 50µM MAG0.

The multi-electrode array consists of 60 electrodes patterned in an 8x8 grid with an inter-electrode distance of 200µm. Each electrode diameter is 30µm. Data was sampled at 20kHz and recorded for off-line analysis. The voltage trace was filtered with

a high band pass of 200Hz. Spikes that crossed threshold was then sorted using Offline Sorter (Plexon, Dallas, TX) to isolate single units from the recordings. Principal component analysis was performed on all of the unsorted waveforms, and the values of the principal component scores for all the waveform were plotted. Clusters of points in the principal component space allowed for the isolation of single units. To ensure accurate sorting by the Offline Sorter, all spike clusters were manually inspected in principal component space. The histograms were binned at 100ms. Data were analyzed with MatLab (v7.7; Mathworks, Natick, MA).

Local Field Potential Recordings-All other cortical work, plus stimulation

All experiments were approved by the Animal Care and Use Committee at the University of California, Berkeley**.** A week prior to recordings, Sprague Dawley rats were injected $5x10^{13}$ vg/ml of AAV5 mixed at a ratio of 4:1 with 0.001% Pronase E (n=6) or $5x10^{13}$ vg/ml of AAV5 mixed at a ratio of 4:1 with 0.01% Pronase E (n=2) and injected in the vitreous of one eye and 5µl of PBS in the contralateral eye.

One week post-injection, animals were anesthetized using ketamine (100mg/kg i.p.) and xylazine (10mg/kg i.p) and pupils dilated. Animals were restrained in a stereotaxic apparatus (David Kopf Instruments, Tujunga, CA) and body temperature was maintained at 36^{o}-37^{o}C via a heating blanket (Harvard Apparatus, Holliston, MA). Anesthesia was supplemented with 0.5-1% isofluorane as needed during the recordings. A small craniotomy and durotomy (~$1mm^2$) were performed over the primary visual cortex (2mm lateral to the midline, 0.5mm anterior to lambda). A glass micropipette

(resistance ~0.5-3MΩ) containing saline solution was lowered to 0.4 mm below the surface of the cortex and contralateral to the side of the stimulated eye.

Visual stimulation for LiGluR experiments consisted of 20 -300 ms pulses of 380 nm light (~3mW/mm^2) preceded and followed by 3 sec of 500nm light (~3mW/mm^2) presented at 0.2Hz for 40-50 repeats (Polychrome V, Till Photonics). Visual stimulation for ChannelRhodopsin experiments consisted of 200-300 ms pulses of 500 nm light (~3mW/mm^2) preceded and followed by 3 sec of 700nm light presented at 0.2Hz for 40-50 repeats (Polychrome V, Till Photonics). Sweeps were filtered at 2 kHz, sampled at 10 kHz by a 12 bit digital acquisition board (National Instruments, Austin, TX), and analyzed with custom software running in Matlab (The Mathworks, Natick, MA).

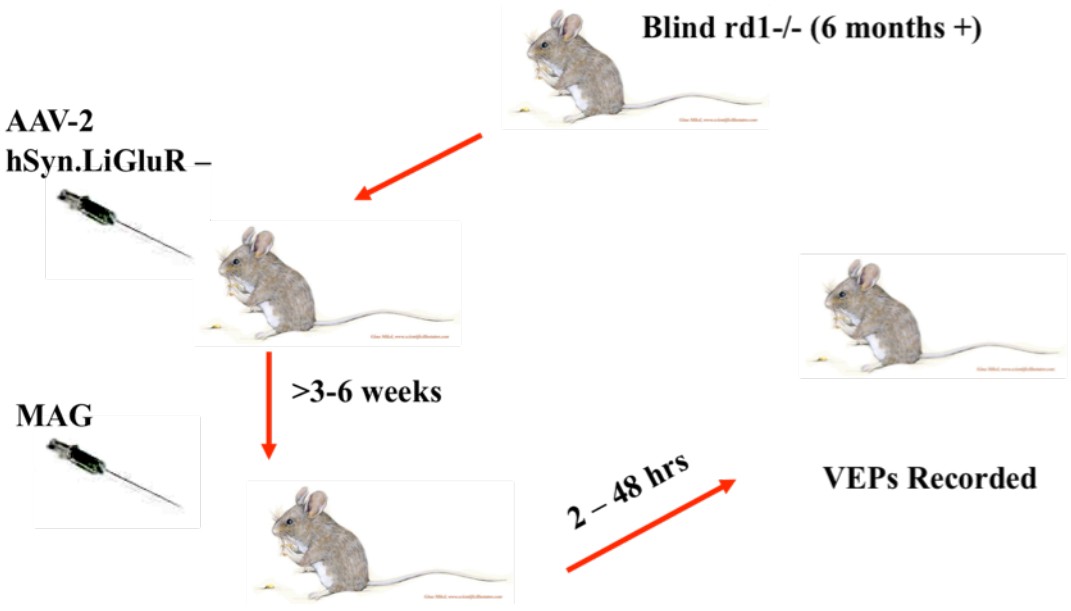

Figure 4.4 Cortical recording experimental protocol. Animals were injected with AAV-2 LiGluR 3-6 weeks before MAG photoswitch injection. VEPs were recorded 2-48 hours post-MAG injection. Rd1-/- animals, 6 months or older were used for all cortical experiments.

Results

Characterization and determination of an appropriate "blind" animal model of retinitis pigmentosa for LiGluR experiments

Electroretinogram analysis indicated no discernable a or b-wave response to light intensities in the range of 0.0001 to 1250 (cd-s)/m^2 from the TgS334-3 rat model of autosomal dominant retinitis pigmentosa. However, local field potential (LFP) recordings in V1 illustrate the maintenance of cortical activity in response to full field flashes of light (Figure 4.5). This response was observed in animals ages P21 up to over a year old.

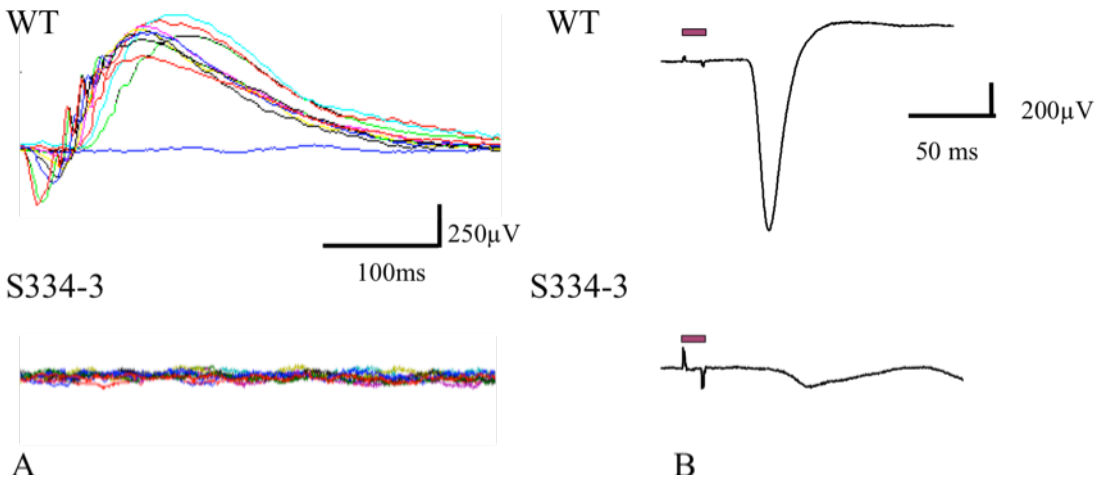

Figure 4.5. Assessment of visual responses in animal models of severe photoreceptor degeneration. Example ERG traces recorded from age matched, dark-adapted wild type and TgS334-3 rats (p45) (a). Responses to twelve light intensities (0 cd/m^2-1250 cd/m^2) were obtained. Responses were averaged across three trials. TgS334-3 rats with severe retinal degeneration do not exhibit a recordable ERG. However, local field potentials

recorded from V1 show responses in the degenerated retina in animals over a year old (b).

Rd1-/- mice possess a mutation in the Pde6β gene that encodes for the beta subunit of the cGMP-PDE. cGMP-PDE is necessary for conversion of cGMP to GMP. This conversion causes photoreceptor cation channels to close upon photoreceptor illumination, hyperpolarizing the cells. Loss of cGMP-PDE function results in the blockage of the photo-transduction cascade (Chang *et al.,* 2002). We tested LFPs (local field potentials) in rd1-/- animals 2.5 months to one year old. Animals six months and older consistantly exhibit no LFP response to bright full field visual stimulation (Figure 4.6). Therefore, all experiments were conducted in rd1-/- animals over the age of six months.

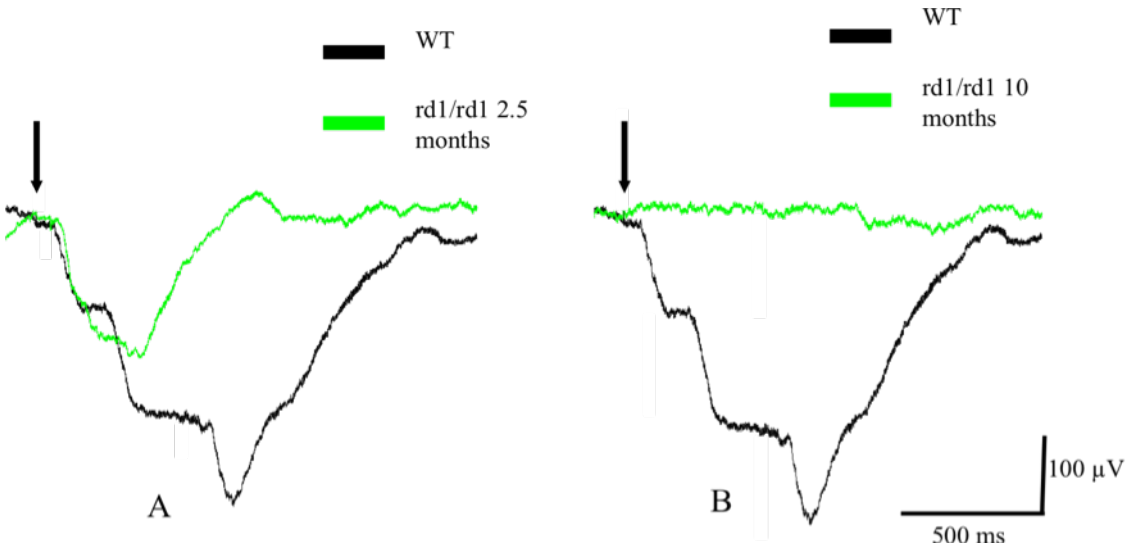

Figure 4.6. Assessment of possible mouse models of severe retinal degeneration by measurement of local field potentials in V1. Black arrows indicate light onset.

Recordings were conducted in WT mice and rd1-/- mice at two and a half months (a) and ten months of age (b). As responses could be elicited from younger animals (up to six months of age), all subsequent cortical experiments were conducted in animals six months or older.

LiGluR expression

An adeno-associated virus (serotype 2; AAV2) genomic vector backbone containing the LiGluR gene driven by the human synapsin promoter was packaged in the AAV2 capsid (Figure 4.3). Three weeks after intravitreal injection, LiGluR expression could be detected by anti-iGluR6/7 immunohistochemistry. Robust expression was achieved throughout the retina, from the optic nerve head to the periphery (Figure 4.7). Occasionally, more localized, intense expression was observed in close proximity to the injection site. This method of LiGluR cDNA delivery allows for non-specific expression in all retinal ganglion cells. LiGluR can be visualized in cell bodies, dendritic arbors throughout the inner plexiform layer, and axons.

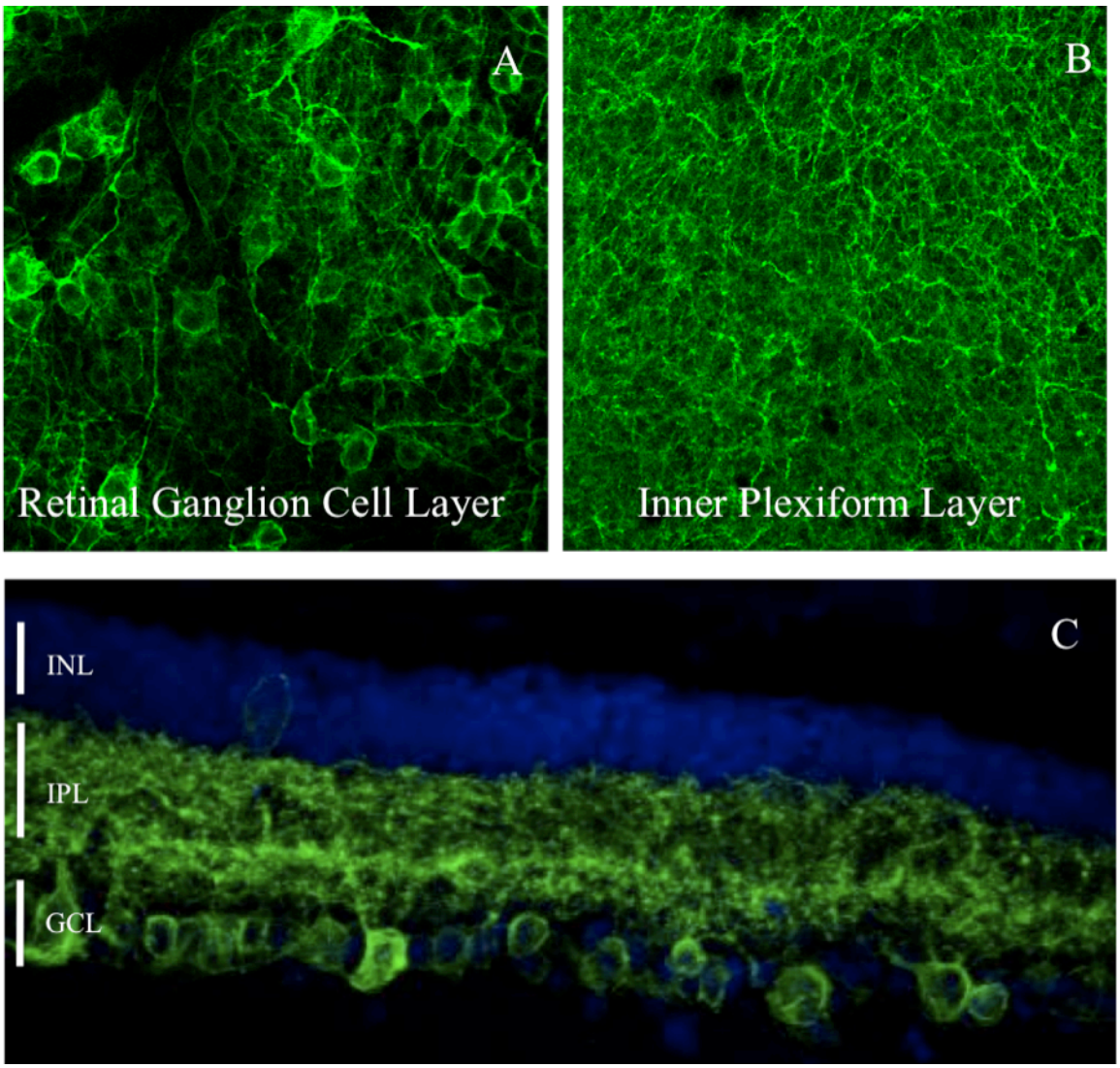

Figure 4.7. AAV2 carrying LiGluR cDNA driven by the human synapsin promoter was injected into the vitreous of six-month-old rd1-/- mice. Expression was confirmed by anti-iGluR6/7 immunohistochemistry (with Alexa-488 secondary antibody). Imaged on Zeiss Confocal Laser Scanning Micropscope (25X). Expression was achieved in retinal ganglion cells without sub-type specificity (a and c), and the occasional amacrine cells. LiGluR expression was present throughout cell bodies and dendritic arbors (a, b, and c).

MAG Toxicity

To initiate the assessment of MAG0 toxicity in the retina, we employed electroretinograms to assess visual function in animals injected with 200μM MAG0, DMSO (1/100), or PBS. These experimental groups were chosen to assess the damaging effects of the injection, the DMSO that is suspended with MAG in order to keep the compound in solution, and MAG0. We discovered that on the day of injection, the a and b-waves are both completely abolished in all groups of animals (Figure 4.8).

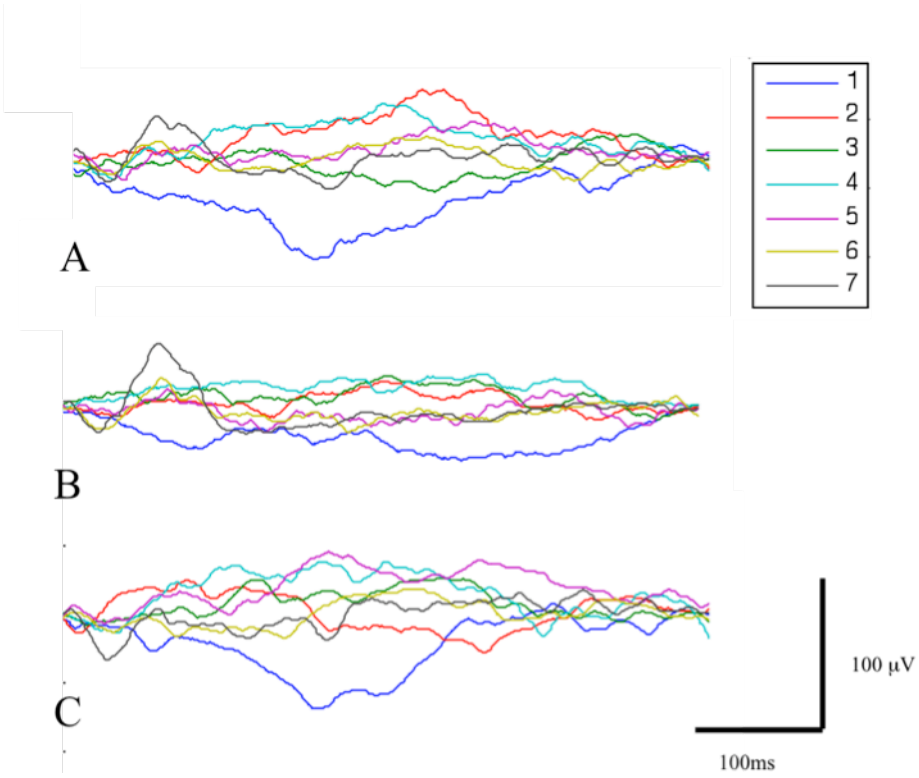

Figure 4.8. On the same day of injection of PBS (a), 1% DMSO (b), or 200μM MAG0 the ERG is completely abolished as demonstrated by no discernable a or b-wave.

By 24 (Figure 4.9) and 48 hours (Figure 4.10) post injection, all responses are partially recovered and at one-week post injection all experimental groups have fully recovered the ERG response (as compared to control, WT, uninjected animal ERG recordings) (Figure 4.11). There was no significant difference in ERG response profiles between experimental groups (Figure 4.12).

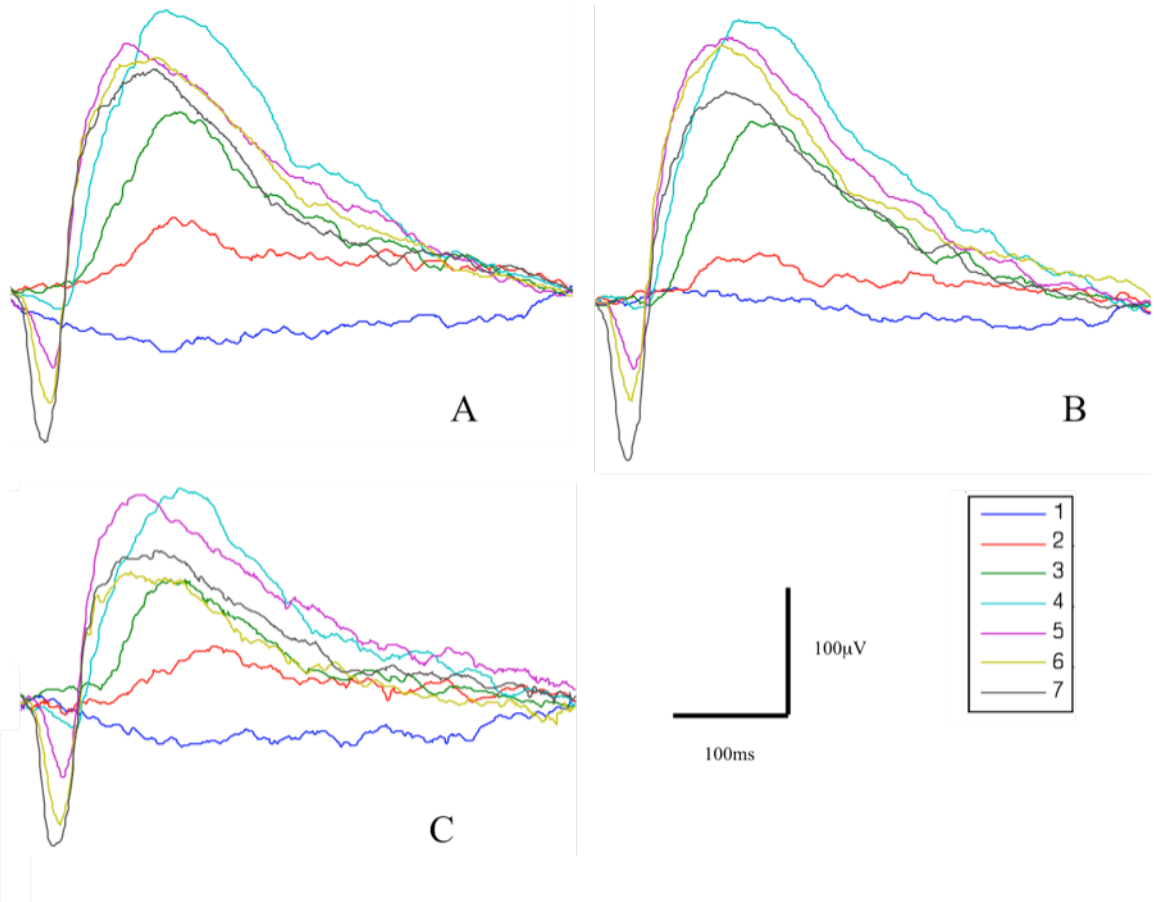

Figure 4.9. At 24 hours post injection the ERG a and b-wave of injected animals are partially recovered (approximately three-quarters of normal a and b-wave amplitude). Of note, there is no significant difference between the ERGs of PBS (a), 1% DMSO (b), or 200µM MAG0 (c) injected animals.

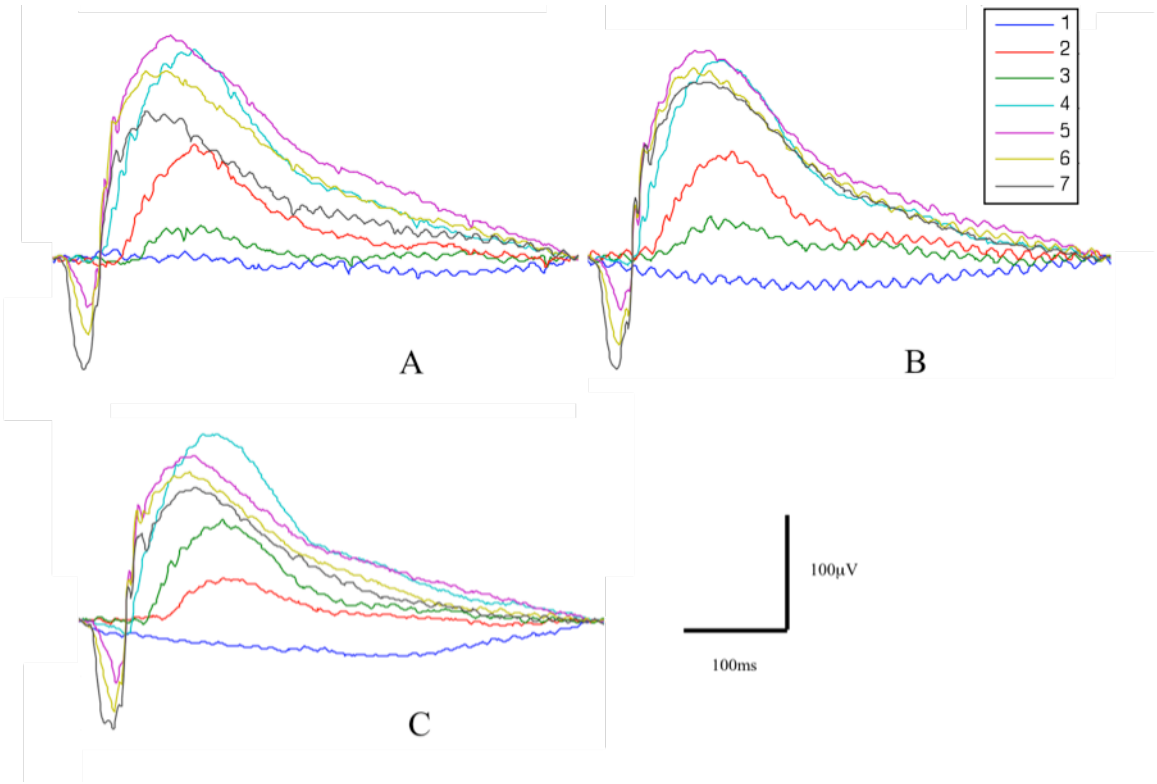

Figure 4.10. At 48 hours post injection the ERG a and b-wave of injected animals are partially recovered. There is no significant difference between the ERGs of PBS (a), 1% DMSO (b), or 200μM MAG0 (c) injected animals.

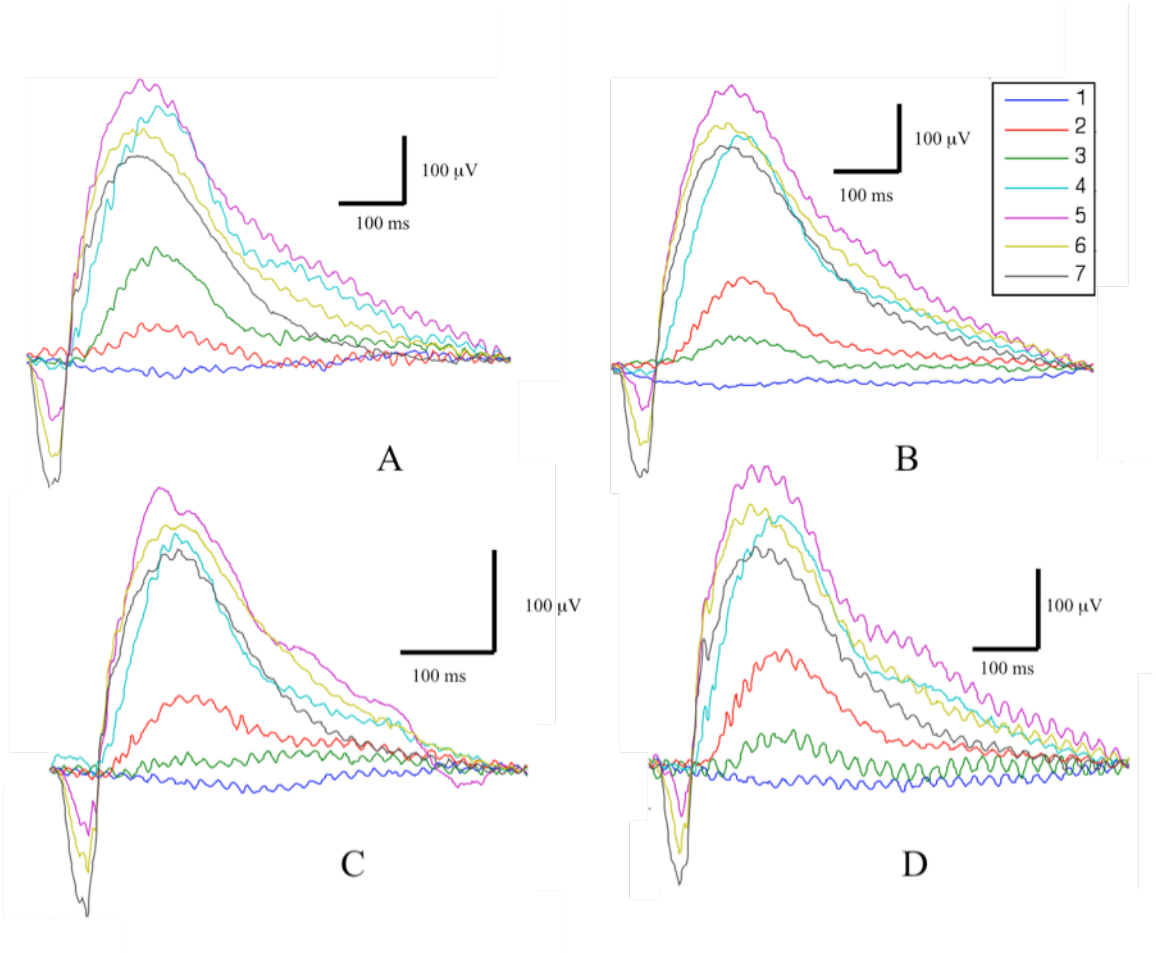

Figure 4.11. By one week post injected, the ERG a and b-wave of injected animals is completely recovered as compared to WT, uninjected animals. There is no significant difference between the ERGs of WT, uninjected animals (d) and PBS (a), 1% DMSO (b), or 200µM MAG0 (c) injected animals

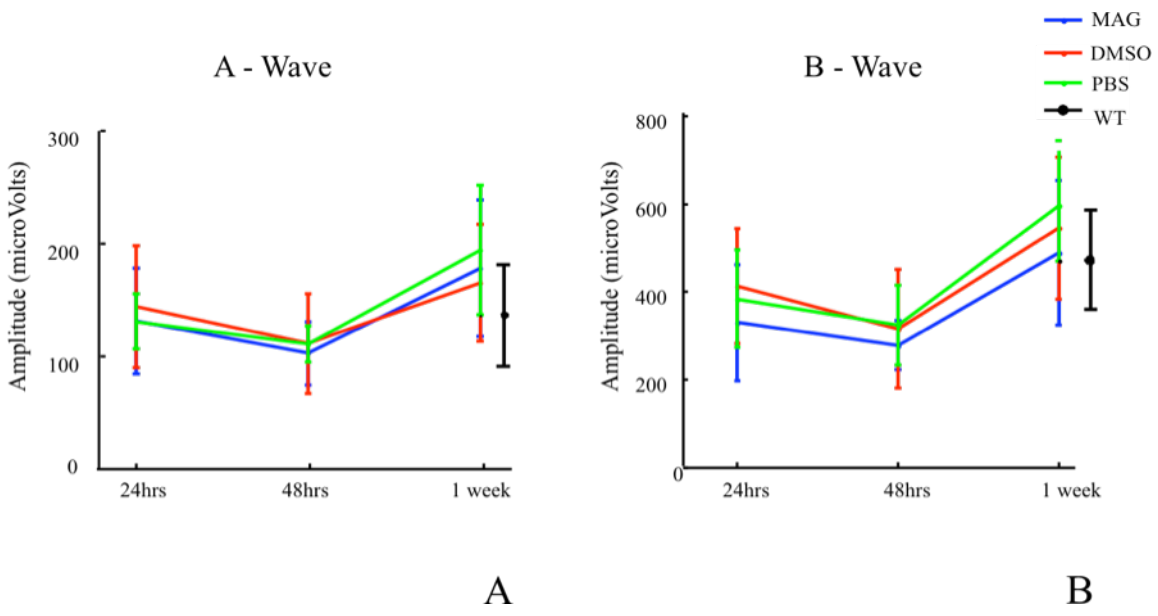

Figure 4.12. Summary of photoswitch toxicity experiments. The ERG a (a) and b-wave (b) is partially recovered 24 and 48 hours after injection of PBS, 1% DMSO, or MAG0. By one week post-injection the ERG is completely recovered. There is no significant difference between the electroretinogram of each experimental group.

These results suggest that neither MAG0 nor the DMSO injected into the eye is toxic at the concentrations used. However, the injection itself is damaging to the eye immediately after surgery as demonstrated by the flat recordings acquired. The loss of electrical retinal activity is likely to be a result of acute increase in intraocular pressure that occurs after injection (Siliprandi *et al.,* 1988).

LiGluR mediated retinal ganglion cell responses *in vitro*

LiGluR mediated electrophysiological responses in retinal ganglion cells were evaluated at the single cell level by multi electrode array recordings. Retinas were dissected from six-month-old rd1-/- animals expressing LiGluR. Continuous spontaneous activity before, during, and after illumination indicated that retinal ganglion cells are healthy, however there is no discernable light response without the presence of MAG0 (Figure 4.13 (a)). After labeling with MAG0, cells respond rapidly to flashes of UV light ranging from 50ms to 5 seconds (Figure 4.13 (b); Figure 4.14). These responses were reproducible as demonstrated by repetitive, consecutive flash stimulus being capable of inducing ensemble cellular spiking. Longer stimuli (5 seconds) caused some receptor desensitization as demonstrate by robust cell ensemble spiking immediately after light onset that slowly diminishes at later points during illumination (Figure 4.13 (b)).

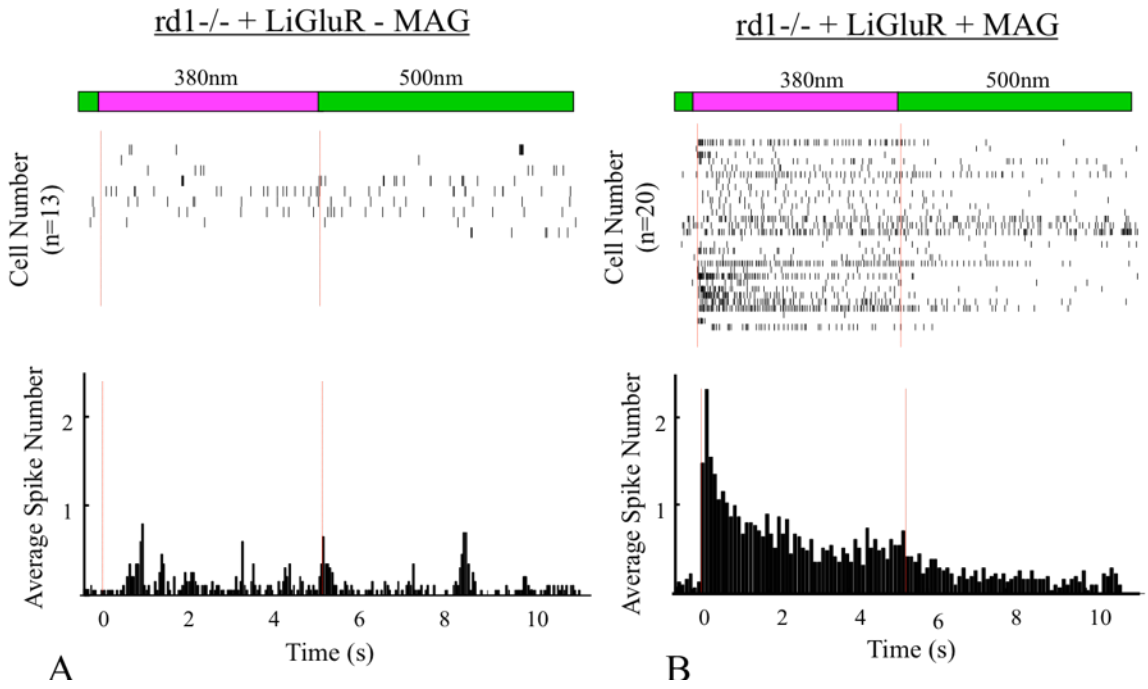

Figure 4.13. Multi-electrode array recordings of LiGluR expressing rd1-/- retinal ganglion cells exhibit illumination dependant activity. When no MAG0 is present, spontaneous activity exists, however illumination does not induce changes in electrophysiological activity (a). When retinal ganglion cells expressing LiGluR are labeled with MAG0, illumination with five seconds of ultraviolet light induces a robust increase in cellular spiking (b). Spiking is silenced upon illumination with 500nm light.

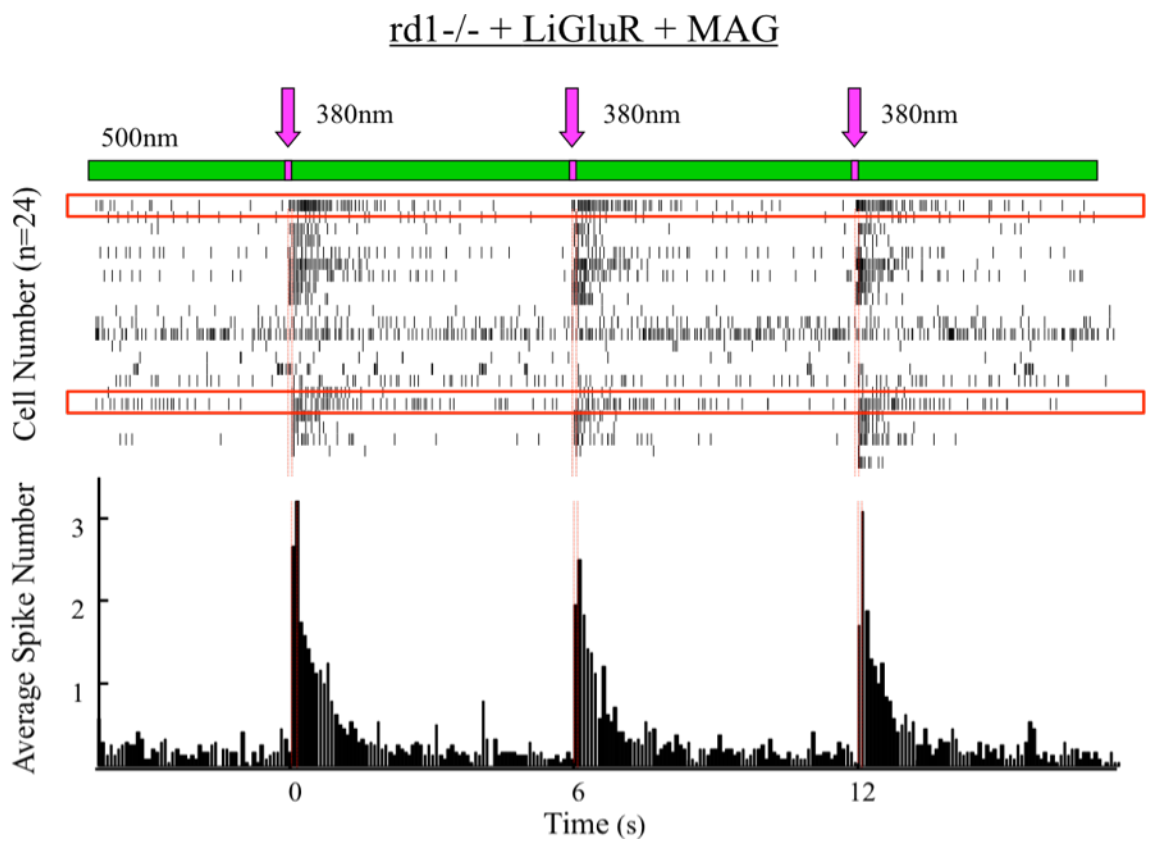

Figure 4.14. Multi-electrode array recordings of LiGluR expressing rd1-/- retinal ganglion cells exhibit illumination dependant activity. When retinal ganglion cells expressing LiGluR are labeled with MAG0, illumination with 50ms of ultraviolet light induces a robust increase in cellular spiking. Spiking is silenced upon illumination with 500nm light. Red bars highlight single cells that demonstrate strong electrophysiological response to UV illumination. Cell spiking is also reproducible as shown by repetitive activation after UV illumination.

To control for the effect MAG0 may have on membrane potential, we conducted multi-unit recordings of rd1-/- retinal ganglion cell activity in retinas labeled with MAG0 but not expressing LiGLuR. If MAG were to have an affect on endogenous

glutamate receptors or proteins that maintain the membrane potential, we would have expected to observe cellular responses to flashes of UV light. Though the cells were healthy as spontaneous firing was observed, MAG0 did not induce spiking without LiGluR expression in ganglion cells (Figure 4.15).

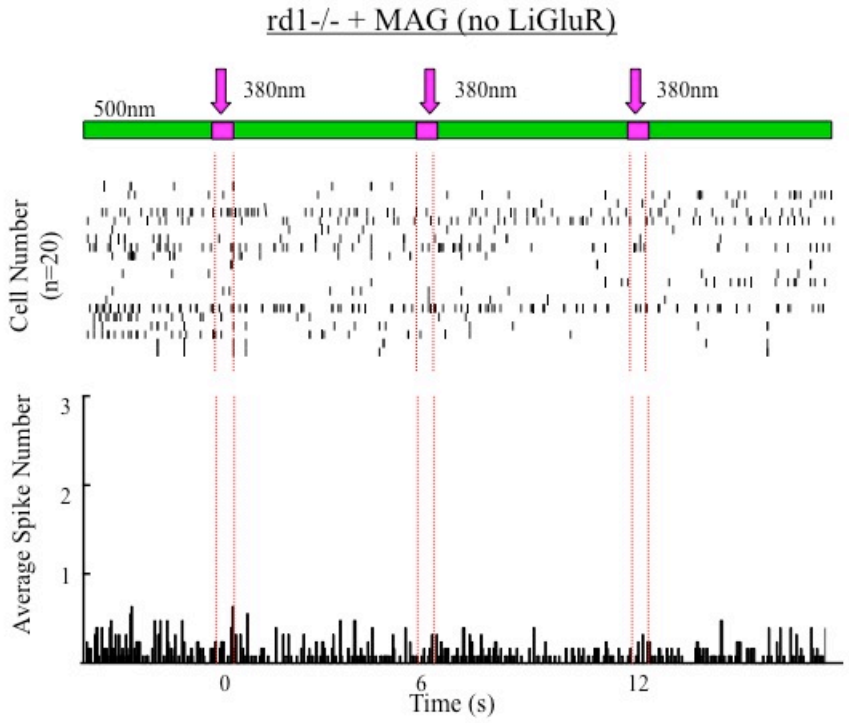

Figure 4.15. MAG0 does not induce cellular activity as demonstrated by multi-unit recording of rd1-/- retinal ganglion cells labeled with MAG0but not expressing LiGluR. Retinas are healthy as demonstrated by spontaneous activity, however UV illumination does not elicit changes in spiking.

***In vivo* LiGluR cell population responses in V1:**

Local field potentials (LFPs) measure visually simulated population responses of cortical neurons in layer 4 and 5 of V1. Local field potentials are intracortical

recordings, therefore are more sensitive than visual evoked potentials that monitor population activity from outside the scull (Figure 4.16 (a)). We utilize a full field flash of light to elicit LFP responses. We have characterized LFP responses at different depths of V1, using variable durations and wavelengths of stimuli (UV, green, white) in wild type animal mice. The duration of the light has little effect on local field potential response size. Responses are largest (~800µV) when the electrode is lowered 600-1000 µm into V1 (Figure 4.16 (b)). There is no significant difference between responses to different wavelengths of light. All experiments measuring responses to different wavelengths of light and cortical depth of recordings were repeated in 6-month-old rd1-/- animals. These experiments demonstrate that rd1-/- animals six months and older have no recordable LFP (Figure 4.16 (b)).

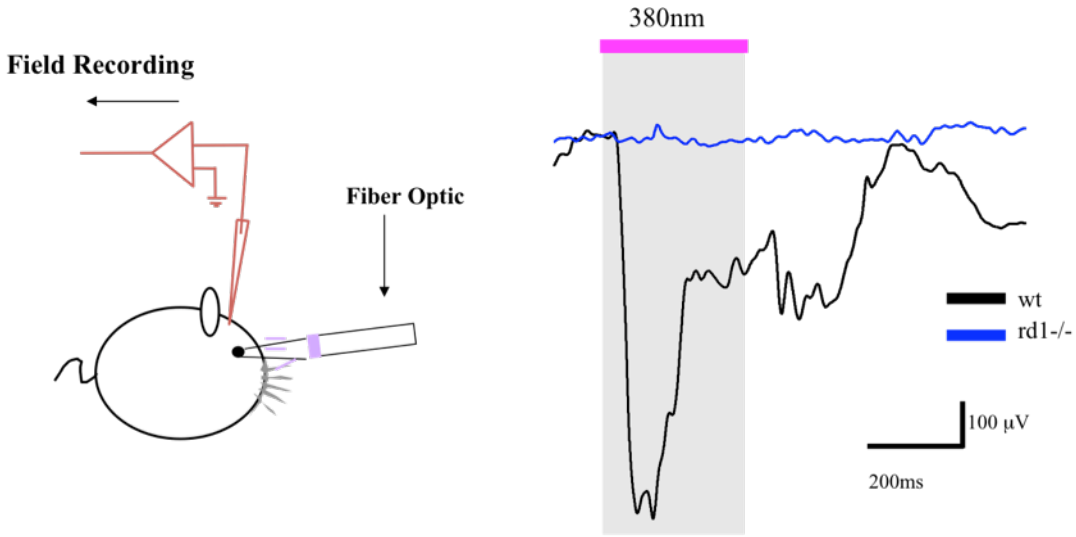

Figure 4.16. Local field potentials were recorded from wild type and rd1-/- mice in response to full field flashes of light (b). An electrode was lowered 600-1000 μm into V1 to record cell population responses to light flashes (a).

We also used local field potential recordings in anesthetized mice to characterize LiGluR-mediated visual responses at the cortical level in response to brief (50ms) and long (300ms) full-field stimulation pulses. Animals (rd1-/-) that had been injected into the left eye with LiGluR (three weeks before recording) were injected with 2μl of prepared (see methods) 200μM MAG0 4-48 hours before recording. We discovered that LiGluR was able to recover approximately 50% of the normal, wild type LFP when mediating light responses from the retinal ganglion cells in rd1-/- animals (Figure 4.17 and 4.19 (b)). As a control, light flash responses were measured from the right eye of the experimental animal where no AAV-2 LiGluR had been injected. Under no circumstances were LFPs observed from the illumination of the control eye.

Flash stimuli were presented over 50-300ms. Shorter illumination resulted in a slight decrease in amplitude of response. We reasoned this might be due to less time for summation of individual RGC responses. In addition, we observed some desensitization to light stimuli when flashes were presented consecutively.

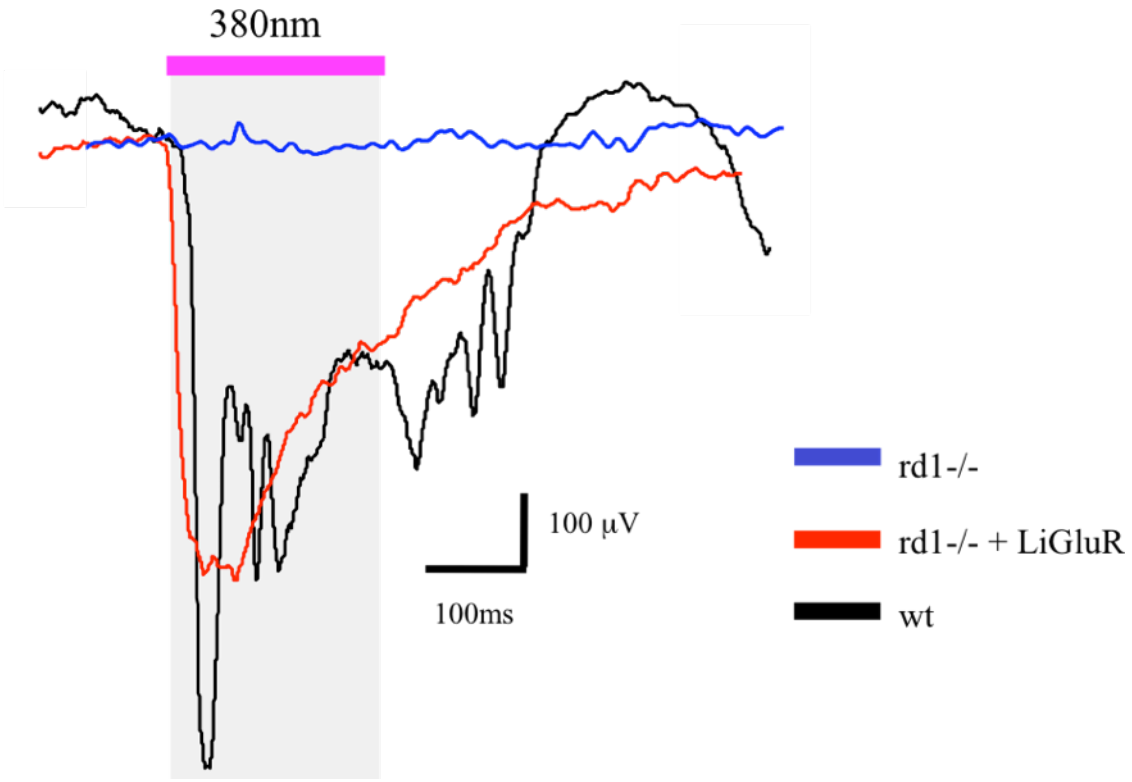

Figure 4.17. LiGluR expression in retinal ganglion cells is capable of driving cortical responses *in vivo*. In fact, LiGluR can recover approximately 50% of the amplitude of a WT LFP. Stimulus presentation to internal control, uninjected (with LiGluR) elicits no response.

The most reliable and robust LiGluR mediated light responses were obtained twenty-four hours post MAG0 injection. We anticipate that the delay in peak sensitivity may be due to a recovery period after intraocular injection. The light necessary to elicit LiGluR mediated responses is 1mW/mm^2, at the cornea. In fact, light intensity is crucial for driving LiGluR responses, intensities any lower elicit smaller and less reliable, or no response at all.

LiGluR wavelength tuning in vivo

To assess peak sensitivity of LiGluR mediated cortical responses, LFPs were recorded in response to varied wavelengths of light (1mW/mm^2) in LiGluR expressing rd1-/- animals. The wavelengths tested ranged from 320nm to 440nm. As expected, we discovered that the wavelength-tuning curve is identical to that obtained when testing LiGluR mediated activity in cultured cells *in vitro* (Gorostiza *et al.,* 2007). In context of translation to the clinic, it is important to note that approximately 60% of the amplitude of cortical response is maintained as the stimulus is moved into the visible range (420nm) (Figure 4.18)

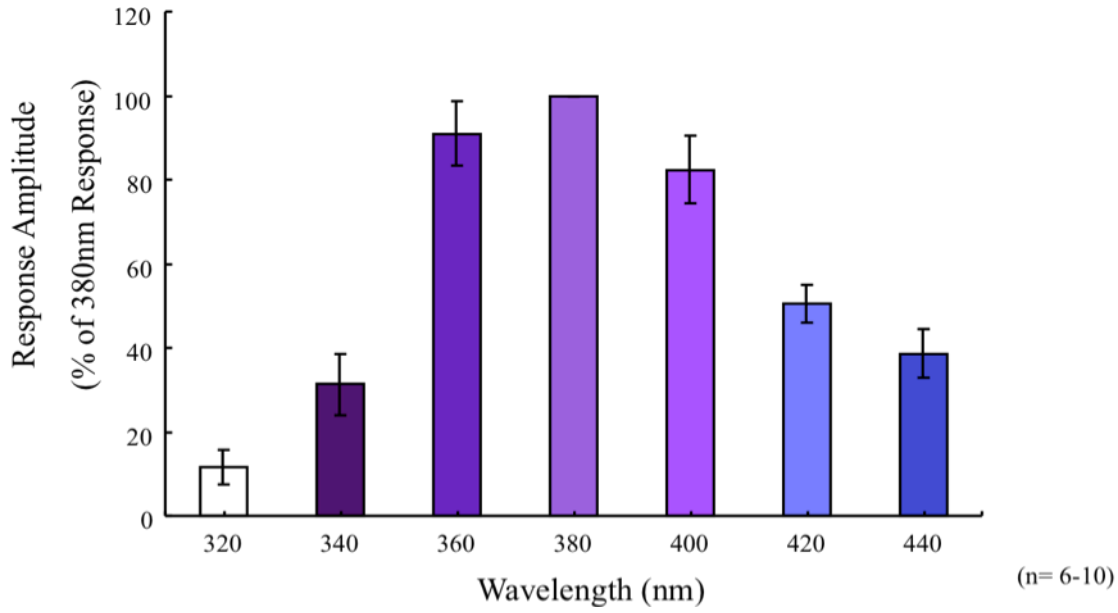

Figure 4.18 The wavelength-tuning curve of LiGluR mediated cortical responses. Average peak amplitude of responses to different wavelengths of light indicates that cortical responses are maintained into the visible range of light (n=6-10/wavelength).

Comparison between WT and LiGluR and Channelrhodopsin2 mediated cortical responses in V1

The naturally occurring, light sensitive channel, channelrhodopsin is another tool for re-introducing light sensitivity to a "blind" retina that has received increasing attention in recent years. There are distinct advantages and disadvantages of this tool, therefore we wanted to compare the cortical responses mediated by LiGluR and ChR2. ChR2 was delivered to retinal ganglion cells of six-month old rd1-/- animals with the exact same experimental approach as LiGluR delivery. ChR2-mCherry was subcloned into an AAV2 vector backbone with the human synapsin promoter driving cDNA expression. Similar titer (to LiGluR) AAV2 vector carrying ChR2 cDNA was injected into rd1-/- animals. Virus was allowed to express for at least three weeks before experiments. We discovered that the peak amplitude of LiGluR mediated local field potentials is over three times greater than responses driven by ChR2 (Figure 4.19). Furthermore, the ChR2 mediated cortical response is about one-eight of the WT response to the same stimuli (intensity and wavelength), while the LiGluR mediated response is approximately 50% of the WT over a population of experimental animals. In addition, LiGluR response peak amplitude is dependant upon the duration of the stimulus (4.20).

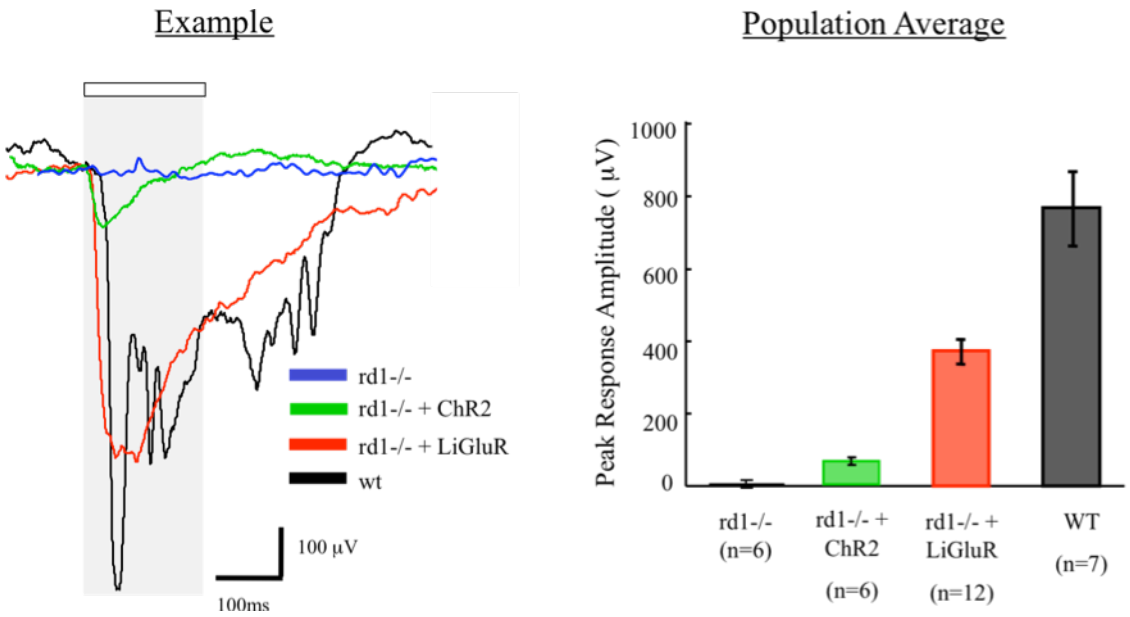

Figure 4.19. LiGluR driven cortical responses in V1 are over three times greater in amplitude in comparison to ChR2 driven responses. Furthermore, a LiGluR response in a population of animals is ~50% of the WT response, while the amplitude of ChR2 driven local field potentials is one-eighth of the WT LFP (n=6-12).

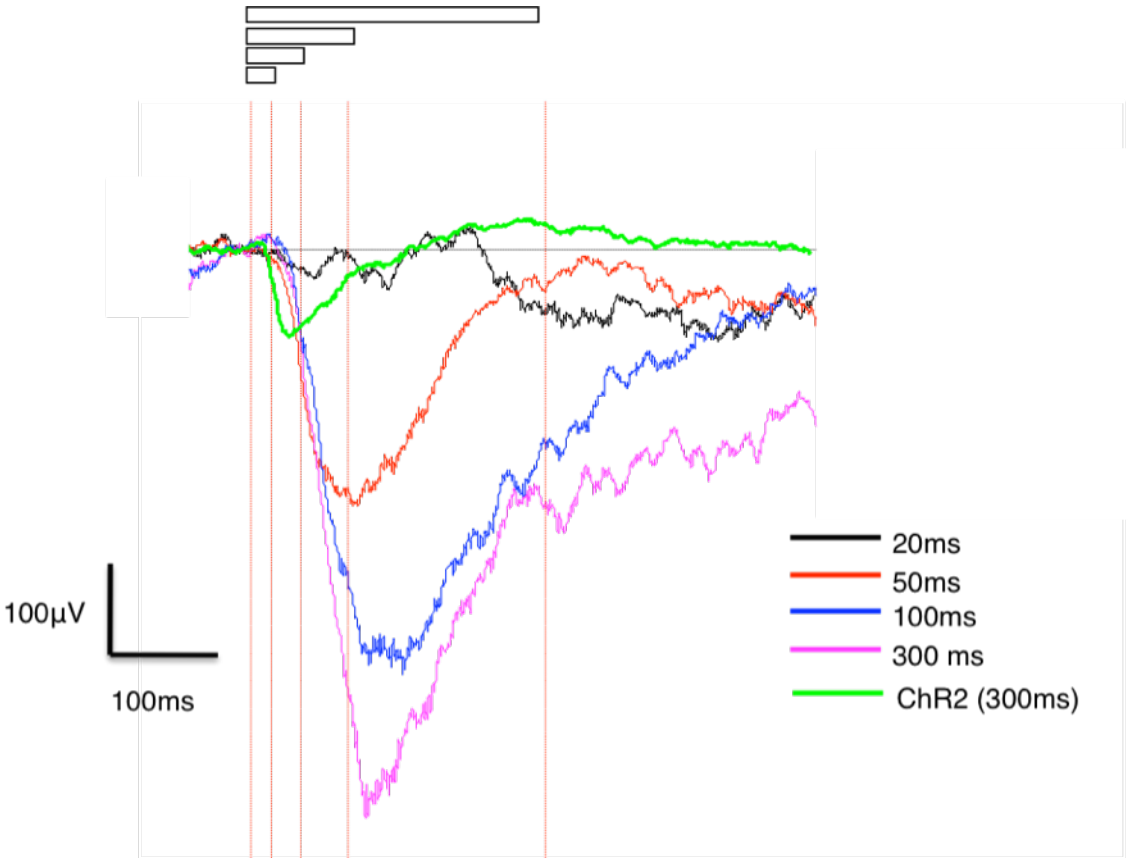

Figure 4.20. LiGluR local field potential response amplitude depends upon the duration of the stimulus. LiGluR was activated with 380nm while ChR2 was activated with 480nm light for 300ms).

Discussion

Patients in the late stages of retinal disease progression currently have few therapeutic options to recover vision. Without photoreceptor activity, visual processing cannot take place, despite the fact that second and third order retinal neurons remain functional. We have developed and assessed a novel therapy for such advanced retinal degenerative states. This therapy utilizes an engineered photosensitive protein, LiGluR, to restore light sensitivity to a blind (lacking photoreceptors) retina. LiGluR expression drives photo-activation of retinal ganglion cells *in vitro* and significantly, to the goal of recovering "vision", this cellular activity is capable of recovering cortical responses to visual stimuli in V1. Together, these results suggest that LiGluR, with further improvement of activation properties, is a promising candidate for a therapeutic aimed at restoring visual function in the late stages of retinal degeneration.

In the current study, we utilized adeno-associated virus to deliver LiGLuR cDNA to retinal ganglion cells in our chosen animal model of retinal disease. This method of gene delivery results in sustained LiGluR expression in all retinal ganglion cell types. A benefit to conferring light sensitivity on third order neurons is that it avoids activating aberrant circuitry in the retina that develops during retinal degeneration (Marc *et al*., 2003). More specifically, in the animal model of retinitis pigmentosa, rd1-/-, second order neurons, namely retinal bipolar cells, undergo dramatic morphological and connectivity modifications during degeneration (Strettoi and Pignatelli, 2000). Bipolar cells never develop normal dendritic arbors and horizontal cells extend neurites into the inner plexiform layer, both events suggest that informational processing at this level would be severely altered. There is also a dramatic decrease in bipolar cell density when

compared to the wild type retina. The expression properties of the mGluR6 receptor (required for ON bipolar cell activation) are compromised, resulting in mis-directed sorting and targeting of the receptor. This series of remodeling events are consistent among various animal models of photoreceptor degeneration (Jones and Marc, 2005). Together, the morphological and biochemical changes that occur at the inner nuclear and inner plexiform layers suggest that re-introducing light sensitivity to the second order neurons of the retina would activate aberrant circuits and limit the restoration of normal visual processing. Moreover, a recent study assessing the morphological, architectural, and survival characteristics of retinal ganglion cells in an animal model of retinitis pigmentosa, found that these properties are remarkably preserved (Mazzoni *et al.,* 2008). Therefore, retinal ganglion cells are currently a more desirable cellular substrate for conferring light sensitivity on the retina by introducing photosensitive proteins as a treatment for late stage photoreceptor degeneration.

Bipolar cell changes during retinal degeneration are likely to be due to diminished and abnormal input from photoreceptive cells; therefore conferring light sensitivity on bipolar cells early in degeneration may limit remodeling (Strettoi and Pignatelli, 2000). If proper bipolar cell function and connectivity were maintained, these cells would be the ideal targets for photosensitive protein therapy. Bipolar cells are core components of natural retinal circuits, therefore activation of subtypes of these cells would contribute to the restoration of appropriate visual processing, such as organizing visual information into the ON and OFF pathways of the retina. Furthermore, the convergence of bipolar cell axons on multiple third order neurons will provide

amplification of signal and promote downstream retinal processing and filtering of visual information.

We are currently in the process of developing methods to efficiently target LiGluR to retinal bipolar cells. Previous studies that have employed channelrhodopsin to confer light sensitivity on retinal bipolar cells utilized electroporation of ChR2 cDNA driven by an mGluR6 promoter fragment (Lagali *et al*., 2008). However, this method of gene delivery does not achieve sustained plasmid transfection of cells. We aim to attain sustained and restricted bipolar cell transduction by utilizing an optimized adeno-associated viral vector that escapes ubiquitination when a surface-exposed capsid tyrosine is mutated (Zhong *et al.,* 2008). The mutated tyrosine residue normally targets AAV viral particles for ubiquitination and proteasome-mediated degradation. This mutation in the capsid leads to a ten fold increase in AAV accumulation in the nucleus and subsequently up to a log higher gene expression. Preliminary data suggests that this vector does target (non-specifically) bipolar cells when the ubiquitous chicken beta actin promoter drives transgene expression after both an intravitreal and subretinal injection (data not shown). However, expression in bipolar cells is much greater when the vector is injected into the subretinal space (Liu *et al.,* 2009 ARVO Abstract 3011). We are also utilizing the ON bipolar cell specific promoter (a generous gift from the Roska and Cepko labs) to drive specific expression in ON bipolar cells (Lagali *et al.,* 2008). As an important goal of our work is to avoid the dangers of the subretinal injection (see Chapters 2a and b), we hope to circumvent the use of the subretinal method of vector administration. We are in the process of evaluating in detail the intravitreal transduction efficiency and specificity of the described method of bipolar cell targeting. At this point,

it is unclear whether an intravitreal injection of the tyrosine mutant AAV with the Grm6 promoter driving LiGLuR expression in ON bipolar cells will provide high enough transfection efficiency and transgene expression to mediate and enhance recovery of cortical responses.

Our group is currently using directed evolution to engineer superior AAV vectors for cell type specific vector targeting in vivo. More specifically, large and diverse, AAV vector libraries are generated from DNA shuffling and error-prone PCR approaches (Jang *et al.,* 2007; Maheshri *et al.,* 2006). Each variant is subjected to positive selection by infecting specific cell types (in vivo and *in vitro*) and isolating vectors with appropriate and efficient tropism. Members of the group have recently used directed evolution to select variants with enhanced permissivity to astrocytes in vivo (Koerber *et al.,* 2009 *under review*). Of relevance to the retina, these variants efficiently and specifically transduce retinal Müller glia from the vitreous in a restricted manner (Koerber *et al.,* 2009 *under review*; Klimczak *et al.,* under review). To our knowledge, such restricted cellular tropism through intravitreal injection with an AAV vector has not been reported. We plan to utilize this method of viral engineering to enhance LiGluR vector targeting of specific retinal cells, namely bipolar cells, to help restore basic retinal visual processing.

Targeting only one cell type with a single photosensitive protein restricts the restoration of visual processing. In the case of targeting ON bipolar cells, photosensitivity would be re-introduced to the ON channel of processing only. Retinal circuitry processes and filters visual information that includes movement, image contours, and color information (Wässle, 2004). Many different retinal cells are

responsible for processing specific types of visual information (e.g. ON and OFF bipolar and ganglion cells and direction selective ganglion cells). Therefore, it would be beneficial to target photosensitive proteins of opposing or varying properties to different cellular subtypes. For example, the SPARK channel induces cellular depolarization when illuminated by long-wavelength light, the opposite of the necessary wavelength light to activate LiGluR mediated cellular depolarization (Banghart *et al.,* 2004; Chambers and Kramer 2009; Vograf *et al.,* 2006). Therefore separately targeting these engineered proteins to ON or OFF cells in the retina could assist in the restoration of parallel processing. Appropriate and specific cell targeting could be achieved by vector engineering (as described) and the use of cell specific promoters (Greenberg *et al.,* 2007; Greenberg, unpublished data). One benefit of utilizing engineered photosensitive proteins is that the seemingly endless repertoire of receptors and channels found in nature are all substrates for creating novel photoswitches of varying properties.

Our results show that not only does LiGluR confer light sensitivity on retinal ganglion cells *in vitro* but this information can also be translated to the cortex, as demonstrated by LiGluR driven local field potentials in V1. This response was at least half of the amplitude of WT LFPs driven by the same visual stimulus. Though this method of recovering visual input to the cortex is promising, optimizing certain photoswitch properties is necessary to translate such a therapy to the clinic. Firstly, the wavelength of LiGluR activation needs to be shifted into the visible range. Currently, peak LiGluR sensitivity is 380nm *in vitro* (Gorostiza *et al.,* 2007) and in vivo (Figure 4.18). Sixty percent of peak LiGluR mediated LFP maximum amplitude is maintained as the activation wavelength is moved into the visible range, which is promising but not

ideal. Studies on lens spectral transmittance have shown that the rat lens filters 40-50% of 360nm illumination (Gorgels and Van Norren, 1991). As LiGluR requires an illumination intensity of 1-5mW/mm^2 for maximal activation, and we are providing 1mW/mm^2 at the cornea, lens filtering and the dissipation of light intensity between the cornea and retina is likely to diminish the illumination intensity significantly at the retinal ganglion cells. Therefore, the cortical responses we are obtaining are likely not to include the maximum amount of LiGluR input. If MAG wavelength tuning were shifted into the visible range, we would avoid lens filtering. We are also in the process of developing a stimulus that will provide higher intensity illumination and will focus on the retina. Together, shifting wavelengths and increasing stimulus intensity will optimize and maximize LiGluR activation.

A stimulus of UV light not only restricts optimal activation of LiGluR, but also causes light damage to the retina. Prolonged or intense light exposure can cause irreversible retinal damage as shown by a reduction in ERG amplitudes and photoreceptor degeneration (Noell *et al.,* 1966). Light damage is not restricted to photoreceptive cells. Recent studies have shown such light exposure can cause Müller cell hypertrophy and neurite extensions that interrupt remaining second and third order neuron connectivity and morphology (Marc *et al.,* 2008). Susceptibility to light damage sharply increases when illumination shifts to shorter wavelengths. In fact, the light intensity required for damage is lowest at 380nm and is 100-fold lower than the light intensity required by LiGluR for activation (Van Norren and Schelleken, 1990). Therefore, it would not only be beneficial to shift the wavelength tuning of LiGluR, but also to lower the intensity required for LiGluR activation.

Trauner and colleagues (part of the Nanomedicine Development Center) are working to achieve both increased sensitivity of photosensitive molecules used for engineered protein activation and wavelength tuning curve alterations. In addition, two newly synthesized compounds that can replace azobenzene in MAG are being developed (Marriot *et al.*, 2008). These compounds rapidly and reversibly change conformation upon illumination (like MAG). Optical activation can be achieved with infrared light, which is important for deep penetration of tissue. In addition, one compound (nitrospirobenzopyran (NitroBIPs)) changes fluorescence upon illumination so that photoswitching can be monitored in real time (Marriot *et al.,* 2008). The use of these compounds as receptor photoswitches is currently being assessed, with promising preliminary results (Marriot G, University of Wisconsin; Isacoff EY, University of California at Berkeley).

Another hurdle to optimizing the use of LiGluR as a late stage retinal disease therapy is the method of delivering the photoswitch, MAG. Currently, three weeks or more after vector administration another intraocular injection must be made to introduce MAG one to two days before cortical recordings. Protein turnover in cells requires the introduction of MAG for LiGluR labeling immediately before cortical experiments. More than one injection increases the chances of damage to the eye in the form of a cataract (if the needle touches the lens) and/or infection. Furthermore, as determined by our toxicity experiments, the injection itself causes acute damage to the eye that limits vision (as shown by ERG data; Figures 4.8 and 4.12). Therefore, repeated MAG injections would not be ideal for any clinical therapy. Researchers have developed multiple methods for the sustained delivery of drugs to the retina with the purpose of

avoiding repeated ocular injections (Ogura, 2001). These technologies include the injection of microparticles made of biodegradable material that encapsulate the drug of choice (Moritera *et al.,* 1991). The rate of drug release is controlled by the material of the sphere and can continuously deliver the drug for months (Akula *et al.,* 1994; Moritera *et al.,* 1991). Another technology for more sustained drug delivery is the implantation of a semi-permeable device in the vitreous that can release drug for 1-2 years (Ogura, 2001). Both methods have been used for drug delivery in the clinic, namely to treat cytomegalovirus retinitis in AIDs patients (Akula *et al.,* 1994; Sanborn *et al.,* 1991). Researchers continue to optimize drug delivery to the retina; therefore, there are and will be many ways to improve MAG delivery to avoid multiple ocular injections.

Channelrhodopsin2 is equipped with some photoactivation properties that LiGluR lacks. More specifically, ChR2 sensitivity is in the visible range and it is does not require the addition of an exogenous photoswitch molecule (Nagel *et al.,* 2005). For these reasons, many researchers have pursued the use of channelrhodopsin to develop therapies for late stage degeneration (Bi *et al.,* 2006; Lagali *et al.,* 2008). However, we discovered that LiGluR drives cortical responses in V1 that are over three times larger in amplitude when compared to ChR2. As we introduced ChR2 cDNA in the exact some fashion, it is unlikely to be due to differences in expression profile. To confirm this, we are currently using ELISA to quantify LiGluR and Channelrhodopsin expression in the rd1-/- retina after AAV mediated gene transfer. It is probable that the major reasons for the difference in photoswitch cortical response profiles are that LiGluR is bi-stable and subsequently does not quickly de-activate, maximizing cellular depolarization over the period of stimulation. In fact, we observed that the difference between peak cortical

response amplitude narrows when the stimulus duration is decreased to 50ms (Figure 4.20). Furthermore, the conductance of LiGluR is approximately 5 fold greater than ChR2, which is likely to contribute to enhanced cortical responses (Szobota *et al*., 2007). There has been recent efforts to improve ChR2 properties by creating chimeras and mutant variants of microbial opsins, namely to limit rapid inactivation and improve kinetics (Nagel *et al.,* 2005; Lin *et al.,* 2009). Both of these improvements could alter the observed ChR2 driven cortical responses. Therefore, we are in the process of assessing the new H134R gain of function channelrhodopsin mutant driven local field potentials (Nagel *et al.,* 2005). This new channelrhodospin variant has been shown to mediate larger photocurrents *in vitro* (Nagel *et al.,* 2005).

Local field potential recordings confirm that the cortex receives input from photoactivated retinal ganglion cells expressing LiGluR. However, these experiments do not provide information on the specifics of how this input is organized or processed by the cortex. We are currently characterizing neuronal response properties at the single cell level, by performing wholecell recordings from V1 cells. Specifically, we are interested in examining the relative contribution of the excitatory and inhibitory inputs to the LiGluR mediated responses. These experiments will allow us to compare the cortical circuitry that shapes LiGluR input to a single cell with normal cortical processing of visual stimuli. We will also characterize receptive field, orientation tuning, and direction selectivity properties of the LiGluR mediated input to cortical neurons. Future studies will also use voltage sensitive dye imaging and/or multielectrode recordings in V1 to study the global organization and electrophysiological properties of LiGluR mediated recovered visual responses. We are currently working to develop a high intensity light

source that is capable of delivering complex visual stimuli at the appropriate wavelength and luminance.

One of the best indications that ocular therapy is effective is improved visually guided behavior or reflexes after treatment. To this end, we aim to assess LiGluR driven pupillary reflexes and changes in two-alternative forced choice task behavior in treated "blind" animals. The pupillary reflex is the light induced contraction of the iris. Activated photosensitive rods, cones, and melanopsin expressing ganglion cells send information to pupillomoter centers in the CNS. This information is then sent back to the eye through activation of a series of neurons that ultimately innervate the iris muscle, causing pupil constriction. Assessment of the pupillary reflex is used frequently to determine abnormalties of vision (Acland *et al.,* 2001; Aleman *et al*., 2004; Trejo and Cicerone 1982). Using LiGluR to recover the pupillary reflex and in diseased animals would provide evidence that not only is information being sent to the CNS, but this information is processed in a way that restores a subconscious behavior. To assess vision driven conscious behavior, we are setting up a discrimination task that reinforces behavior (Umino *et al.,* 2006).

In summary, we have developed a promising therapeutic approach for late stage retinal disease as shown by the restoration of visually evoked cortical responses in previously "blind" animals when an engineered photosensitive protein is used to confer light sensitivity on retinal ganglion cells. Though optimization of LiGluR's properties as well as the use of various engineered photosensitive proteins in different cell types to restore basic retinal processing is desirable, the described therapy shows promise for

restoring high resolution photosensitivity to patients suffering from retinal degenerative disease.

Chapter 5

Concluding Remarks

We anticipate that the results presented in this dissertation will help make future gene therapies more efficacious and applicable to a wider spectrum of retinal disease genotypes and stages. There were two key therapeutic approaches addressed in my dissertation: slowing photoreceptor degeneration and reversing vision loss. In the first approach, we have employed Müller glia to mediate the therapeutic effects of recombinant human GDNF to slow retinal degeneration. Secondly, we have conferred light sensitivity on remaining neurons after complete photoreceptor degeneration and achieved visual recovery as shown by cortical responses to flash stimuli. Such treatments could give patients with varied disease genotypes and/or at late stages of disease therapeutic options.

In addition, we have identified natural barriers to viral vector delivery to the outer retina from the vitreous. We have also developed artificial methods and identified natural (disease) states that allow these barriers to be overcome. These data will assist the development of gene delivery techniques that avoid the subretinal injection which causes damage through retinal detachment, limits the spread of therapeutic vector, and poses a high risk of creating a retinal tear or macular hole (Fisher *et al.,* 2005; Maguire *et al.,* 2008).

The results of this dissertation touch upon the limits of gene therapy today. I will review some of the topics within gene therapy that deserve the greatest attention as we move forward to making ocular gene therapy a real option for all retinal disease patients in the clinic.

Ocular Gene Therapy Today

There are many luxuries in retinal disease research that have benefited discoveries and assisted in the translation of basic research to clinical treatments. Firstly, there are numerous animal models, both naturally occurring and transgenic, of inherited retinal disease. These animal models cross species (rodent to dog) and mimic both phenotypic and genetic manifestations of human disease (Acland *et al.,* 2001; Chang *et al.,* 2002). Furthermore, the eye is highly compartmentalized which assists in therapeutic gene/drug delivery, the blood-brain barrier minimizes systemic distribution of therapeutic material, and there is minimal immune response to vector introduction, particularly in the case of the well established gene delivery vehicle, AAV (Auricchio, 2003; Buning *et al*., 2008; Buch *et al*., 2008; Surace and Auricchio, 2003). As the eye is transparent, it is simple to image and conduct intraocular injections. In addition, gene therapy efficacy is easily assessed with noninvasive behavioral, psychophysical, and electrophysiological techniques (Buch *et al.,* 2008). Finally, treatment of only one eye allows the other eye to serve as an internal control. As the phenotypic manifestation of RP is highly variable, such a control is valuable during gene therapy development (Sullivan and Daiger, 1996).

Numerous gene therapy approaches are being generated and validated pre-clinically. These approaches include gene replacement (the introduction of wild-type DNA to replace the mutant endogenous gene activity or lack thereof), RNA mediated knock-down of dominant-negative mutant genes, the delivery of trophic factors to slow photoreceptor death, and genetically introduced retinal prosthetics (Reviewed in Buch *et al.,* 2008). The thorough experimentation conducted in animals models has expedited the implementation of phase I clinical trials in RPE65 loss of function patients (Bainbridge *et al*., 2008; Cideciyan *et al*., 2008; Hauswirth *et al*., 2008; Maguire *et al*., 2008). These proof-of principle gene therapy trials are important examples for the translation of other ocular therapies to the clinic. Drawbacks of these advanced treatments are that they target a very small patient population and are tied to traditional gene delivery techniques that have been improved upon greatly since translation from the rodent. To this end, trophic factor therapy, retinal prosthetics (both genetic and chip based), stem cell therapy, and vector engineering are emerging methods that could improve and expand treatment options.

Gene Delivery

The success of gene therapy depends upon the capability of a gene delivery vector to efficiently transduce the targeted retinal cell. Adeno-associated virus, which was employed for most of the work in this thesis, is the most widely used and promising gene delivery vehicle today (Hauswirth *et al.,* 2008; Lebherz *et al.,* 2008; Mueller and Flotte, 2008). AAV is non-pathogenic and able to infect the majority of retinal cells (Auricchio, 2003; Buch *et al*., 2008; Harvey *et al*., 2002; Lebherz *et al*., 2008; Martin *et*

al., 2002; Rolling, 2004). Furthermore, long-term transgene expression is achieved following a single treatment (Buning *et al.,* 2008). The limitations of AAV include the small packaging capacity (4.7kb), time to transgene expression after administration (approximately three weeks in rodent), inability to restrictively transduce (or mediate transgene expression in) a single cell type, and the requirement of a subretinal injection to deliver the vector to the outer retina.

Much effort is being made to address AAV's limitations. Firstly, we hope that our described results identifying and manipulating barriers to AAV transduction of outer retinal neurons and RPE from the vitreous will help avoid the subretinal injection. The discovery of new viral serotypes and engineering of the viral capsid has helped to manipulate vector tropism properties (Allocca *et al.,* 2007; Jang *et al.,* 2007; Koerber *et al., under review;* Maheshri *et al.,* 2006). Another method of restricting and enhancing transgene expression is the use of cell type specific promoters. This method has been employed to target transgene expression to rods, cones, Müller cells, and specific sub-types of retinal ganglion cells (Chen *et al.,* 2004; Flannery *et al.,* 1997; Greenberg *et al.,* 2007; Greenberg, unpublished data; Glushakova *et al.,* 2006; Komáromy *et al.,* 2008; Li *et al.,* 2008)

Researchers have identified specific approaches to enhancing AAV transduction efficiency and decreasing time to onset of transgene expression. Mutating a tyrosine residue in the AAV2 capsid allows the virus to escape ubiquitination and proteosome degradation, thereby enhancing vector transduction efficiency and kinetics (Zhong *et al.,* 2008). Complementary strand DNA synthesis is the rate-limiting step for transgene expression after AAV transduction (Ferrari *et al.,* 1996). Researchers developed a self-

complementary AAV vector that avoids this rate-limiting step and expedites the speed of transgene expression after AAV infection (Yokoi *et al.,* 2007). However, self-complementary vectors possess inverted repeat genomes, thus even further limiting the packaging capacity of the virus. As engineering AAV capsid proteins becomes more common, it is possible this method could be used to increase vector-packaging capacity. Current research is addressing the limitations of AAV mediated gene therapy techniques. However, much work needs to continue to optimize these methods and assess the side effects of manipulating the virus, viral genome, or delivery techniques before these methods make it to the clinic.

Summary

The goal of this dissertation was to develop safer and more efficacious gene delivery techniques and gene therapy approaches that could target a larger population of retinal degenerative disease patients. Though the work discussed in this dissertation requires optimization and further exploration to assess the translational potential, we hope this original body of research lays the groundwork for superior treatments for ocular disease in the future.

References

1. Acland, G. M. et al. Long-term restoration of rod and cone vision by single dose rAAV-mediated gene transfer to the retina in a canine model of childhood blindness. Mol Ther 12, 1072-82 (2005).

2. Acland, G. M. et al. Gene therapy restores vision in a canine model of childhood blindness. Nat Genet 28, 92-5 (2001).

3. Aguirre, G. K. et al. Canine and human visual cortex intact and responsive despite early retinal blindness from RPE65 mutation. PLoS Med 4, e230 (2007).

4. Ahuja, S. et al. rd1 mouse retina shows imbalance in cellular distribution and levels of TIMP-1/MMP-9, TIMP-2/MMP-2 and sulfated glycosaminoglycans. Ophthalmic Res 38, 125-36 (2006).

5. Airaksinen, M. S. & Saarma, M. The GDNF family: signalling, biological functions and therapeutic value. Nat Rev Neurosci 3, 383-94 (2002).

6. Akache, B. et al. The 37/67-kilodalton laminin receptor is a receptor for adeno-associated virus serotypes 8, 2, 3, and 9. J Virol 80, 9831-6 (2006).

7. Akula, S. K. et al. Treatment of cytomegalovirus retinitis with intravitreal injection of liposome encapsulated ganciclovir in a patient with AIDS. Br J Ophthalmol 78, 677-80 (1994).

8. Aleman, T. S. et al. Impairment of the transient pupillary light reflex in Rpe65(-/-) mice and humans with leber congenital amaurosis. Invest Ophthalmol Vis Sci 45, 1259-71 (2004).

9. Alexander, J. J. & Hauswirth, W. W. Prospects for retinal cone-targeted gene therapy. Drug News Perspect 21, 267-71 (2008).

10. Ali, R. R. et al. Restoration of photoreceptor ultrastructure and function in retinal degeneration slow mice by gene therapy. Nat Genet 25, 306-10 (2000).

11. Alilain, W. J. et al. Light-induced rescue of breathing after spinal cord injury. J Neurosci 28, 11862-70 (2008).

12. Allocca, M. et al. Serotype-dependent packaging of large genes in adeno-associated viral vectors results in effective gene delivery in mice. J Clin Invest 118, 1955-64 (2008).

13. Allocca, M. et al. Novel adeno-associated virus serotypes efficiently transduce murine photoreceptors. J Virol 81, 11372-80 (2007).

14. Amendola, M., Venneri, M. A., Biffi, A., Vigna, E. & Naldini, L. Coordinate dual-gene transgenesis by lentiviral vectors carrying synthetic bidirectional promoters. Nat Biotechnol 23, 108-16 (2005).

15. Andrieu-Soler, C. et al. Intravitreous injection of PLGA microspheres encapsulating GDNF promotes the survival of photoreceptors in the rd1/rd1 mouse. Mol Vis 11, 1002-11 (2005).

16. Arroyo, J. G., Yang, L., Bula, D. & Chen, D. F. Photoreceptor apoptosis in human retinal detachment. Am J Ophthalmol 139, 605-10 (2005).

17. Auricchio, A. Pseudotyped AAV vectors for constitutive and regulated gene expression in the eye. Vision Res 43, 913-8 (2003).

18. Auricchio, A. et al. Exchange of surface proteins impacts on viral vector cellular specificity and transduction characteristics: the retina as a model. Hum Mol Genet 10, 3075-81 (2001).

19. Awatramani, G. B. & Slaughter, M. M. Origin of transient and sustained responses in ganglion cells of the retina. J Neurosci 20, 7087-95 (2000).

20. Ayling, O. G., Harrison, T. C., Boyd, J. D., Goroshkov, A. & Murphy, T. H. Automated light-based mapping of motor cortex by photoactivation of channelrhodopsin-2 transgenic mice. Nat Methods 6, 219-24 (2009).

21. Bainbridge, J. W. et al. Effect of gene therapy on visual function in Leber's congenital amaurosis. N Engl J Med 358, 2231-9 (2008).

22. Baker, P. S. & Brown, G. C. Stem-cell therapy in retinal disease. Curr Opin Ophthalmol 20, 175-81 (2009).

23. Baloh, R. H., Enomoto, H., Johnson, E. M., Jr. & Milbrandt, J. The GDNF family ligands and receptors - implications for neural development. Curr Opin Neurobiol 10, 103-10 (2000).

24. Banghart, M., Borges, K., Isacoff, E., Trauner, D. & Kramer, R. H. Light-activated ion channels for remote control of neuronal firing. Nat Neurosci 7, 1381-6 (2004).

25. Bartlett, J. S., Wilcher, R. & Samulski, R. J. Infectious entry pathway of adeno-associated virus and adeno-associated virus vectors. J Virol 74, 2777-85 (2000).

26. Becquet, F., Courtois, Y. & Goureau, O. Nitric oxide decreases in vitro phagocytosis of photoreceptor outer segments by bovine retinal pigmented epithelial cells. J Cell Physiol 159, 256-62 (1994).

27. Berndt, A., Yizhar, O., Gunaydin, L. A., Hegemann, P. & Deisseroth, K. Bi-stable neural state switches. Nat Neurosci 12, 229-34 (2009).

28. Bessant, D. A., Ali, R. R. & Bhattacharya, S. S. Molecular genetics and prospects for therapy of the inherited retinal dystrophies. Curr Opin Genet Dev 11, 307-16 (2001).

29. Bi, A. et al. Ectopic expression of a microbial-type rhodopsin restores visual responses in mice with photoreceptor degeneration. Neuron 50, 23-33 (2006).

30. Bloomfield, S. A. & Miller, R. F. A functional organization of ON and OFF pathways in the rabbit retina. J Neurosci 6, 1-13 (1986).

31. Bourque, M. J. & Trudeau, L. E. GDNF enhances the synaptic efficacy of dopaminergic neurons in culture. Eur J Neurosci 12, 3172-80 (2000).

32. Boyden, E. S., Zhang, F., Bamberg, E., Nagel, G. & Deisseroth, K. Millisecond-timescale, genetically targeted optical control of neural activity. Nat Neurosci 8, 1263-8 (2005).

33. Bringmann, A. et al. Muller cells in the healthy and diseased retina. Prog Retin Eye Res 25, 397-424 (2006).

34. Bringmann, A. & Reichenbach, A. Role of Muller cells in retinal degenerations. Front Biosci 6, E72-92 (2001).

35. Buch, P. K., Bainbridge, J. W. & Ali, R. R. AAV-mediated gene therapy for retinal disorders: from mouse to man. Gene Ther 15, 849-57 (2008).

36. Buning, H., Perabo, L., Coutelle, O., Quadt-Humme, S. & Hallek, M. Recent developments in adeno-associated virus vector technology. J Gene Med 10, 717-33 (2008).

37. Callaway, E. M. & Yuste, R. Stimulating neurons with light. Curr Opin Neurobiol 12, 587-92 (2002).

38. Candiello, J. et al. Biomechanical properties of native basement membranes. Febs J 274, 2897-908 (2007).

39. Cao, W., Wen, R., Li, F., Cheng, T. & Steinberg, R. H. Induction of basic fibroblast growth factor mRNA by basic fibroblast growth factor in Muller cells. Invest Ophthalmol Vis Sci 38, 1358-66 (1997).

40. Chai, L. & Morris, J. E. Distribution of heparan sulfate proteoglycans in embryonic chicken neural retina and isolated inner limiting membrane. Curr Eye Res 13, 669-77 (1994).

41. Chai, L. & Morris, J. E. Heparan sulfate in the inner limiting membrane of embryonic chicken retina binds basic fibroblast growth factor to promote axonal outgrowth. Exp Neurol 160, 175-85 (1999).

42. Chambers, J. J. & Kramer, R. H. Light-activated ion channels for remote control of neural activity. Methods Cell Biol 90, 217-32 (2008).

43. Chang, B. et al. Retinal degeneration mutants in the mouse. Vision Res 42, 517-25 (2002).

44. Chang, G. Q., Hao, Y. & Wong, F. Apoptosis: final common pathway of photoreceptor death in rd, rds, and rhodopsin mutant mice. Neuron 11, 595-605 (1993).

45. Chen, J. et al. The human blue opsin promoter directs transgene expression in short-wave cones and bipolar cells in the mouse retina. Proc Natl Acad Sci U S A 91, 2611-5 (1994).

46. Cho, E. Y., Choi, H. L. & Chan, F. L. Expression pattern of glycoconjugates in rat retina as analysed by lectin histochemistry. Histochem J 34, 589-600 (2002).

47. Choi, V. W., McCarty, D. M. & Samulski, R. J. AAV hybrid serotypes: improved vectors for gene delivery. Curr Gene Ther 5, 299-310 (2005).

48. Cideciyan, A. V. et al. Human gene therapy for RPE65 isomerase deficiency activates the retinoid cycle of vision but with slow rod kinetics. Proc Natl Acad Sci U S A 105, 15112-7 (2008).

49. Costantini, F. & Shakya, R. GDNF/Ret signaling and the development of the kidney. Bioessays 28, 117-27 (2006).

50. Cowey, A., Stoerig, P. & Williams, C. Variance in transneuronal retrograde ganglion cell degeneration in monkeys after removal of striate cortex: effects of size of the cortical lesion. Vision Res 39, 3642-52 (1999).

51. Daiger, S. P., Bowne, S. J. & Sullivan, L. S. Perspective on genes and mutations causing retinitis pigmentosa. Arch Ophthalmol 125, 151-8 (2007).

52. Dalkara, D., Kolstad K.D., Caporale N., Visel M., Klimczak R.R., Schaffer, D.V., Flannery, J.G.Inner Limiting Membrane Barriers to AAV Mediated Retinal Transduction from the Vitreous. Mol Ther (2009).

53. de Kozak, Y., Cotinet, A., Goureau, O., Hicks, D. & Thillaye-Goldenberg, B. Tumor necrosis factor and nitric oxide production by resident retinal glial cells from rats presenting hereditary retinal degeneration. Ocul Immunol Inflamm 5, 85-94 (1997).

54. den Hollander, A. I., Roepman, R., Koenekoop, R. K. & Cremers, F. P. Leber congenital amaurosis: genes, proteins and disease mechanisms. Prog Retin Eye Res 27, 391-419 (2008).

55. Dinculescu, A., Glushakova, L., Min, S. H. & Hauswirth, W. W. Adeno-associated virus-vectored gene therapy for retinal disease. Hum Gene Ther 16, 649-63 (2005).

56. Dorrell, M. I. et al. Antioxidant or neurotrophic factor treatment preserves function in a mouse model of neovascularization-associated oxidative stress. J Clin Invest (2009).

57. Dryja, T. P., Hahn, L. B., Reboul, T. & Arnaud, B. Missense mutation in the gene encoding the alpha subunit of rod transducin in the Nougaret form of congenital stationary night blindness. Nat Genet 13, 358-60 (1996).

58. Dubois-Dauphin, M. et al. Early postnatal Muller cell death leads to retinal but not optic nerve degeneration in NSE-Hu-Bcl-2 transgenic mice. Neuroscience 95, 9-21 (2000).

59. Eisenfeld, A. J., Bunt-Milam, A. H. & Sarthy, P. V. Muller cell expression of glial fibrillary acidic protein after genetic and experimental photoreceptor degeneration in the rat retina. Invest Ophthalmol Vis Sci 25, 1321-8 (1984).

60. Faktorovich, E. G., Steinberg, R. H., Yasumura, D., Matthes, M. T. & LaVail, M. M. Photoreceptor degeneration in inherited retinal dystrophy delayed by basic fibroblast growth factor. Nature 347, 83-6 (1990).

61. Faktorovich, E. G., Steinberg, R. H., Yasumura, D., Matthes, M. T. & LaVail, M. M. Basic fibroblast growth factor and local injury protect photoreceptors from light damage in the rat. J Neurosci 12, 3554-67 (1992).

62. Ferrari, F. K., Samulski, T., Shenk, T. & Samulski, R. J. Second-strand synthesis is a rate-limiting step for efficient transduction by recombinant adeno-associated virus vectors. J Virol 70, 3227-34 (1996).

63. Fisher, S. K. & Lewis, G. P. Muller cell and neuronal remodeling in retinal detachment and reattachment and their potential consequences for visual recovery: a review and reconsideration of recent data. Vision Res 43, 887-97 (2003).

64. Fisher, S. K., Lewis, G. P., Linberg, K. A. & Verardo, M. R. Cellular remodeling in mammalian retina: results from studies of experimental retinal detachment. Prog Retin Eye Res 24, 395-431 (2005).

65. Flannery, J. G. et al. Efficient photoreceptor-targeted gene expression in vivo by recombinant adeno-associated virus. Proc Natl Acad Sci U S A 94, 6916-21 (1997).

66. Fontaine, V., Kinkl, N., Sahel, J., Dreyfus, H. & Hicks, D. Survival of purified rat photoreceptors in vitro is stimulated directly by fibroblast growth factor-2. J Neurosci 18, 9662-72 (1998).

67. Fork, R. L. Laser stimulation of nerve cells in Aplysia. Science 171, 907-8 (1971).

68. Frasson, M. et al. Glial cell line-derived neurotrophic factor induces histologic and functional protection of rod photoreceptors in the rd/rd mouse. Invest Ophthalmol Vis Sci 40, 2724-34 (1999).

69. Gao, G. et al. Clades of Adeno-associated viruses are widely disseminated in human tissues. J Virol 78, 6381-8 (2004).

70. Glushakova, L. G., Timmers, A. M., Pang, J., Teusner, J. T. & Hauswirth, W. W. Human blue-opsin promoter preferentially targets reporter gene expression to rat s-cone photoreceptors. Invest Ophthalmol Vis Sci 47, 3505-13 (2006).

71. Goncalves, M. A. Adeno-associated virus: from defective virus to effective vector. Virol J 2, 43 (2005).

72. Gorgels, T. G. & van Norren, D. Spectral transmittance of the rat lens. Vision Res 32, 1509-12 (1992).

73. Gorostiza, P. & Isacoff, E. Y. Optical switches for remote and noninvasive control of cell signaling. Science 322, 395-9 (2008).

74. Gorostiza, P. et al. Mechanisms of photoswitch conjugation and light activation of an ionotropic glutamate receptor. Proc Natl Acad Sci U S A 104, 10865-70 (2007).

75. Green, E. S. et al. Two animal models of retinal degeneration are rescued by recombinant adeno-associated virus-mediated production of FGF-5 and FGF-18. Mol Ther 3, 507-15 (2001).

76. Greenberg, K. P., Geller, S. F., Schaffer, D. V. & Flannery, J. G. Targeted transgene expression in muller glia of normal and diseased retinas using lentiviral vectors. Invest Ophthalmol Vis Sci 48, 1844-52 (2007).

77. Gregory-Evans, K., Chang, F., Hodges, M. D. & Gregory-Evans, C. Y. Ex vivo gene therapy using intravitreal injection of GDNF-secreting mouse embryonic stem cells in a rat model of retinal degeneration. Mol Vis 15, 962-73 (2009).

78. Grieger, J. C., Choi, V. W. & Samulski, R. J. Production and characterization of adeno-associated viral vectors. Nat Protoc 1, 1412-28 (2006).

79. Gruter, O. et al. Lentiviral vector-mediated gene transfer in adult mouse photoreceptors is impaired by the presence of a physical barrier. Gene Ther 12, 942-7 (2005).

80. Gu, S. M. et al. Mutations in RPE65 cause autosomal recessive childhood-onset severe retinal dystrophy. Nat Genet 17, 194-7 (1997).

81. Guillonneau, X. et al. Fibroblast growth factor (FGF) soluble receptor 1 acts as a natural inhibitor of FGF2 neurotrophic activity during retinal degeneration. Mol Biol Cell 9, 2785-802 (1998).

82. Halfter, W., Dong, S., Dong, A., Eller, A. W. & Nischt, R. Origin and turnover of ECM proteins from the inner limiting membrane and vitreous body. Eye 22, 1207-13 (2008).

83. Halfter, W. & Schurer, B. Disruption of the pial basal lamina during early avian embryonic development inhibits histogenesis and axonal pathfinding in the optic tectum. J Comp Neurol 397, 105-17 (1998).

84. Hanein, S. et al. Leber congenital amaurosis: comprehensive survey of the genetic heterogeneity, refinement of the clinical definition, and genotype-phenotype correlations as a strategy for molecular diagnosis. Hum Mutat 23, 306-17 (2004).

85. Harada, T. et al. Modification of glial-neuronal cell interactions prevents photoreceptor apoptosis during light-induced retinal degeneration. Neuron 26, 533-41 (2000).

86. Harvey, A. R. et al. Intravitreal injection of adeno-associated viral vectors results in the transduction of different types of retinal neurons in neonatal and adult rats: a comparison with lentiviral vectors. Mol Cell Neurosci 21, 141-57 (2002).

87. Hauck, S. M. et al. GDNF family ligands trigger indirect neuroprotective signaling in retinal glial cells. Mol Cell Biol 26, 2746-57 (2006).

88. Hauswirth, W. et al. Phase I Trial of Leber Congenital Amaurosis due to RPE65 Mutations by Ocular Subretinal Injection of Adeno-Associated Virus Gene Vector: Short-Term Results. Hum Gene Ther (2008).

89. Heegaard, S., Jensen, O. A. & Prause, J. U. Structure and composition of the inner limiting membrane of the retina. SEM on frozen resin-cracked and enzyme-digested retinas of Macaca mulatta. Graefes Arch Clin Exp Ophthalmol 224, 355-60 (1986).

90. Hims, M. M., Diager, S. P. & Inglehearn, C. F. Retinitis pigmentosa: genes, proteins and prospects. Dev Ophthalmol 37, 109-25 (2003).

91. Huang, S. H. et al. Autosomal recessive retinitis pigmentosa caused by mutations in the alpha subunit of rod cGMP phosphodiesterase. Nat Genet 11, 468-71 (1995).

92. Humayun, M. S. et al. Pattern electrical stimulation of the human retina. Vision Res 39, 2569-76 (1999).

93. Jacobson, S. G. et al. Defining the residual vision in leber congenital amaurosis caused by RPE65 mutations. Invest Ophthalmol Vis Sci 50, 2368-75 (2009).

94. Jacobson, S. G. et al. Identifying photoreceptors in blind eyes caused by RPE65 mutations: Prerequisite for human gene therapy success. Proc Natl Acad Sci U S A 102, 6177-82 (2005).

95. Jacobson, S. G. et al. Disease boundaries in the retina of patients with Usher syndrome caused by MYO7A gene mutations. Invest Ophthalmol Vis Sci 50, 1886-94 (2009).

96. Jang, J. H., Lim, K. I. & Schaffer, D. V. Library selection and directed evolution approaches to engineering targeted viral vectors. Biotechnol Bioeng 98, 515-24 (2007).

97. Janssen, A. et al. Effect of late-stage therapy on disease progression in AAV-mediated rescue of photoreceptor cells in the retinoschisin-deficient mouse. Mol Ther 16, 1010-7 (2008).

98. Jones, B. W. & Marc, R. E. Retinal remodeling during retinal degeneration. Exp Eye Res 81, 123-37 (2005).

99. Jurasek, J., Johnson, P., Olafson, R. W. & Smillie, L. B. An improved fractionation system for pronase on CM-sephadex. Can J Biochem 49, 1195-201 (1971).

100. Kaludov, N., Brown, K. E., Walters, R. W., Zabner, J. & Chiorini, J. A. Adeno-associated virus serotype 4 (AAV4) and AAV5 both require sialic acid binding for hemagglutination and efficient transduction but differ in sialic acid linkage specificity. J Virol 75, 6884-93 (2001).

101. Kandel, E. R., Schwartz, J. H. & Jessell, T. M. Principles of Neural Science (McGraw-Hill, New York, 2000).

102. Kateriya, S., Nagel, G., Bamberg, E. & Hegemann, P. "Vision" in single-celled algae. News Physiol Sci 19, 133-7 (2004).

103. Kay, M. A., Glorioso, J. C. & Naldini, L. Viral vectors for gene therapy: the art of turning infectious agents into vehicles of therapeutics. Nat Med 7, 33-40 (2001).

104. Klein, R. et al. WPRE-mediated enhancement of gene expression is promoter and cell line specific. Gene 372, 153-61 (2006).

105. Klimczak, R. R., Koerber, J. T., Dalkara, D., Flannery, J. & Schaffer, D. V. A novel evolved adeno-associated viral variant for efficient, targeted intravitreal transduction of Muller cells. PLoS One Under Review (2009).

106. Koerber, J. T. et al. Molecular evolution of adeno-associated virus for enhanced glial gene delivery. Mol Ther under review (2009).

107. Komaromy, A. M. et al. Targeting gene expression to cones with human cone opsin promoters in recombinant AAV. Gene Ther 15, 1049-55 (2008).

108. Kordower, J. H. et al. Neurodegeneration prevented by lentiviral vector delivery of GDNF in primate models of Parkinson's disease. Science 290, 767-73 (2000).

109. Lagali, P. S. et al. Light-activated channels targeted to ON bipolar cells restore visual function in retinal degeneration. Nat Neurosci 11, 667-75 (2008).

110. Landers, R. A., Rayborn, M. E., Myers, K. M. & Hollyfield, J. G. Increased retinal synthesis of heparan sulfate proteoglycan and HNK-1 glycoproteins following photoreceptor degeneration. J Neurochem 63, 737-50 (1994).

111. Lau, D. et al. Retinal degeneration is slowed in transgenic rats by AAV-mediated delivery of FGF-2. Invest Ophthalmol Vis Sci 41, 3622-33 (2000).

112. LaVail, M. M., Gorrin, G. M. & Repaci, M. A. Strain differences in sensitivity to light-induced photoreceptor degeneration in albino mice. Curr Eye Res 6, 825-34 (1987).

113. LaVail, M. M. et al. Multiple growth factors, cytokines, and neurotrophins rescue photoreceptors from the damaging effects of constant light. Proc Natl Acad Sci U S A 89, 11249-53 (1992).

114. LaVail, M. M. et al. Ribozyme rescue of photoreceptor cells in P23H transgenic rats: long-term survival and late-stage therapy. Proc Natl Acad Sci U S A 97, 11488-93 (2000).

115. LaVail, M. M. et al. Protection of mouse photoreceptors by survival factors in retinal degenerations. Invest Ophthalmol Vis Sci 39, 592-602 (1998).

116. Le Meur, G. et al. Restoration of vision in RPE65-deficient Briard dogs using an AAV serotype 4 vector that specifically targets the retinal pigmented epithelium. Gene Ther 14, 292-303 (2007).

117. Lebherz, C., Maguire, A., Tang, W., Bennett, J. & Wilson, J. M. Novel AAV serotypes for improved ocular gene transfer. J Gene Med 10, 375-82 (2008).

118. Lester, H. A. et al. Electrophysiological experiments with photoisomerizable cholinergic compounds: review and progress report. Ann N Y Acad Sci 346, 475-90 (1980).

119. Lewis, G. P., Charteris, D. G., Sethi, C. S. & Fisher, S. K. Animal models of retinal detachment and reattachment: identifying cellular events that may affect visual recovery. Eye 16, 375-87 (2002).

120. Lewis, G. P. et al. The ability of rapid retinal reattachment to stop or reverse the cellular and molecular events initiated by detachment. Invest Ophthalmol Vis Sci 43, 2412-20 (2002).

121. Lewis, G. P. & Fisher, S. K. Up-regulation of glial fibrillary acidic protein in response to retinal injury: its potential role in glial remodeling and a comparison to vimentin expression. Int Rev Cytol 230, 263-90 (2003).

122. Lewis, G. P., Sethi, C. S., Linberg, K. A., Charteris, D. G. & Fisher, S. K. Experimental retinal reattachment: a new perspective. Mol Neurobiol 28, 159-75 (2003).

123. Li, Q., Timmers, A. M., Guy, J., Pang, J. & Hauswirth, W. W. Cone-specific expression using a human red opsin promoter in recombinant AAV. Vision Res 48, 332-8 (2008).

124. Liang, F. Q. et al. Long-term protection of retinal structure but not function using RAAV.CNTF in animal models of retinitis pigmentosa. Mol Ther 4, 461-72 (2001).

125. Liewald, J. F. et al. Optogenetic analysis of synaptic function. Nat Methods 5, 895-902 (2008).

126. Lin, J. Y., Lin, M. Z., Steinbach, P. & Tsien, R. Y. Characterization of engineered channelrhodopsin variants with improved properties and kinetics. Biophys J 96, 1803-14 (2009).

127. Linden, R., Rehen, S. K. & Chiarini, L. B. Apoptosis in developing retinal tissue. Prog Retin Eye Res 18, 133-65 (1999).

128. Lundkvist, A. et al. Under stress, the absence of intermediate filaments from Muller cells in the retina has structural and functional consequences. J Cell Sci 117, 3481-8 (2004).

129. MacLaren, R. E. et al. Retinal repair by transplantation of photoreceptor precursors. Nature 444, 203-7 (2006).

130. Maguire, A. M. et al. Safety and efficacy of gene transfer for Leber's congenital amaurosis. N Engl J Med 358, 2240-8 (2008).

131. Maheshri, N., Koerber, J. T., Kaspar, B. K. & Schaffer, D. V. Directed evolution of adeno-associated virus yields enhanced gene delivery vectors. Nat Biotechnol 24, 198-204 (2006).

132. Marc, R. E. & Jones, B. W. Retinal remodeling in inherited photoreceptor degenerations. Mol Neurobiol 28, 139-47 (2003).

133. Marc, R. E. et al. Neural reprogramming in retinal degeneration. Invest Ophthalmol Vis Sci 48, 3364-71 (2007).

134. Marc, R. E., Jones, B. W., Watt, C. B. & Strettoi, E. Neural remodeling in retinal degeneration. Prog Retin Eye Res 22, 607-55 (2003).

135. Marc, R. E. et al. Extreme retinal remodeling triggered by light damage: implications for age related macular degeneration. Mol Vis 14, 782-806 (2008).

136. Marlhens, F. et al. Mutations in RPE65 cause Leber's congenital amaurosis. Nat Genet 17, 139-41 (1997).

137. Marriott, G. et al. Optical lock-in detection imaging microscopy for contrast-enhanced imaging in living cells. Proc Natl Acad Sci U S A 105, 17789-94 (2008).

138. Martin, K. R., Klein, R. L. & Quigley, H. A. Gene delivery to the eye using adeno-associated viral vectors. Methods 28, 267-75 (2002).

139. Maw, M. A. et al. Mutation of the gene encoding cellular retinaldehyde-binding protein in autosomal recessive retinitis pigmentosa. Nat Genet 17, 198-200 (1997).

140. Mayer, G. & Heckel, A. Biologically active molecules with a "light switch". Angew Chem Int Ed Engl 45, 4900-21 (2006).

141. Mayer, M. L. Crystal structures of the GluR5 and GluR6 ligand binding cores: molecular mechanisms underlying kainate receptor selectivity. Neuron 45, 539-52 (2005).

142. Mazzoni, F., Novelli, E. & Strettoi, E. Retinal ganglion cells survive and maintain normal dendritic morphology in a mouse model of inherited photoreceptor degeneration. J Neurosci 28, 14282-92 (2008).

143. McCarty, D. M. Self-complementary AAV vectors; advances and applications. Mol Ther 16, 1648-56 (2008).

144. McGee Sanftner, L. H., Abel, H., Hauswirth, W. W. & Flannery, J. G. Glial cell line derived neurotrophic factor delays photoreceptor degeneration in a transgenic rat model of retinitis pigmentosa. Mol Ther 4, 622-9 (2001).

145. McLaughlin, M. E., Ehrhart, T. L., Berson, E. L. & Dryja, T. P. Mutation spectrum of the gene encoding the beta subunit of rod phosphodiesterase among patients with autosomal recessive retinitis pigmentosa. Proc Natl Acad Sci U S A 92, 3249-53 (1995).

146. Mester, V. & Kuhn, F. Internal limiting membrane removal in the management of full-thickness macular holes. Am J Ophthalmol 129, 769-77 (2000).

147. Min, S. H. et al. Prolonged recovery of retinal structure/function after gene therapy in an Rs1h-deficient mouse model of x-linked juvenile retinoschisis. Mol Ther 12, 644-51 (2005).

148. Miyoshi, H., Takahashi, M., Gage, F. H. & Verma, I. M. Stable and efficient gene transfer into the retina using an HIV-based lentiviral vector. Proc Natl Acad Sci U S A 94, 10319-23 (1997).

149. Moritera, T. et al. Microspheres of biodegradable polymers as a drug-delivery system in the vitreous. Invest Ophthalmol Vis Sci 32, 1785-90 (1991).

150. Mueller, C. & Flotte, T. R. Clinical gene therapy using recombinant adeno-associated virus vectors. Gene Ther 15, 858-63 (2008).

151. Nagel, G. et al. Light activation of channelrhodopsin-2 in excitable cells of Caenorhabditis elegans triggers rapid behavioral responses. Curr Biol 15, 2279-84 (2005).

152. Nagel, G. et al. Channelrhodopsins: directly light-gated cation channels. Biochem Soc Trans 33, 863-6 (2005).

153. Naldini, L. et al. In vivo gene delivery and stable transduction of nondividing cells by a lentiviral vector. Science 272, 263-7 (1996).

154. Narfstrom, K. et al. Functional and structural evaluation after AAV.RPE65 gene transfer in the canine model of Leber's congenital amaurosis. Adv Exp Med Biol 533, 423-30 (2003).

155. Nelson, R., Famiglietti, E. V., Jr. & Kolb, H. Intracellular staining reveals different levels of stratification for on- and off-center ganglion cells in cat retina. J Neurophysiol 41, 472-83 (1978).

156. Newman, E. & Reichenbach, A. The Muller cell: a functional element of the retina. Trends Neurosci 19, 307-12 (1996).

157. Nguyen, Q. T., Parsadanian, A. S., Snider, W. D. & Lichtman, J. W. Hyperinnervation of neuromuscular junctions caused by GDNF overexpression in muscle. Science 279, 1725-9 (1998).

158. Noell, W. K., Walker, V. S., Kang, B. S. & Berman, S. Retinal damage by light in rats. Invest Ophthalmol 5, 450-73 (1966).

159. Numano, R. et al. Nanosculpting reversed wavelength sensitivity into a photoswitchable iGluR. Proc Natl Acad Sci U S A 106, 6814-9 (2009).

160. Ogura, Y. Drug delivery to the posterior segments of the eye. Adv Drug Deliv Rev 52, 1-3 (2001).

161. Ozaki, S., Radeke, M. J. & Anderson, D. H. Rapid upregulation of fibroblast growth factor receptor 1 (flg) by rat photoreceptor cells after injury. Invest Ophthalmol Vis Sci 41, 568-79 (2000).

162. Ozaki, S., Radeke, M. J. & Anderson, D. H. Rapid upregulation of fibroblast growth factor receptor 1 (flg) by rat photoreceptor cells after injury. Invest Ophthalmol Vis Sci 41, 568-79 (2000).

163. Pang, J. J. et al. Gene therapy restores vision-dependent behavior as well as retinal structure and function in a mouse model of RPE65 Leber congenital amaurosis. Mol Ther 13, 565-72 (2006).

164. Park, T. K. et al. Intravitreal delivery of AAV8 retinoschisin results in cell type-specific gene expression and retinal rescue in the Rs1-KO mouse. Gene Ther (2009).

165. Petreanu, L., Mao, T., Sternson, S. M. & Svoboda, K. The subcellular organization of neocortical excitatory connections. Nature 457, 1142-5 (2009).

166. Petrs-Silva, H. et al. High-efficiency transduction of the mouse retina by tyrosine-mutant AAV serotype vectors. Mol Ther 17, 463-71 (2009).

167. Philpott, N. J. & Thrasher, A. J. Use of nonintegrating lentiviral vectors for gene therapy. Hum Gene Ther 18, 483-9 (2007).

168. Pickard, G. E. et al. Intravitreal injection of the attenuated pseudorabies virus PRV Bartha results in infection of the hamster suprachiasmatic nucleus only by retrograde transsynaptic transport via autonomic circuits. J Neurosci 22, 2701-10 (2002).

169. Pittler, S. J. & Baehr, W. Identification of a nonsense mutation in the rod photoreceptor cGMP phosphodiesterase beta-subunit gene of the rd mouse. Proc Natl Acad Sci U S A 88, 8322-6 (1991).

170. Pothos, E. N., Davila, V. & Sulzer, D. Presynaptic recording of quanta from midbrain dopamine neurons and modulation of the quantal size. J Neurosci 18, 4106-18 (1998).

171. Qing, K. et al. Human fibroblast growth factor receptor 1 is a co-receptor for infection by adeno-associated virus 2. Nat Med 5, 71-7 (1999).

172. Raymond, P. A., Barthel, L. K. & Rounsifer, M. E. Immunolocalization of basic fibroblast growth factor and its receptor in adult goldfish retina. Exp Neurol 115, 73-8 (1992).

173. Reme, C. E., Grimm, C., Hafezi, F., Wenzel, A. & Williams, T. P. Apoptosis in the Retina: The Silent Death of Vision. News Physiol Sci 15, 120-124 (2000).

174. Rolling, F. Recombinant AAV-mediated gene transfer to the retina: gene therapy perspectives. Gene Ther 11 Suppl 1, S26-32 (2004).

175. Rolling, F. et al. Gene therapeutic prospects in early onset of severe retinal dystrophy: restoration of vision in RPE65 Briard dogs using an AAV serotype 4 vector that specifically targets the retinal pigmented epithelium. Bull Mem Acad R Med Belg 161, 497-508; discussion 508-9 (2006).

176. Roska, B., Molnar, A. & Werblin, F. S. Parallel processing in retinal ganglion cells: how integration of space-time patterns of excitation and inhibition form the spiking output. J Neurophysiol 95, 3810-22 (2006).

177. Roska, B. & Werblin, F. Vertical interactions across ten parallel, stacked representations in the mammalian retina. Nature 410, 583-7 (2001).

178. Saari, J. C. The sights along route 65. Nat Genet 29, 8-9 (2001).

179. Sanborn, G. E. et al. Sustained-release ganciclovir therapy for treatment of cytomegalovirus retinitis. Use of an intravitreal device. Arch Ophthalmol 110, 188-95 (1992).

180. Sastry, L., Johnson, T., Hobson, M. J., Smucker, B. & Cornetta, K. Titering lentiviral vectors: comparison of DNA, RNA and marker expression methods. Gene Ther 9, 1155-62 (2002).

181. Schultz, B. R. & Chamberlain, J. S. Recombinant adeno-associated virus transduction and integration. Mol Ther 16, 1189-99 (2008).

182. Semina, E. V. et al. Mutations in laminin alpha 1 result in complex, lens-independent ocular phenotypes in zebrafish. Dev Biol 299, 63-77 (2006).

183. Shastry, B. S. Signal transduction in the retina and inherited retinopathies. Cell Mol Life Sci 53, 419-29 (1997).

184. Siliprandi, R., Bucci, M. G., Canella, R. & Carmignoto, G. Flash and pattern electroretinograms during and after acute intraocular pressure elevation in cats. Invest Ophthalmol Vis Sci 29, 558-65 (1988).

185. Sineshchekov, O. A., Govorunova, E. G. & Spudich, J. L. Photosensory functions of channelrhodopsins in native algal cells. Photochem Photobiol 85, 556-63 (2009).

186. Sinn, P. L., Sauter, S. L. & McCray, P. B., Jr. Gene therapy progress and prospects: development of improved lentiviral and retroviral vectors--design, biosafety, and production. Gene Ther 12, 1089-98 (2005).

187. Smith, A. J. et al. AAV-Mediated gene transfer slows photoreceptor loss in the RCS rat model of retinitis pigmentosa. Mol Ther 8, 188-95 (2003).

188. Steinberg, R. H. et al. in ARVO abstract: S226 (1997).

189. Strettoi, E. & Pignatelli, V. Modifications of retinal neurons in a mouse model of retinitis pigmentosa. Proc Natl Acad Sci U S A 97, 11020-5 (2000).

190. Sullivan, L. S. & Daiger, S. P. Inherited retinal degeneration: exceptional genetic and clinical heterogeneity. Mol Med Today 2, 380-6 (1996).

191. Summerford, C. & Samulski, R. J. Membrane-associated heparan sulfate proteoglycan is a receptor for adeno-associated virus type 2 virions. J Virol 72, 1438-45 (1998).

192. Surace, E. M. & Auricchio, A. Adeno-associated viral vectors for retinal gene transfer. Prog Retin Eye Res 22, 705-19 (2003).

193. Surace, E. M. & Auricchio, A. Versatility of AAV vectors for retinal gene transfer. Vision Res 48, 353-9 (2008).

194. Szobota, S. et al. Remote control of neuronal activity with a light-gated glutamate receptor. Neuron 54, 535-45 (2007).

195. Travis, G. H. Mechanisms of cell death in the inherited retinal degenerations. Am J Hum Genet 62, 503-8 (1998).

196. Trejo, L. J. & Cicerone, C. M. Retinal sensitivity measured by the pupillary light reflex in RCS and albino rats. Vision Res 22, 1163-71 (1982).

197. Triolo, D. et al. Loss of glial fibrillary acidic protein (GFAP) impairs Schwann cell proliferation and delays nerve regeneration after damage. J Cell Sci 119, 3981-93 (2006).

198. Tso, M. O. et al. Apoptosis leads to photoreceptor degeneration in inherited retinal dystrophy of RCS rats. Invest Ophthalmol Vis Sci 35, 2693-9 (1994).

199. Umino, Y., Frio, B., Abbasi, M. & Barlow, R. A two-alternative, forced choice method for assessing mouse vision. Adv Exp Med Biol 572, 169-72 (2006).

200. Valter, K., van Driel, D., Bisti, S. & Stone, J. FGFR1 expression and FGFR1-FGF-2 colocalisation in rat retina: sites of FGF-2 action on rat photoreceptors. Growth Factors 20, 177-88 (2002).

201. van Norren, D. & Schellekens, P. Blue light hazard in rat. Vision Res 30, 1517-20 (1990).

202. Verma, I. M. et al. in Genes and Resistance to Disease (eds. Boulyjenkov, V., Berg, K. & Christen, Y.) 147-153 (Springer, New York, 2000).

203. Volgraf, M. et al. Allosteric control of an ionotropic glutamate receptor with an optical switch. Nat Chem Biol 2, 47-52 (2006).

204. Vollrath, D. et al. Correction of the retinal dystrophy phenotype of the RCS rat by viral gene transfer of Mertk. Proc Natl Acad Sci U S A 98, 12584-9 (2001).

205. Wahlin, K. J., Campochiaro, P. A., Zack, D. J. & Adler, R. Neurotrophic factors cause activation of intracellular signaling pathways in Muller cells and other cells of the inner retina, but not photoreceptors. Invest Ophthalmol Vis Sci 41, 927-36 (2000).

206. Walters, R. W. et al. Binding of adeno-associated virus type 5 to 2,3-linked sialic acid is required for gene transfer. J Biol Chem 276, 20610-6 (2001).

207. Wang, C. Y. et al. Ca(2+) binding protein frequenin mediates GDNF-induced potentiation of Ca(2+) channels and transmitter release. Neuron 32, 99-112 (2001).

208. Wang, H. et al. High-speed mapping of synaptic connectivity using photostimulation in Channelrhodopsin-2 transgenic mice. Proc Natl Acad Sci U S A 104, 8143-8 (2007).

209. Wassle, H. Parallel processing in the mammalian retina. Nat Rev Neurosci 5, 747-57 (2004).

210. Weber, M. et al. Recombinant adeno-associated virus serotype 4 mediates unique and exclusive long-term transduction of retinal pigmented epithelium in rat, dog, and nonhuman primate after subretinal delivery. Mol Ther 7, 774-81 (2003).

211. Weiland, J. D., Liu, W. & Humayun, M. S. Retinal prosthesis. Annu Rev Biomed Eng 7, 361-401 (2005).

212. Wen, R. et al. Injury-induced upregulation of bFGF and CNTF mRNAS in the rat retina. J Neurosci 15, 7377-85 (1995).

213. Werblin, F., Roska, B. & Balya, D. Parallel processing in the mammalian retina: lateral and vertical interactions across stacked representations. Prog Brain Res 131, 229-38 (2001).

214. Wickham, L. et al. Glial and neural response in short-term human retinal detachment. Arch Ophthalmol 124, 1779-82 (2006).

215. Wu, S. M., Gao, F. & Maple, B. R. Functional architecture of synapses in the inner retina: segregation of visual signals by stratification of bipolar cell axon terminals. J Neurosci 20, 4462-70 (2000).

216. Wu, W. C. et al. Gene therapy for detached retina by adeno-associated virus vector expressing glial cell line-derived neurotrophic factor. Invest Ophthalmol Vis Sci 43, 3480-8 (2002).

217. Wu, Z., Asokan, A. & Samulski, R. J. Adeno-associated virus serotypes: vector toolkit for human gene therapy. Mol Ther 14, 316-27 (2006).

218. Wu, Z., Miller, E., Agbandje-McKenna, M. & Samulski, R. J. Alpha2,3 and alpha2,6 N-linked sialic acids facilitate efficient binding and transduction by adeno-associated virus types 1 and 6. J Virol 80, 9093-103 (2006).

219. Yanez-Munoz, R. J. et al. Effective gene therapy with nonintegrating lentiviral vectors. Nat Med 12, 348-53 (2006).

220. Yokoi, K. et al. Ocular gene transfer with self-complementary AAV vectors. Invest Ophthalmol Vis Sci 48, 3324-8 (2007).

221. Yu, D. & Silva, G. A. Stem cell sources and therapeutic approaches for central nervous system and neural retinal disorders. Neurosurg Focus 24, E11 (2008).

222. Yu, J. H. & Schaffer, D. V. Selection of novel vesicular stomatitis virus glycoprotein variants from a peptide insertion library for enhanced purification of retroviral and lentiviral vectors. J Virol 80, 3285-92 (2006).

223. Zack, D. J. Neurotrophic rescue of photoreceptors: are Muller cells the mediators of survival? Neuron 26, 285-6 (2000).

224. Zemelman, B. V., Lee, G. A., Ng, M. & Miesenbock, G. Selective photostimulation of genetically chARGed neurons. Neuron 33, 15-22 (2002).

225. Zhang, F., Aravanis, A. M., Adamantidis, A., de Lecea, L. & Deisseroth, K. Circuit-breakers: optical technologies for probing neural signals and systems. Nat Rev Neurosci 8, 577-81 (2007).

226. Zhang, F. et al. Red-shifted optogenetic excitation: a tool for fast neural control derived from Volvox carteri. Nat Neurosci 11, 631-3 (2008).

227. Zhang, F., Wang, L. P., Boyden, E. S. & Deisseroth, K. Channelrhodopsin-2 and optical control of excitable cells. Nat Methods 3, 785-92 (2006).

228. Zhang, F. et al. Multimodal fast optical interrogation of neural circuitry. Nature 446, 633-9 (2007).

229. Zhang, X., Cheng, M. & Chintala, S. K. Kainic acid-mediated upregulation of matrix metalloproteinase-9 promotes retinal degeneration. Invest Ophthalmol Vis Sci 45, 2374-83 (2004).

230. Zhao, S. et al. Improved expression of halorhodopsin for light-induced silencing of neuronal activity. Brain Cell Biol 36, 141-54 (2008).

231. Zhong, L. et al. Next generation of adeno-associated virus 2 vectors: point mutations in tyrosines lead to high-efficiency transduction at lower doses. Proc Natl Acad Sci U S A 105, 7827-32 (2008).